**CHAPTER 8**

# Glaciers and glacial geology

*Fire and Ice*
Some say the world will end in fire
Some say in ice.
From what I've tasted of desire
I hold with those who favor fire.
But if I had to perish twice,
I think I know enough of hate
To say that for destruction ice
Is also great
And would suffice.

Robert Frost

**Figure 8.0** Kennicott Glacier, Wrangell–St. Elias National Park, Alaska. Mt. Blackburn graces the left skyline. Little Ice Age moraines bound the ides of the glacier roughly 16 km from its present terminus near the town of McCarthy. (photograph by R. S. Anderson)

## In this chapter

we address the processes that modify landscapes once occupied by glaciers. These large mobile chunks of ice are very effective agents of change in the landscape, sculpting distinctive landforms, and generating prodigious amounts of sediment. Our task is broken into two parts, which form the major divisions of the chapter: (1) understanding the physics of how glaciers work, the discipline of glaciology, which is prerequisite for (2) understanding how glaciers erode the landscape, the discipline of glacial geology.

Although glaciers are interesting in their own right, and lend to alpine environments an element of beauty of their own, they are also important geomorphic actors. Occupation of alpine valleys by glaciers leads to the generation of such classic glacial signatures as U-shaped valleys, steps and overdeepenings now occupied by lakes in the long valley profiles, and hanging valleys that now spout waterfalls. Even coastlines have been greatly affected by glacial processes. Major fjords, some of them extending to water depths of over 1 km, punctuate the coastlines of western North America, New Zealand and Norway. We will discuss these features and the glacial erosion processes that lead to their formation.

It is the variation in the extent of continental scale ice sheets in the northern hemisphere that has driven the 120–150 m fluctuations in sea level over the last three million years. On tectonically rising coastlines, this has resulted in the generation of marine terraces, each carved at a sea level highstand corresponding to an interglacial period.

Ice sheets and glaciers also contain high-resolution records of climate change. Extraction and analysis of cores of ice reveal detailed layering, chemistry, and air bubble contents that are our best terrestrial paleoclimate archive for comparison with the deep sea records obtained through ocean drilling programs.

The interest in glaciers is not limited to Earth, either. As we learn more about other planets in the solar system, attention has begun to focus on the potential that Martian ice caps could also contain paleoclimate information. And further out into the solar system are bodies whose surfaces are at mostly water ice. Just how these surfaces deform upon impacts of bolides, and the potential for unfrozen water at depth, are topics of considerable interest in the planetary sciences community.

Finally, glaciers are worth understanding in their own right, as they are pathways for hikers, suppliers of water to downstream communities, and sources of catastrophic floods and ice avalanches. The surfaces of glaciers are littered with cracks and holes, some of which are dangerous. But these hazards can either be avoided or lessened if we approach them with some knowledge of their origin. How deep are crevasses? How are crevasses typically oriented, and why? What is a moulin? What is a medial moraine, what is a lateral moraine? Are they mostly ice or mostly rock? How does the water discharge from a glacial outlet stream vary through a day, and through a year?

## Glaciology: what are glaciers and how do they work?

A glacier is a natural accumulation of ice that is in motion due to its own weight and the slope of its surface. The ice is derived from snow, which slowly loses porosity to approach a density of pure ice. This evolution is shown in Figure 8.1. Consider a small alpine valley. In general, it snows more at high altitudes than it does at low altitudes. And it melts more at low altitudes than it does at high. If there is some place in the valley where it snows more in the winter than it melts in the summer, there will be a net accumulation of snow there. The down-valley limit of this accumulation is the snowline, the first place where you would encounter snow on a climb of the valley in the late fall. If this happened year after year, a wedge of snow would accumulate each year, compressing the previous years' accumulations. The snow slowly compacts to produce firn in a process akin to the metamorphic reactions in a mono-mineralic rock near its pressure melting point. Once thick enough,

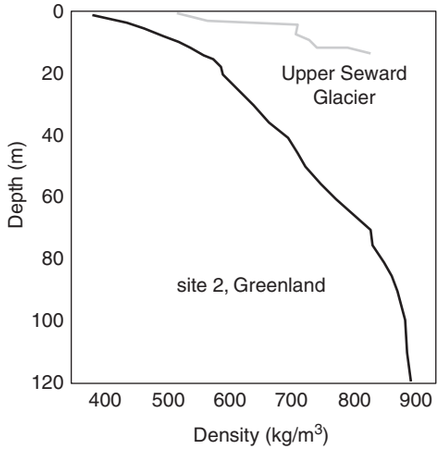


**Figure 8.1** Density profiles in two very different glaciers, the upper Seward Glacier in coastal Alaska being very wet, the Greenland site being very dry. The metamorphism of snow is much more rapid in the wetter case; firn achieves full ice densities by 20 m on the upper Seward and takes 100 m in Greenland. Ice with no pore space has a density of 917 kg/m$^3$. (after Paterson, 1994, Figure 2.2, reproduced with permission from Elsevier)

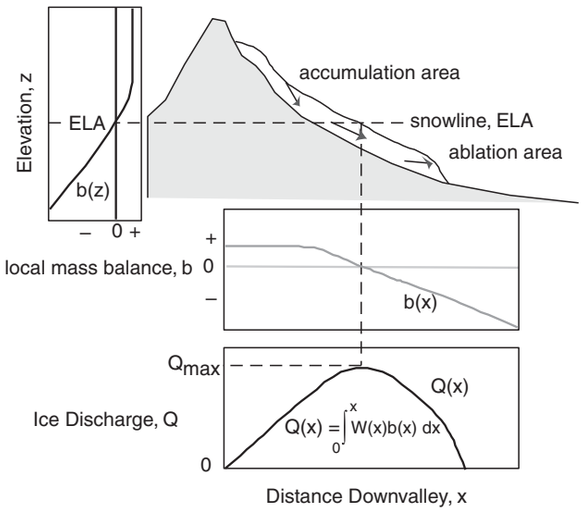


**Figure 8.2** Schematic diagrams of a glacier (white) in mountainous topography (gray) showing accumulation and ablation areas on either side of the equilibrium line. Mapped into the vertical, *z* (left-hand diagram), the net mass balance profile, *b*(*z*), is negative at elevations below the ELA and positive above it. We also show the net balance mapped onto the valley- parallel axis, *x* (follow dashed line downward), generating the net balance profile *b*(*x*). At steady state the ice discharge of the glacier must reflect the integral of this net balance profile (bottom diagram). The maximum discharge should occur at roughly the down-valley position of the ELA. Where the discharge goes again to zero determines the terminus position.

this growing wedge of snow-ice can begin to deform under its own weight, and to move downhill. At this point, we would call the object a glacier. It is only by the motion of the ice that ice can be found further down the valley than the annual snowline.

A glacier can be broken into two parts, as summarized in Figure 8.2: the accumulation area, where there is net accumulation of ice over the course of a year, and the ablation area, where there is net loss of ice. The two are separated by the equilibrium line, at which a balance (or equilibrium) exists between accumulation and ablation. This corresponds to a long-term average of the snowline position. The equilibrium line altitude, or the ELA, is a very important attribute of a glacier. In a given climate, it is remarkably consistent among close-by valleys, and at least crudely approximates the elevation at which the mean annual temperature is 0°C.

The ice of the world is contained primarily in the great ice sheets. Antarctica represents roughly 70 m of sea level equivalent of water, Greenland roughly 7 m, and all the small glaciers and ice caps of the world roughly 2 m. We note, however, that the small ice bodies of the globe are contributing disproportionately to the present sea level rise.

## Types of glaciers: a bestiary of ice

First of all, note that sea ice is fundamentally different from glacier ice. Sea ice is frozen seawater; it is not born of snow. It is usually a few meters thick at the best, with pressure ridges and their associated much deeper keels being a few tens of meters thick. Icebreakers can plow through sea ice. They cannot plow through icebergs, which are calved from the fronts of tidewater glaciers, and can be more than a hundred meters thick. It is icebergs that pose a threat to shipping.

Glaciers can be classified in several ways, using size, the thermal regime, the location in the landscape, and even the steadiness of a glacier's speed. Some of these classifications overlap, as we will see. We will start with the thermal distinctions, as they play perhaps the most important role in determining the degree to which a glacier can modify the landscape.

The temperatures of *polar glaciers* are well below the freezing point of water throughout except, in some cases, at the bed. They are found at both very high latitudes and very high altitudes, reflecting the very cold mean annual temperatures there. As is seen in Figure 8.3, to first order, a thermal profile in these glaciers would look like one in rock, increasing with depth in a geothermal profile that differs from one in rock only in that the conductivity and density of ice is different from that of rock.

In contrast to these glaciers, *temperate glaciers* are those in which the mean annual temperature is very close to the pressure-melting point of ice, all the way to the bed. The distinction is clearly seen in Figure 8.3. They derive their name from their location in temperate climates whose mean annual temperatures are closer to 0°C than at much higher elevations or latitudes. The importance of the thermal regime lies in the fact that being close to the melting point at the base allows the ice to slide along the bed in a process called regelation, which we will discuss later in the chapter. It is this process of sliding that allows temperate glaciers to erode their beds through both abrasion and quarrying. Polar glaciers are gentle on the landscape, perhaps even protecting it from subaerial mechanical weathering

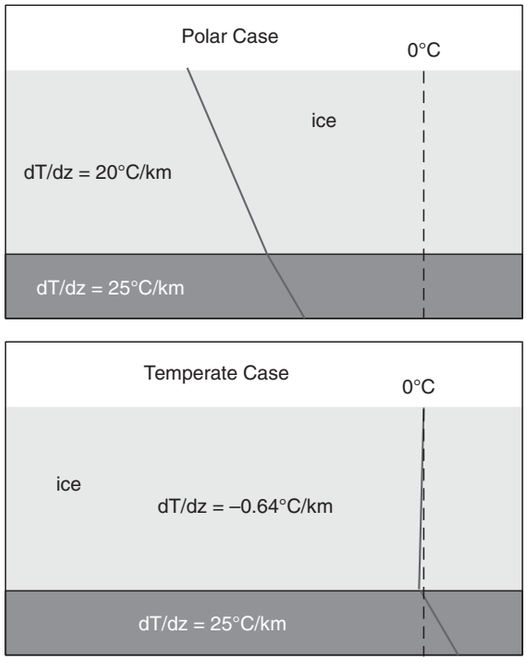


**Figure 8.3** Temperature profiles in polar (top) and temperate (bottom) glacier cases. Slight kink in profile in the polar case reflects the different thermal conductivities of rock and ice. Roughly isothermal profile in the temperate case is allowed by the downward advection of heat by melt water. Temperature is kept very near the pressure-melting point throughout, meaning it declines slightly (see phase diagram of water, Figure 1.2).

processes that would otherwise attack it. How does a temperate glacier remain close to the melting point throughout, being almost isothermal? Recall that associated with the phase change of water is a huge amount of energy. In a temperate glacier, significant water melts at the surface, and is translated to depth within the firn, and even deeper in the glacier along three-grain intersections. Glacier ice is after all a porous substance. If this water encounters any site that is below the freezing point, it will freeze, yielding its energy, which in turn warms up the surrounding ice. So heat is efficiently moved from the surface to depth by moving water – it is advected. This is a much more efficient process of heat transport than is conduction, and can maintain the entire body of a glacier at very near the freezing point.

A straightforward distinction can be made in terms of size. Valley glaciers occupy single valleys. Ice caps cover the tops of peaks and drain down several valleys on the sides of the peak. Ice sheets can exist in the absence of any pre-existing topography, and can be much larger by orders of magnitude than ice caps. The greatest contemporary examples are the ice sheets of east and west Antarctica, and of Greenland, with diameters of thousands of kilometers, and thicknesses of kilometers. Their even larger relatives in the last glacial maximum (LGM), the combined Laurentide and Cordillera, and the Fennoscandian Ice Sheets, covered half of North America and half of Europe, respectively.

Tidal glaciers are those that dip their toes in the sea, and lose some fraction of their mass through the calving of icebergs (as opposed to loss solely by melting). These are the glaciers of concern to shipping, be it the shipping plying the waters of the Alaskan coastline, or the ocean liners plying the waters off Greenland.

Most glaciers obey what we mean when we use the adjective "glacial." Glacial speeds might be a few meters to a few kilometers per year, and will be the same the next year and the next. We speak of glacial speeds as being slow and steady. The exceptions to this are surging glaciers and their cousins embedded in ice sheet margins, the ice streams, which appear to be in semi-perpetual surge. These ill-behaved glaciers (meaning they don't fit our expectations) are the subjects of intense modern study. They may hold the key to understanding the rapid fluctuations of climate in the late Pleistocene, which in turn are important to understand as they lay the context for the modern climate system that humans are modifying significantly.

All of these we will visit in turn, but first let us lay out the basics of how glaciers work.

## Mass balance

The glaciological community, traditionally an intimate mix of mountain climbers and geophysicists, has a long and proud tradition of being quite formal in its approach to the health of glaciers and their mechanics. Once again, the problem comes down to a balance, this time of mass of ice. One may find in the bible of the glaciologists, Paterson's *The Physics of Glaciers*, now in its third edition (Paterson, 1994), at least one chapter on mass balance alone (see Further reading in this chapter for more suggestions of other excellent textbooks). One may formalize the

illustration of the mass balance shown in Figure 8.2 with the following equation:

$$\frac{\partial H}{\partial t} = b(z) - \frac{1}{W(z)}\frac{\partial Q}{\partial x} \tag{8.1}$$

where $H$ is ice thickness, $W$ is the glacier width, and $Q$ the ice discharge per unit width [$= L^2/T$]. Mass can be lost or gained through all edges of the block we have depicted (the top, the base, and the up- and down-ice sides). Here $b$ represents the "local mass balance" on the glacier surface, the mass lost or gained over an annual cycle. It is usually expressed as a thickness of ice surface, i.e., meters of water equivalent. This quantity is positive where there is a net gain of ice mass over an annual cycle, and negative where there is a net loss. The elevation at which the mass balance crosses zero defines the "equilibrium line altitude," or the ELA, of the glacier. Because it is an altitude, it is a horizontal line in Figure 8.2. The mass balance reflects all of the meteorological forcing of the glacier, both the snow added over the course of the year, and the losses dealt by the combined effects of ablation (melt) and sublimation. Where the annual mass balance is positive, it has snowed more than it melts in a year, and vice versa. To first order, because it snows more at higher altitudes, and melts more at lower altitudes, the mass balance always has a positive gradient with elevation. Examples of mass balance profiles from a variety of glaciers in differing climates are shown in Figure 8.4. Note the positive mass balance gradient in each case, which is especially well marked in the ablation or wastage zones. One can easily pick out the ELA for each glacier. The ELA varies greatly, being lowest in high latitudes (where it is cold and the ablation is low) and nearest coastlines (where the winter accumulation is high due to proximity of oceanic water sources). A classic illustration of the latitudinal dependence is drawn from work of Porter *et al*., reproduced in Figure 8.5. The modern ELAs, as deduced from snowlines and mass balance surveys, are everywhere much higher than the ELAs reconstructed (more on how to do this later; see Figure 8.19) from the last glacial maximum (LGM) at roughly 18 ka. In places the rise in ELA is up to 1 km!

One may measure the health of a glacier by the total mass balance, reflecting whether in a given year there has been a net loss or gain of ice from the entire

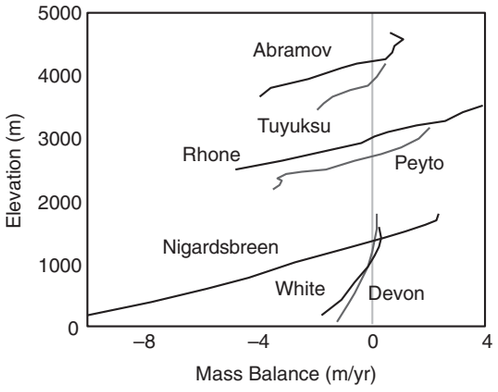


**Figure 8.4** Specific mass balance profiles from several glaciers around the world, showing the variability of the shape of the profiles. Mass balance gradients (slopes on this plot) are quite similar, especially in ablation zones (where the local balance $b < 0$), except for those in the Canadian Arctic (Devon and White ice caps). (adapted from Oerlemans and Fortuin, 1992, Figure 1, with permission of the American Association for the Advancement of Science)

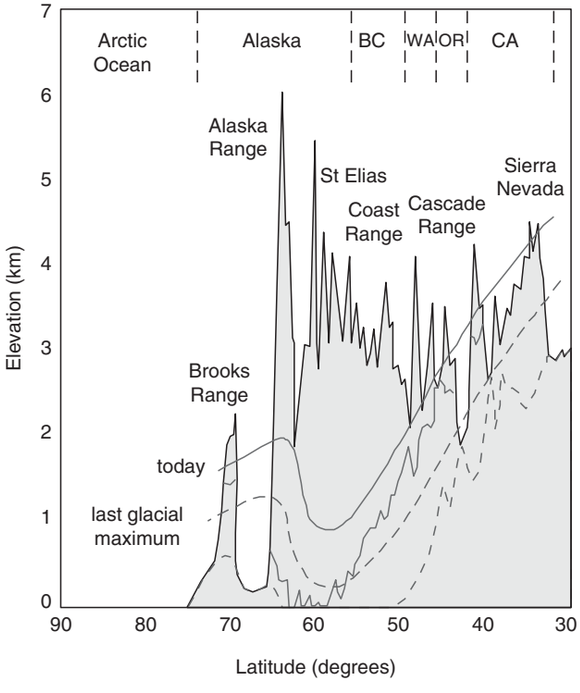


**Figure 8.5** Profiles of topography (gray), equilibrium line elevation (ELA, top) and glacial extent (bottom) (solid, present day; dashed, last glacial maximum (LGM)) along the spine of Western North America from California to the Arctic Ocean. Note the many-hundred meter lowering of the ELA in the LGM, and the corresponding greater extent of the glacial coverage of the topography. (after Skinner *et al*., 1999, with permission from John Wiley & Sons)

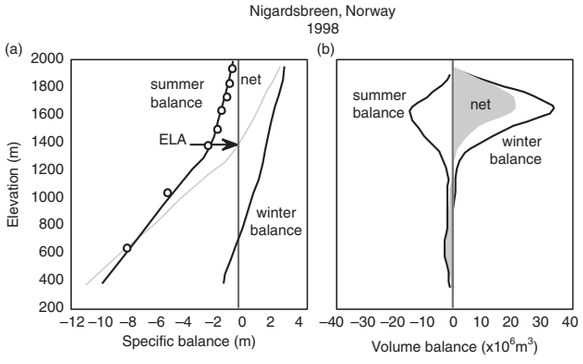


**Figure 8.6** Mass balance profiles for the year 1998 on the Nigardsbreen, a coastal Norwegian glacier. (a) Specific balance in meters of water equivalent. Winter balance from snow probe surveys, summer balance from stake network (circles). Net balance is shown in gray; net balance is zero at 1350 m, which is the ELA. (b) The volume balance derived by the product of the specific balance with the altitudinal distribution or hypsometry of the glacier. That the glacier has so much more area at high elevations is reflected in the high contribution of accumulation to the net balance of the glacier (gray fill). In 1998, the net balance is highly positive; there is more gray area to the right of the 0 balance line than to the left), so that the integral of the gray fill is $> 0$. In this year the positive total balance represents a net increase of roughly 1 m water equivalent over the entire glacier. (after data in Kjøllmoen, 1999)

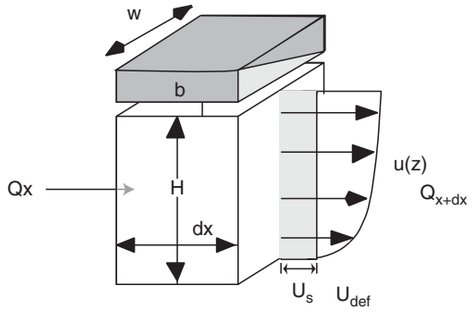


**Figure 8.7** (a) Mass balance for a section of glacier of width *W*, down-glacier length d*x*, and height *H*. Inputs or outputs through the top of the box dictate the local mass balance, *b*. Downglacier discharge of ice into the left-hand side of the box, $Q_x$, and out the right-hand side, $Q_{x+dx}$, include contributions from basal sliding (shading) and internal ice deformation. (after MacGregor *et al*., 2000, Figure 2)

glacier. This is simply the spatial integral of the product of the local mass balance with the hypsometry (area vs. elevation) of the valley:

$$B = \int_0^{z_{\max}} b(z)W(z)\mathrm{d}z \tag{8.2}$$

This exercise is carried out annually on numerous glaciers worldwide. See Figure 8.6 for an example from the Nigardsbreen, Norway. The Norwegians are interested in the health of their glaciers because they control fresh water supplies, but also because a significant portion of their electrical power comes from subglacially tapped hydropower sources.

It is a common misconception that a considerable amount of melting takes place at the base of a glacier, because after all the Earth is hot. Note the scales on the mass balance profiles. In places, many meters can be lost by melting associated with solar radiation. Recall that the heat flux through the Earth's crust is about 41 mW/m$^2$ (defined as one heat flow unit, HFU), a trivial flux when contrasted with the high heat fluxes powered in one or another way by the sun (about 1000 W/m$^2$). The upward heat flux from the Earth is sufficient to melt about 5 cm of ice per year. As far as the mass balance of a glacier is concerned, then, there is little melt at the base.

If nothing else were happening but the local mass gain or loss from the ice surface, a new lens of snow would accumulate, which would be tapered off by melt to a tip at the ELA (or snowline) each year. Each successive wedge would thicken the entire wedge of snow above the snowline, and would increase the slope everywhere. But something else *must* happen, because we find glaciers poking their snouts well below the ELA, below the snowline. How does this happen? Ice is in motion. This is an essential ingredient in the definition of a glacier. Otherwise we are dealing with a snowfield. The $Q$ terms in the mass balance expression reflect the fact that ice can move downhill, powered by its own weight. Ice has two technologies for moving, one by basal sliding, in which the entire glacier moves at a rate dictated by the slip at the bed, the other by internal deformation, like any other fluid (see Figure 8.7). We will return to a more detailed treatment of these processes in a bit. Know for now that the ice discharge per unit width of glacier, $Q$, is the product of the mean velocity of the ice column, $\bar{U}$, and the thickness of the glacier, $H$.

Given only this knowledge, we can construct a model of a glacier in steady state, one in which none of the variables of concern in the mass balance expression are changing with time. Setting the

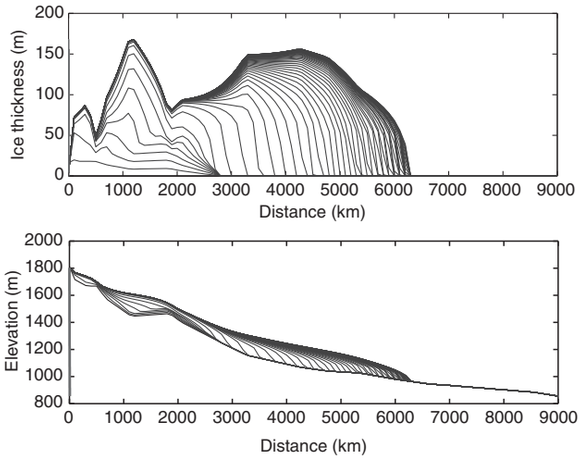


**Figure 8.8** Model of glacier evolution on bedrock profile from Bench Glacier valley, Alaska, shown in evenly spaced time steps out to 600 years. Climate is assumed to be steady, with a prescribed mass balance profile. top: profiles of ice thickness through time. bottom: glacier draped on bedrock profile. The glacier reaches approximately steady state at ~500 years. Measured maximum ice thickness of 180 m is well reproduced by the final model glacier, implying that the mass balance profile $b(x)$ is well chosen.

left-hand side to zero, we see that there must be a balance between the local mass balance of ice dictated by the meteorological forcing (the climate) and the local gradient in the ice discharge:

$$Q(x) = \int_0^x b(x)W(x)\mathrm{d}x \tag{8.3}$$

Here we have taken $x$ to be 0 at the up-valley end of the glacier. If we ignore for the moment the width function $W(x)$, reflecting the geometry (or really the hypsometry) of the valley, the discharge will follow the integral of the mass balance. For small $x$, high up in the valley, since the local mass balance is positive there the ice discharge must increase with distance down-valley; conversely, it must decrease with distance below that associated with the ELA, as the mass balance is negative there. The ice discharge must therefore go through a maximum at the ELA. To illustrate this, we show in Figure 8.8 a simulation of the evolution of a small alpine glacier in its valley, starting with no ice and evolving to steady state. We impose a mass balance profile shown in the figure, and hold it steady from the start of the model run. The simulations shown represent 600 years, and the glacier comes into roughly steady state within 400 years. Similar modeling exercises have been used recently to explore the sensitivity of alpine glaciers to climate changes in the past and in the future (e.g., Oerlemans 1994, 2001, 2005).

This exercise also yields another interesting result. In steady state, we find that within the accumulation area, the ice discharge must be increasing down-valley in order to accommodate the new snow (ultimately ice) arriving on its top. Conversely, the ice discharge must be decreasing with down-valley distance in the ablation region. This has several important glaciological and glacial geological consequences. First, the vertical component of the trajectories of the ice parcels must be downward in the accumulation zone and upward in the ablation zone, as shown in all elementary figures of glaciers, including Figure 8.2. As a corollary, debris embedded in the ice is taken toward the bed in the accumulation zone and away from it in the ablation zone. Glaciers tend to have concave up-valley contours above the ELA, and convex contours below (hence you can approximately locate the ELA on a map of a glacier simply by finding the contour that most directly crosses the glacier without bending either up- or down-valley). Debris therefore moves away from the valley walls in the accumulation zone and toward them in the ablation zone. This is reflected in the fact that lateral moraines begin at roughly the ELA. This observation is useful if one is trying to reconstruct past positions of glaciers in a valley, or more particularly to locate the past position of the ELA. As the ELA is often taken as a proxy for the 0° isotherm, it is a strong measure of climate, and hence a strong target for paleoclimate studies.

This straightforward exercise should serve as a motivation for understanding the mechanics of ice motion. These mechanics are at the core of all such simulations. It is what separates one type of glacier from another. And whether a glacier can slide on its bed or not dictates whether it can erode the bed or not – and hence whether the glacier can be an effective means of modifying the landscape.

## Ice deformation

Like any other fluid on a slope, ice deforms under its own weight. It does so at very slow rates, which are

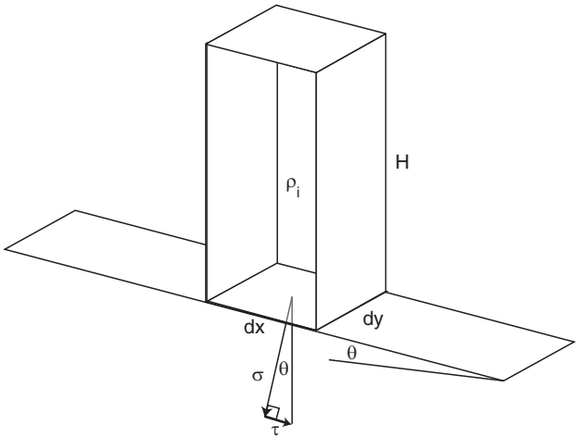


**Figure 8.9** Definition of normal and shear stresses imposed by a column of material (here ice) resting on a sloping plane.

dictated by the high viscosity of the ice. As the viscosity is temperature dependent, increasing greatly as the temperature declines, the colder the glacier is the slower it deforms. Although the real picture is considerably more complicated than that we will describe here (see Hooke, 2005, and Paterson, 1994, for recent detailed treatments), the essence of the physics is as follows. Consider a slab of ice resting on a plane inclined at an angle to the horizontal, as sketched in Figure 8.9. We wish to write a force balance for this chunk of ice. It is acted upon by body forces (fields like gravitational fields and magnetic fields). As ice is not magnetic, the relevant body force is simply that due to gravity. The weight of any element of ice is $mg$ where $m$ is the mass of the slab, or its density times its volume, (d$x$d$y$d$z$). One may decompose the weight vector into one acting parallel to the bed and one acting normal to the bed. As shown in the figure, the normal stress, $\sigma$, (recall that a stress is a force divided by the area of the surface, d$x$d$y$) acting on the slab on its top side is $\rho g(H - z)\cos\,\theta$, and at its base $\rho gH\,\cos\,\theta$.

Now that we have an expression for the stresses within the slab, we introduce its material behavior, or rheology, the relationship describing the reaction of the material to the stresses acting upon it. To anticipate, our goal is to derive an expression for the velocity of the ice as a function of height above the bedrock–ice interface, or the bed of the glacier. The rheology will relate the stresses to the spatial *gradient* of the velocity in the vertical direction. We will then have to integrate this expression to obtain the velocity.

In a simple fluid, Newton demonstrated that there is a linear relation between the shear stress acting on a parcel of the fluid and the shear strain rate of that fluid. These are therefore called "linear" or Newtonian fluids. Although ice is more complicated, we will walk through the derivation using a linear fluid first, and then take the parallel path through the expressions relevant to ice. The problem requires several steps:

5. Development of an expression for the pattern of shear stress within the material.
6. Development of an expression to describe the rheology of the material.
7. Combination of these to obtain an expression relating the rate of strain to the position within the material.
8. Integration of the strain rate to obtain the velocity profile.

## The pattern of stress

At any level within a column of material resting on a slope, the shear stress is the component of the weight of the overlying material that acts parallel to the bed, divided by the cross-sectional area of the column, while the normal stress is that acting normal to the surface. These are illustrated in Figure 8.9. The weight is of course the mass times the acceleration, here that due to gravity, and the mass is the density times the volume. If we take the density to be uniform with depth in the column, this yields the expression for the shear stress as a function of height above the bed, $z$:

$$\tau = \rho_i g(H - z)\sin(\theta) \tag{8.4}$$

Here the quantity $H - z$ represents the height of the overlying column of material, which is exerting the stress on the underlying material. Note that we have not yet identified the nature of the material – i.e., we have not yet specified how the material responds to this stress. This is a general expression for the vertical profile of shear stress within a brick, a column of rock on a slope, or in a fluid such as water, lava, or ice on a slope. As long as the material density is uniform, the stress increases linearly with depth into the material, as plotted in Figure 8.10, reaching a maximum at the bed. Importantly, the shear stress is said to "vanish"

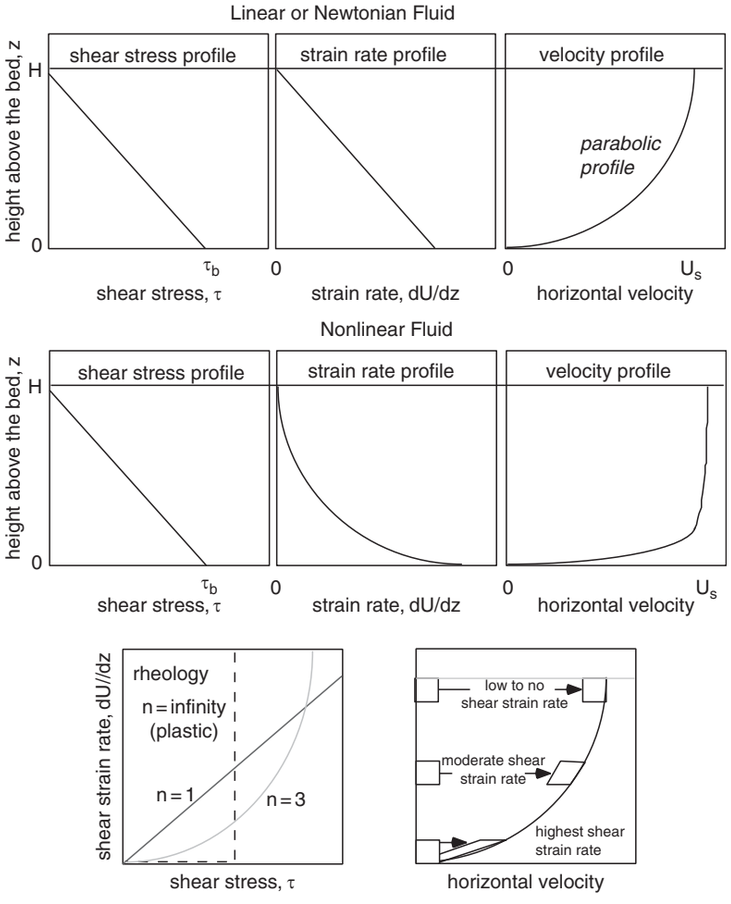


**Figure 8.10** Diagrams to aid in the derivation of the velocity profiles in linear fluids (top row) and in nonlinear fluids (second row). In each row the shear stress profile is the same, linearly increasing from 0 at the top of the fluid to the basal shear stress $\tau_b$ at the base. The middle box shows the shear deformation rate profile, d*U*/d*z*(*z*), and the third box shows its integral, the velocity profile, *U*(*z*). Bottom box shows graphically the shear strain associated with three different levels in the fluid. Shear strain can be measured by the change in angles in a box with originally orthogonal sides.

at the surface; nothing magic here, it is simply zero where $z = H$. The shear stress exerted by the overlying column of air is negligible (until we begin worrying about entrainment of small sand and dust particles in Chapter 14).

## The rheology

Now we must address the response of the material to this applied shear stress. This is called the rheology of the material. In the case of a solid or elastic rheology, there is a finite and specific strain of the material that results from an applied stress. Consider a rubber band. You apply a stress to it, a force per unit area of the rubber. The band stretches a certain amount. The strain of the rubber, $\varepsilon$, is defined as the change in length divided by the original length:

$$\varepsilon = \frac{\Delta L}{L_o} \tag{8.5}$$

where $L_o$ is the original length. This is called the linear strain, the strain of the material along a line. This is associated with the changes of length in the direction of the applied force, here a normal force. Note that strain is dimensionless. In the case of elastic solids, this strain is both finite and reversible: when the force is taken away, the material returns to its original shape. The relationship between the stress and the resulting strain is captured by this simplified rheological statement for an elastic solid:

$$\varepsilon = \frac{1}{E}\sigma \tag{8.6}$$

where $\sigma$ is the applied stress, and $E$ is Young's modulus. The higher the Young's modulus, the more stress it takes to accomplish a given strain. For completeness, we must recognize that in an elastic material the strain in one dimension is connected to the strain in another direction; the rubber band thins as you stretch it. The material constant that relates strain in

one dimension to strain in orthogonal directions is Poisson's ratio, $\nu$.

There is another type of strain, called a shear strain, which results from a shear stress. Rather than changes in length, this is captured as changes in angle. Consider a material on which we have scribed a right angle. Shear strain of the material results in a change to this angle. Again, it is dimensionless (radians). A given stress results in a given strain, here a shear stress and a shear strain:

$$\varepsilon_{xz} = \frac{1+\nu}{E}\tau_{xz} \tag{8.7}$$

For further discussion of strains and stresses in elastic materials, see for example Turcotte and Schubert (2002).

Now let us consider a fluid rather than a solid. They differ fundamentally because an applied stress can result in an infinite strain of the material. Imagine a plate on which you pour some molasses or treacle. Tip the plate; in so doing you exert a shear stress on the molasses. The molasses keeps moving as long as you keep the plate tilted. There is no specific strain associated with an applied stress, and we cannot therefore use an elastic rheology to describe the behavior. However, one could instead relate a specific *rate* of strain to the applied stress. In the case of a shear stress, the resulting shear strain rate is equivalent to the velocity gradient in the direction of shear (see Figure 8.10). In other words, for the case at hand of a fluid on a tipped plate (or bedrock valley floor), the shear stress results in a strain rate that is captured in the vertical gradient of the horizontal velocity with respect to the vertical, $\mathrm{d}U/\mathrm{d}z$:

$$\dot{\varepsilon}_{xz} = \frac{\mathrm{d}U}{\mathrm{d}z} = \frac{1}{\mu}\tau_{xz} \tag{8.8}$$

The parameter $\mu$ that dictates the scale of the response is called the viscosity of the fluid. This is called variously a Newtonian viscous rheology, or a linear viscous rheology. The shear strain rate is related linearly to the shear stress.

Combining this mathematical representation of a linear viscous fluid with that for the shear stress as a function of depth (the stress profile), we obtain an expression for the shear strain rate at all levels within the fluid.

$$\frac{\mathrm{d}U}{\mathrm{d}z} = \frac{\rho_i g \sin(\theta)}{\mu}(H - z) \tag{8.9}$$

This is shown in Figure 8.10. Note that the profile of shear strain rate mimics the shear stress profile in that it is zero at the surface of the fluid, and linearly increases to a maximum at the bed. What does this mean for the velocity profile? At the surface, there can be no shear strain rate. Equivalently, the velocity profile must have no slope to it at the surface. The gradient (slope) of the velocity profile then increases linearly toward the bed.

We obtain the velocity itself by integrating the strain rate with respect to $z$. This is a definite integral, from 0 to some level $z$ in the fluid:

$$U(z) = \frac{\rho_i g \sin(\theta)}{\mu}\left(Hz - \frac{z^2}{2}\right) \tag{8.10}$$

While the contribution due to internal deformation (flow) is indeed zero at the bed, to this must be added any slip along the bed. In most fluids, the "no slip condition" is applied, as molecules within the fluid interact with stationary ones in the bed to bring the velocity smoothly to zero at the bed. Ice, we will see below, is different. First, it can change phase at the bed, and second, it can slide as a block against the bed. Ignoring this for the moment, the resulting profile of velocity is shown in Figure 8.10, where you can see that the features we expected are displayed: there is no gradient at the top of the flow, and the highest gradient in the velocity is found at the bed.

Three other quantities are easily extracted from this analysis: the surface velocity, which we would like to have because we can measure it, the average velocity, and the integral of the velocity, which is equivalent to the ice discharge per unit width of the glacier. The surface velocity is simply $U(H)$, which is

$$U_s = \frac{\rho g H^2 \sin\theta}{2\mu} \tag{8.11}$$

The average velocity can be obtained formally by application of the mean value theorem to the problem:

$$\bar{y} = \frac{1}{b-a}\int_a^b y(x)\mathrm{d}x \tag{8.12}$$

In the case at hand, the variable is the velocity, and the limits are 0 and $H$:

$$\bar{U} = \frac{1}{H-0}\int_0^H U(z)\mathrm{d}z \tag{8.13}$$

We find that the average velocity is

$$\bar{U} = \frac{\rho g H^2 \sin\theta}{3\mu} = \frac{2}{3} U_s \tag{8.14}$$

or two-thirds of the surface velocity. Note on the graph of velocity vs. depth in Figure 8.10 where this mean velocity would be encountered in the profile. It is closer to the bed than to the surface, and is in fact at about six-tenths of the way to the bed from the surface.

The integral of the velocity, or the discharge per unit width of flow, is the product of the mean velocity and the flow depth, and is therefore

$$Q = \bar{U}H = \frac{\rho g H^3 \sin\theta}{3\mu} \tag{8.15}$$

Note the strong (cubic) dependence on the depth of the flow.

## Ice wrinkles 1: Glen's flow law

While the equations derived above illustrate the approach one takes to flow problems in general, they are not appropriate for ice. Ice differs from many fluids in that the relationship between the shear stress and the strain rate (the rheology) is not linear. Instead, the rheology is roughly cubic, as shown in Figure 8.10. Ice is therefore said to have a nonlinear rheology. A more general rheological relation can be written

$$\frac{dU}{dz} = A\tau^n = \left[A\tau^{n-1}\right]\tau \tag{8.16}$$

where $n$ is an exponent that one needs to determine experimentally, and the constant $A$ is called the "flow-law parameter." We have already dealt with the linear ($n = 1$) case. Glen's experiments (Glen, 1952) revealed that $n$ is approximately 3 for ice. The term in brackets represents the inverse of an effective viscosity: $\frac{1}{[A\tau^{n-1}]}$. This expression implies that, as the shear stress increases, the effective viscosity declines, and radically so for all $n > 1$. The consequence is that ice near the bed (under high shear stress) behaves as if it is much less stiff than ice near the surface. We can now again combine this equation for the relationship between the shear strain rate and the shear stress (the rheology) with that for shear stress profile to obtain the profile of shear strain rate:

$$\frac{dU}{dz} = A[\rho_i g \sin(\theta)]^3 (H - z)^3 \tag{8.17}$$

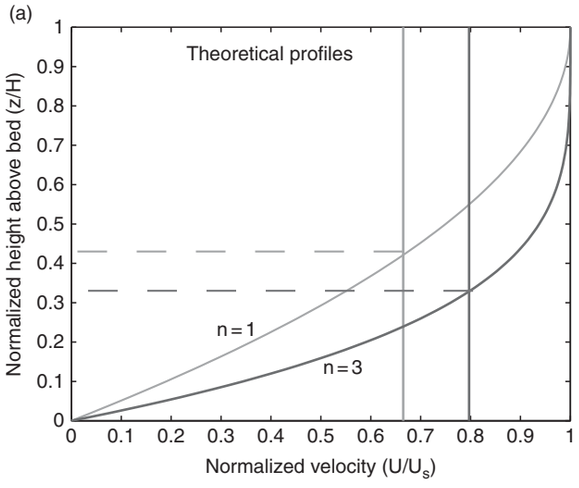


**Figure 8.11(a)** Theoretical flow profiles for $n = 1$ (thin line) and $n = 3$ (bold line) fluids, normalized against maximum height above bed and maximum flow speed. The mean speed is shown as the vertical lines, and the position above the bed at which this mean speed would be measured is signified by the dashed horizontal lines. As the nonlinearity of the rheology increases, the mean speed approaches the surface speed, and the depth at which it would be measured is found nearer the bed.

This may then be integrated to yield the velocity profile:

$$U(z) = A[\rho_i g \sin(\theta)]^3 \left[H^3 z - \frac{3z^2H^2}{2} + z^3 H - \frac{z^4}{4}\right] \tag{8.18}$$

The resulting velocity profile is significantly different from that for the linear rheology case. In Figures 8.10 we show it crudely, and in Figure 8.11(a) more formally. In particular, much more of the change in speed of the ice with distance from the bed is accomplished very near the bed. The flow looks much more "plug-like."

Again, we can obtain the surface speed by evaluation of the velocity at $z = H$:

$$U(H) = U_s = A[\rho_i g \sin(\theta)]^3 \left[\frac{H^4}{4}\right] \tag{8.19}$$

The specific discharge of ice is obtained by integrating the profile from 0 to $H$:

$$Q = A[\rho_i g \sin(\theta)]^3 \left[\frac{H^5}{5}\right] \tag{8.20}$$

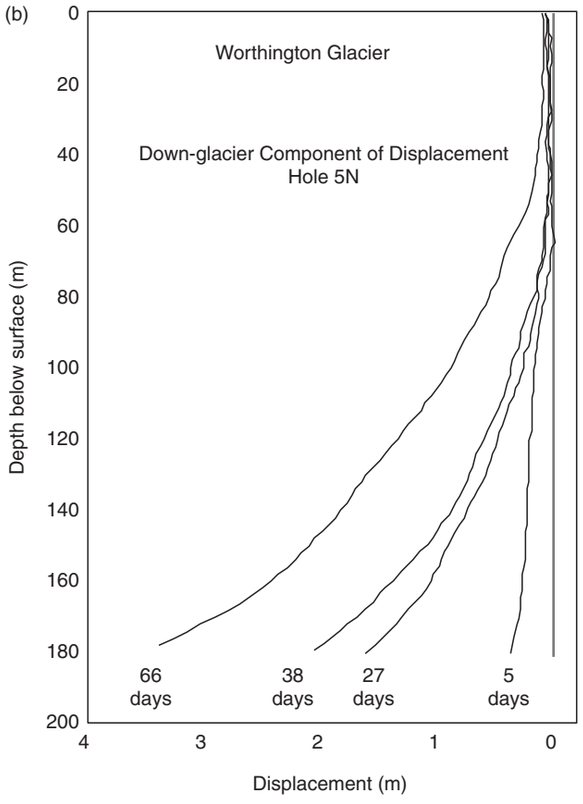


**Figure 8.11(b)** Four measured deformation profiles of an initially straight vertical borehole drilled almost to the bed of the Worthington Glacier, Alaska. Ice depth at this location is roughly 190 m. Measurements made with borehole inclinometer; only the down-glacier component of deformation is shown. Profiles are shown relative to the surface position. (after J. T. Harper, pers. comm. 1996; see Harper *et al*., 1998, Figure 2, with permission from the American Association for the Advancement of Science)

and the average speed is obtained by using the mean value theorem, or by recognizing that the average speed is simply $Q/H$:

$$\bar{U} = A[\rho_i g \sin(\theta)]^3 \left[\frac{H^4}{5}\right] \tag{8.21}$$

This is shown as the dashed line in Figure 8.11(a). Note that this average speed is related to the surface speed through

$$\bar{U} = \frac{4}{5}U_s = \frac{n+1}{n+2}U_s \tag{8.22}$$

As the nonlinearity of the flow law, expressed by $n$, increases, the mean speed approaches the surface speed. The flow profiles for $n = 1$ and $n = 3$ cases are compared in Figure 8.11(a), in which we also show the mean speeds for both cases. That the velocities are normalized to the maximum speed (that at the surface, $U_s$) makes it straightforward to see the how the mean speed relates to the maximum in both cases. As $n$ increases, the maximum speed becomes a better proxy for the mean speed, and the mean speed could occur closer to the bed.

It is also important to realize that the nonlinearity of the flow law results in a very sensitive dependence of the ice discharge on both ice thickness and ice surface slope. The ice discharge, $Q = \bar{U}H$, varies as the fifth power of ice thickness and the third power of the ice surface slope. A doubling of the ice discharge on a given slope can be accomplished by ice that is only $2^{(1/5)}$ or about 3% thicker!

Note that, in the formulations above, we have assumed that the flow-law parameter, $A$, is uniform with depth. While this is a good approximation in temperate glaciers, in which the temperatures are close to the pressure melting point throughout, the assumption breaks down badly in polar glaciers. Both experiments and theory show that the flow-law parameter is sensitive to temperature:

$$A = f(T_k) = A_o e^{-\frac{E_a}{RT_k}} \tag{8.23}$$

where $A_o$ is a reference flow-law parameter, $E_a$ is the activation energy, $R$ is the universal gas constant, and $T_k$ is the absolute temperature. Recommended values for $A_o$ are as follows: at 0°C: $2.1 \times 10^{-16}\,\mathrm{yr^{-1}\ Pa^{-3}}$, at –5°C: $7.5 \times 10^{-17}\,\mathrm{yr^{-1}\,Pa^{-3}}$, at –10°C: $1.5 \times 10^{-17}\,\mathrm{yr^{-1}\ Pa^{-3}}$.

As the temperature decreases, the argument of the exponential factor becomes more negative and $A$ declines. Since the effective viscosity varies as $1/A$, the viscosity therefore increases. (For discussion see Turcotte and Schubert, 2002, chapter 7.) Using the values for activation energy for ice ($61 \times 10^3$ J/mole) and the universal gas constant (8.31 J/mole-K), the flow-law parameter and hence the effective viscosity (both shown in Figure 8.13) are expected to vary over four orders of magnitude in the temperature range relevant to Earth's glaciers and ice sheets. Let's think about the implications of this for the shape of the velocity profile. As temperature decreases with height above the bed, $z$, the flow-law parameter will decrease rapidly. The ice effectively

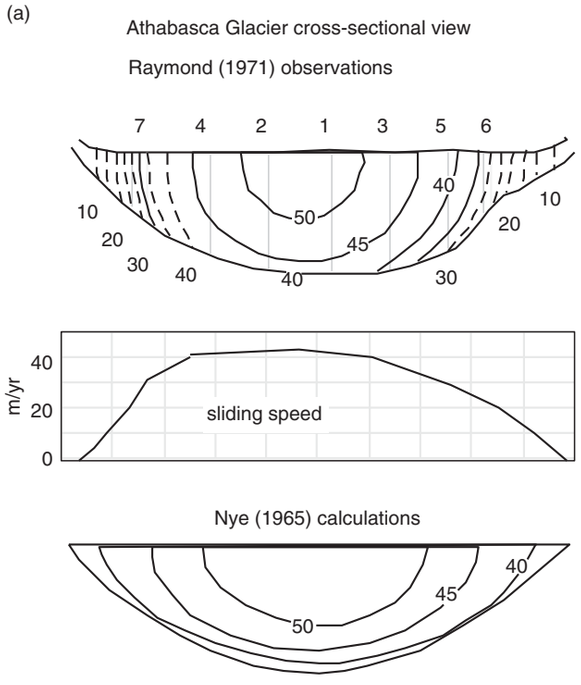


**Figure 8.12(a)** Top: distribution of down-valley ice speeds in cross section of the Athabasca Glacier, Canada, as interpolated from measurements in seven boreholes (labeled gray lines), from Raymond (1971). Center: cross-valley distribution of sliding speed as deduced by the intersection of the velocity contours with the bed in top panel. Note strong broad peak in the sliding speed in the center of the glacier. Bottom: flow field as predicted Nye (1965) theory for flow in a parabolic channel, to which a uniform sliding speed has been added. (after Paterson, 1994, Figure 11.11, reproduced with permission from Elsevier)

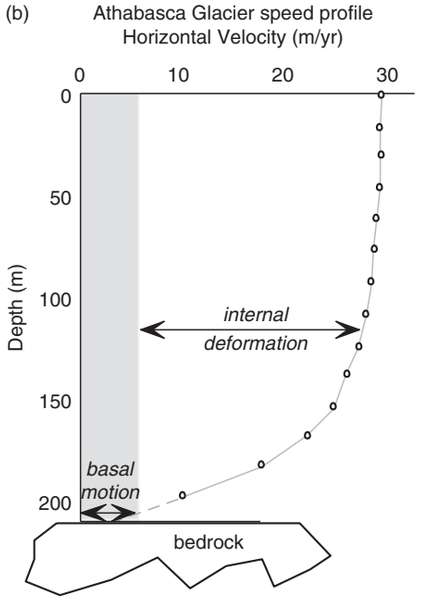


**Figure 8.12(b)** Velocity profile of the Athabasca Glacier, Canada, derived from inclinometry of a borehole and measurement of surface displacement of the borehole top. Projection to the base yields estimate of the contribution from motion of the ice relative to the rock, or basal motion (gray box). (data from Savage and Paterson (1963))

stiffens with height above the bed. This reduces the rate of strain, or the velocity gradient, and the flow profile should look even more plug-like than in the uniform temperature case. This extreme sensitivity of the rheology to temperature requires that the modeling of ice sheets incorporate the evolution of the temperature field. Such models are said to require thermo-mechanical coupling.

While experiments on small blocks of ice inspired the exploration of the nonlinear rheology of ice, it is field measurements of entire glacial profiles that have been used to test the theory. This information comes largely from the deformation of boreholes in glaciers. Boreholes are initially drilled straight downward using hot tips, and later steam drills. Using an inclinometer, the dip of the hole is measured at each of many depths, from which the profile may be constructed. The location of the top of the hole may also be tracked using either GPS or optical surveying, so that we know its speed. The deformation speeds may then be deduced as a function of depth, to be contrasted with theory, as shown in Figure 8.11(b) and in Figure 8.12(b) (see Harper *et al.*, 1998, 2001). Note that the difference in motion between the bottom and top of the hole may now be calculated. Knowing the speed of the top and the difference in the speed of the top and bottom of the hole, one can subtract the two to determine any motion of the base of the hole that is unaccounted for. This leftover motion we call "basal motion." This consists of motion of the ice relative to the rock, and can be either direct sliding of the ice over rock, or deformation of an intervening layer of water-saturated sediments (basal till).

## Ice wrinkles 2: sliding/regelation

While the physics of internal deformation are interesting and can accomplish the translation of large masses

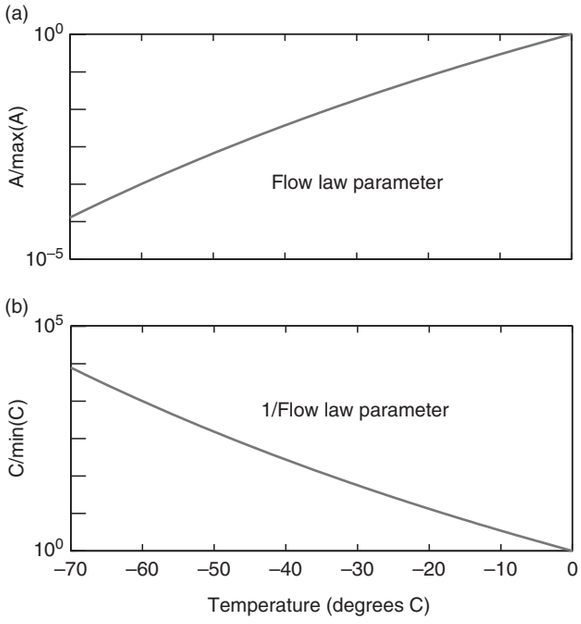


**Figure 8.13** Dependence of flow-law parameter on temperature. (a) Flow law parameter, *A*, and (b) inverse of flow-law parameter, which scales the effective viscosity. Vertical axes are normalized to their values at the pressure melting point. Noting the logarithmic vertical axis, the effective viscosity will rise by four orders of magnitude over the 70°C range depicted.

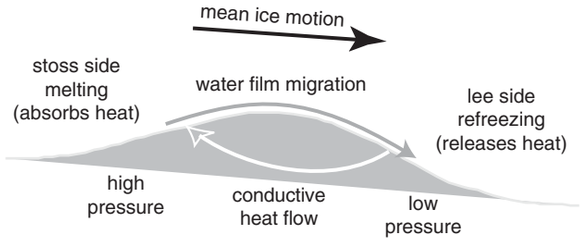


**Figure 8.14** Schematic diagram of the regelation process by which temperate glaciers move around small bumps on the glacier bed. Ice melts on the high-pressure (stoss) side of the bump, moves around it as a thin water film, and refreezes in the low-pressure shadow on the lee side. The heat released by refreezing is conducted back through the bump to be used in the melting process. This is therefore an excellent case of coupling between thermal and fluid mechanics problems.

of ice down valleys, some large segment of the glacier population has yet another process to allow transport of ice down valleys. If the ice near the bed of the glacier is near the melting point, the ice can slide across the bed. As it is only by this mechanism that the bed of the glacier can be modified by the motion of ice above it, it is sliding that is the focus of glacial geologic studies.

Sliding of the ice is permitted by a special property of water: high pressure promotes melting. A corollary to this is that the high pressure phase of water is ice, its solid phase. This makes ice very different from, say, quartz or olivine, whose melted liquid state is lighter than their solid, and for which higher pressure therefore promotes the change of phase from the solid to the liquid. This can be seen in the phase diagram for the water system we first introduced in Figure 1.2. The negative slope (of –0.0074°C/bar, or $7.4 \times 10^{-8}$°C/Pa) on the P–T plot, separating the water and ice phases, is what differentiates water from most other substances.

Consider the conditions at the bed of a temperate glacier, which by definition is at its freezing point throughout (meaning at all points the temperature lies along the phase boundary, declining at 0.0074°C/11 m of depth). The glacier rests on a sloping valley floor that is not perfectly smooth, but has bumps and swales in it depicted in Figure 8.14. We probably would all agree that the ice is not accelerating (changing its velocity) very much. If it is doing so, it is doing so very slowly, meaning that the accelerations are very slight. This means, through Newton's law $F = ma$, that the forces on the ice are essentially balanced. There is also heat arriving at the base of the glacier from beneath the glacier, at a rate sufficient to melt about 5 cm of ice per year. This is not much melt, but given that the ice is already at the pressure melting point, there ought to be a thin layer of water present at the bed. You might think this would make it pretty slippery. For a slab of ice d$x$ long in the down-valley direction, the force promoting down-valley motion is the down-valley component of the weight of the ice, or $dx\rho g H\sin(\theta)$. What is resisting this, especially if there is a thin layer of water there, which is very weak in shear? Given that the shear resistance is therefore nearly zero, the forces resisting the down-valley motion of the ice are those associated with pressure variations associated with the bumps in the bed. In order to prevent acceleration of the ice, there must be a net component of the normal stress that is directly up-glacier. There must therefore be higher pressures on the up-valley sides of bumps than on the down-valley sides of bumps. Of course in the direction normal to the mean bed, the

pressure must be that exerted by the normal component of the ice weight, or $\mathrm{d}x\rho g\, H\cos(\theta)$.

But if the pressure fluctuates about some mean, say that of the pressure melting point of ice, then increasing the pressure a little bit on the up-valley side of a bump will promote melting of the ice, and decreasing it a little bit on the back of the bump will promote freezing of water. Given the phase diagram of the $H_2O$ system, this must happen. In fact, the water film so generated on the up-valley side of the bumps is forced into motion for the very same reason: liquid water responds to pressure gradients by flowing from high pressures toward low pressures. Putting the two patterns together, we find that that a parcel of basal ice performs something of a magic act to get past bumps in the bed. The ice melts on the up-valley sides of bumps, flows around the bump as a thin water film, and refreezes on the low-pressure down-valley sides of the bump. This process is called regelation, which is French for "refreezing."

Regelation is most effective in moving ice past small-scale bumps in the bed. Melting of water consumes energy, and refreezing of water releases energy, the same amount per unit volume of ice. That's nice – as no net energy must be added to the system. The problem is that the site where energy is needed to melt ice is different from where it is released upon refreezing. They are separated by the length of the bump. This heat energy must be transported through the bump or through the ice above it by conduction as shown in Figure 8.14. Heat conduction is dictated by the temperature gradient: the temperature difference between the two sites, divided by the distance between them. Therefore, the closer the sites, or the smaller the wavelength the bump, the more efficient the process.

It turns out that very large bumps can be circumvented by another process that makes them easy to get around as well. The situation is diagramed in Figure 8.15. For long wavelength bumps, only a small-scale perturbation of the flow field in the ice itself is required to move past the bump, meaning that the ice does not have to regelate to get by the bump. This leaves intermediate sized bumps, with wavelengths of around 0.5 to 1 m, as the hardest bumps for the basal ice to move past. These have been called the "controlling wavelengths" for the basal sliding process. We will see that these details of the sliding process are strongly reflected in the patterns of erosion at the bed of a temperate glacier.

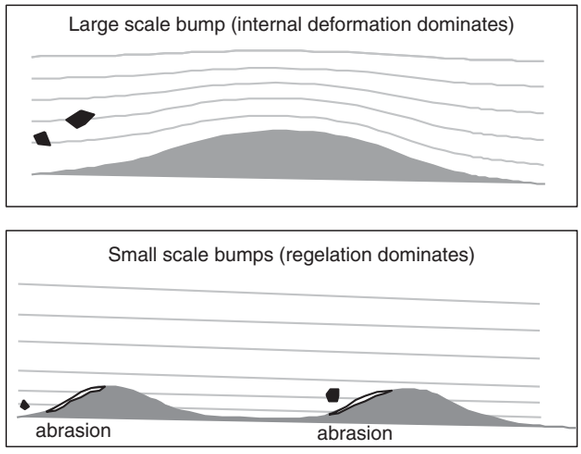


**Figure 8.15** Trajectories of clasts embedded in basal ice as it encounters big (top) and little (bottom) bumps in the bed. Ice can deform sufficiently to accommodate the larger bumps, allowing clasts in the ice to ride over the bumps. In the small-bump case, the ice trajectories intersect the bed, reflecting the regelation mechanism. Clasts in the ice will be brought forcefully into contact with the bed, and cause abrasion of the front (stoss) sides of these bumps, leading to their elimination.

Direct evidence for the existence of this thin film of subglacial water, and the operation of the regelation mechanism, comes from several sources. One of the more striking is to be found on limestone bedrock, where the susceptibility of calcite to solution allows the subglacial water system to be read in great detail (Hallet, 1976). One sees on the upslope sides of small bumps little dissolution pits, and on the down-glacier sides precipitates. In fact, the precipitates take the form of small stalactites that grow almost horizontally, anchored to the downslope sides of the bumps. These interesting forms are easily visible in the photographs of Figure 8.16. This pattern of solution and re-precipitation is argued to represent the solution of calcite by the very pure water film, and its expulsion from solution as the water refreezes on the downslope side of the bump. The film is thought to be only microns thick. The ice produced by the regelation process is distinct in at least two senses from that produced originally from snow. It has a strong isotopic signature associated with fractionation that occurs upon both melting and refreezing. And it is largely bubble-free. Typical glacial ice is bubbly from air originally trapped in the ice as it metamorphoses from firn to ice. The bubbles give rise to the white

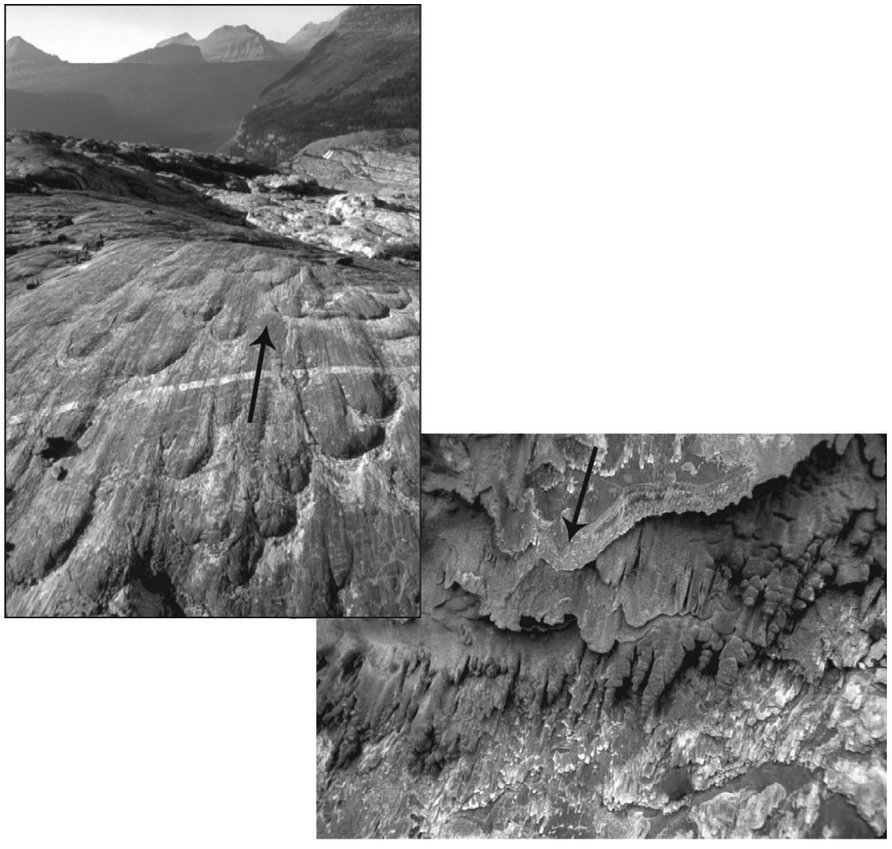

**Figure 8.16** Details of the recently deglaciated bed of Blackfoot Glacier, Montana. Top: view downglacier. Bumps in the bed localized by argillitic partings in the limestone bedrock show dissolutional roughening on the stoss (up-valley) sides, and re-precipitation of calcite (white) in the lee. (see Hallet, 1976) Bottom: detail of the subglacially precipitated calcite, glacier flow top to bottom. (photographs by R. S. Anderson)

color of the ice. In the regelation process, the air in the bubbles is allowed to escape upon melting on the stoss sides of bumps, and is not incorporated into the regelation ice in the lee of the bumps. Thus basal ice can take on a beautifully complex blue and white streaked look, clear blue in the regelation ice and white due to bubbles in the original ice.

Concurrent measurement of glacier sliding and of local basal water pressure has led to the hypothesis that sliding is promoted by high water pressures. This is captured in the expression

$$U_{\text{slide}} = c\frac{\tau_{\text{b}}^{p}}{\{P_{\text{i}} - P_{\text{w}}\}^{q}} \tag{8.24}$$

where $c$ is a constant that serves to scale the sliding speed and whose dimensions depends upon $p$ and $q$, and $p$ and $q$ determine the sensitivity of the sliding to $\tau_{\text{b}}$, and to $P_i - P_{\text{w}}$, respectively. The expression in the denominator, the difference between the normal stress exerted by the ice overburden ($\rho_{\text{i}}gH$) and the local water pressure, $P_{\text{w}}$, is called the effective stress. As the water pressure approaches that of the ice overburden, the effective stress goes to zero and sliding ought to become very rapid (infinite, if we take it to the limit of zero effective pressure). This state we also call the flotation condition: the full pressure of the column of ice overhead is being supported by the water pressure. Given the density difference between water and ice, this would correspond to a water table in the glacier at a height of $\rho_{\text{i}}/\rho_{\text{w}}$, or roughly nine-tenths of the ice thickness. Note as well that within this expression it is the water pressure at the bed that can change rapidly, while both the normal and shear stresses associated with the ice column cannot. This suggests that a way to document sliding or basal motion of a glacier is by measuring the temporal variations in the speed of a monument on the surface of the glacier.

The details of the relation between water pressure and sliding rate are the target of modern glacial research. Water pressures are very difficult to measure in the field, as they require drilling holes in the glacier

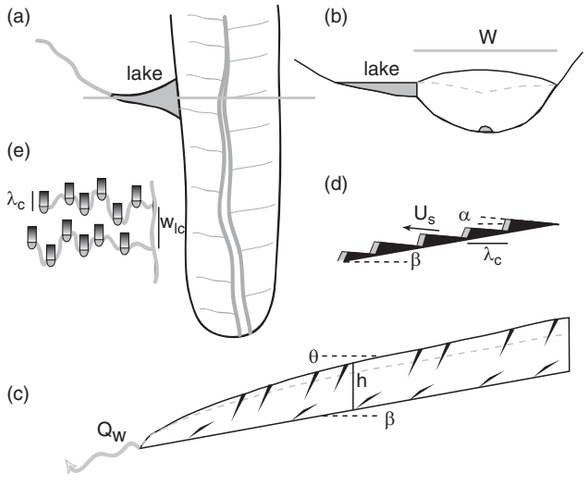


**Figure 8.17** Sketch of the hydrological system in a glacier. (a) Map view showing subglacial tunnel system and tributaries to it that, in turn, connect sets of cavities in the lee of bumps (shown in plan view in E and in cross section in D). (b) Cross-valley profile through the glacier at the location of a side-glacier lake ponded by the ice, showing subglacial tunnel and a hypothetical water table (dashed). (c) Long-valley cross section of the glacier showing crevasses and the water table, with water discharging in the exit stream. (after Kessler and Anderson, 2004, Figure 1, with permission from the American Geophysical Union)

that connect to the water system at the bed. When this is done, the pressures vary considerably both in time and in space. We do not know at present how best to average these pressures, nor the length scale over which such a measurement must be made in order to be relevant to sliding. The bottom line, however, is that the glacial hydrologic system evolves anew every year (see review in Fountain and Walder, 1998). This system is complex, and consists of several interacting elements shown schematically in Figure 8.17. Water is generated at the glacier surface by melt. This percolates into the snow and/or runs off on the ice surface to find a conduit that takes it into the subsurface. This often consists of a moulin (a vertical hollow shaft) or the base of a crevasse. At the bed, the hydrologic system consists of three elements: a thin film of water at the ice-bedrock interface we have already talked about, a set of cavities in the lee of bumps in the bed, and conduits or tunnels. These two larger-scale elements close down significantly in the winter when the melt water input is turned off: most of the water drains out of the system, leaving cavities and tunnels as voids that collapse by viscous closure of the ice. These structures, the pipes and little distributed reservoirs of the subglacial system, must therefore be born anew each melt season. This is what makes the glacial hydrologic system so interesting, and it is intimately related to the seasonal cycle of sliding that is now well documented. As the melt season begins, water that makes its way toward the bed does not have an efficient set of conduits through which to drain. It therefore backs up in the glacier, raising the water table and therefore pressurizing the subglacial system as the column of water piles up. This allows sliding to begin, which in turn opens up cavities in the lees of bumps. Nearer the terminus, a tunnel system begins to grow, forced open by high rates of melt as water flows through the tunnel under a high water pressure gradient toward the terminus. As water flows through this nascent system, it widens due to frictional dissipation of heat, out-competing the tendency of the ice to move toward the conduit. The lower pressure conduit is therefore inserted into the glacier from the terminus upglacier. As it reaches a particular location, it serves as a low-pressure boundary condition for the adjacent cavities, and can serve to bleed the water out of cavities, which in turns lowers the water pressure in the local glacier. As the conduit system elongates, it therefore bleeds off the pressures that were sustaining the sliding of the glacier, and terminates the sliding event. In the meanwhile, the conduit system grows until it can accommodate the rate of water input from the glacier surface. This basic explanation of "spring sliding events" has been modeled as well, and shows the up-glacier evolution of the system (see Kessler and Anderson, 2004).

Documentation of such dynamics requires high-frequency measurements of glacier position. This was accomplished first with computer-controlled laser distance ranging systems that automatically ranged to targets on the ice, for example at Storglacieren, Sweden. Recent work on small to medium alpine glaciers has begun to utilize GPS measurements to document the detailed surface motion history of a glacier through a melt season. One example from the Bench Glacier in Alaska (e.g., R. Anderson *et al*., 2004c; MacGregor *et al*., 2005) is shown in Figure 8.18. While the uplift of glaciers during these speedup events has lead to models of enhanced sliding over upglacier tilted blocks in the bed for some time (e.g., Iken and Truffer (1997)), these new measurements in concert with records of stream discharge

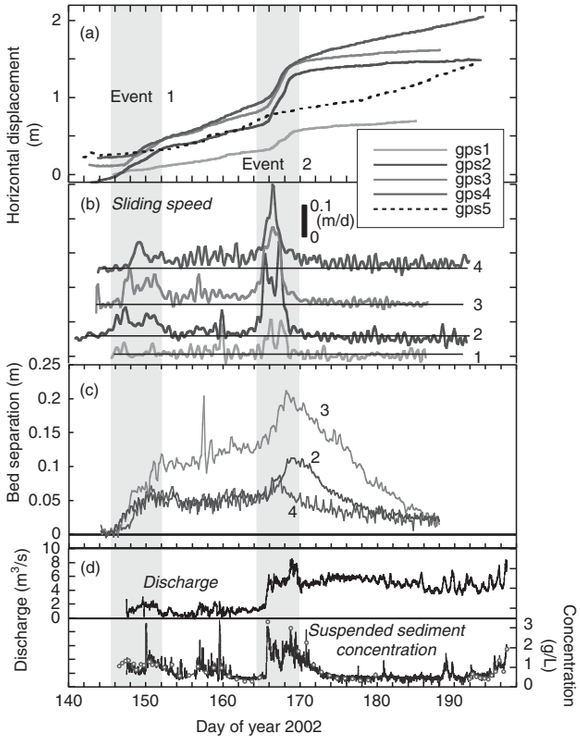


**Figure 8.18** The record of surface motion of five GPS monuments on the surface of 100–180 m-thick Bench Glacier, Alaska (a), their speeds (b), the uplift of the surface not attributable to surface-parallel motion (c), and both the discharge and the suspended sediment concentration of the exit stream (d). Acceleration associated with increases in sliding occurred in two events separated by two weeks of roughly steady sliding. The termination of the second event coincides with a major increase in stream discharge, interpreted to reflect completion of the subglacial conduit that bleeds high pressures from the glacier bed. Uplift of the surface reflects block sliding up stoss slopes of bumps in the bed, and collapse of the resulting cavities after termination of sliding. (after S. P. Anderson *et al*., 2004c, Figure 7, with permission from the American Geophysical Union)

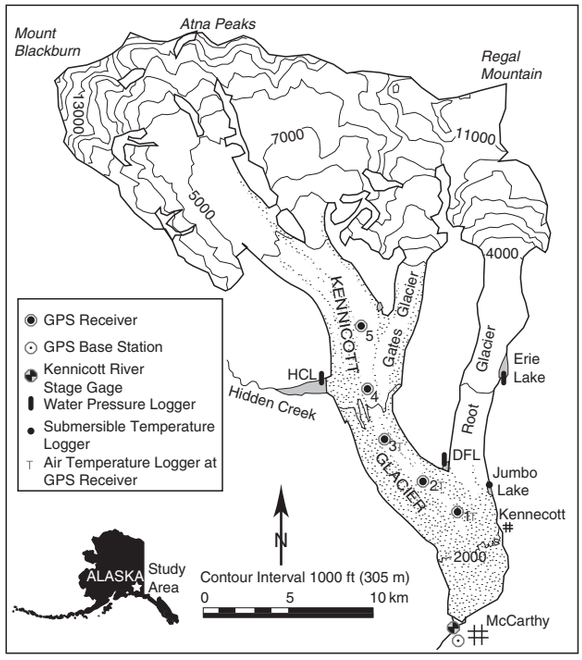


**Figure 8.19** Map of Kennicott Glacier, Alaska, with instrumentation deployed in summer 2006. Outburst floods from Hidden Creek Lake (HCL) serve as a probe of the relationship between the hydrologic system of the glacier and its sliding. History of displacements of GPS monuments on the glacier surface allow the separation of steady flow and non-steady basal motion. Pressure gages at HCL and at Donoho Falls lake (DFL), and river gaging at the exit river in McCarthy provide constraints on how the hydrologic system behaves. (after Bartholomaus *et al*., 2007, Figure 1, with permission from Nature Publishing Group)

have generated a coherent model of alpine glacier sliding mechanics. The picture of basal motion that has emerged from study of the Kennicott glacier in Alaska, shown in the map of Figure 8.19, is one in which the glacier slides whenever the water inputs to the glacier exceed the capacity of the plumbing system of the glacier to pass that water (Bartholomaus *et al*., 2007). This is shown in the melt-season record in Figure 8.20, and is broken out into several timescales in Figure 8.21. The water therefore accumulates in the glacier, which must result in pressurization of the basal water system. The Kennicott Glacier serves as particularly good natural experiment in that a side-glacier lake called Hidden Creek Lake visible in Figure 8.19 outbursts each year, and has done so for at least the last century. This slug of water passes through subglacial tunnel to the terminus, generating a flood that for decades washed out the railroad bridge across which copper ore from the Kennicott mines was taken to market. Passage of this water through the tunnel greatly perturbs the subglacial water system, promoting a sliding event documented in both Figures 8.20 and 8.21 that exceeds background speeds by a factor of six. The detailed trajectory of the GPS monument on the ice surface also holds clues for what must be happening at the base of the glacier. In both the Bench Glacier and the Kennicott Glaciers, rapid sliding coincides with departure of the trajectory of

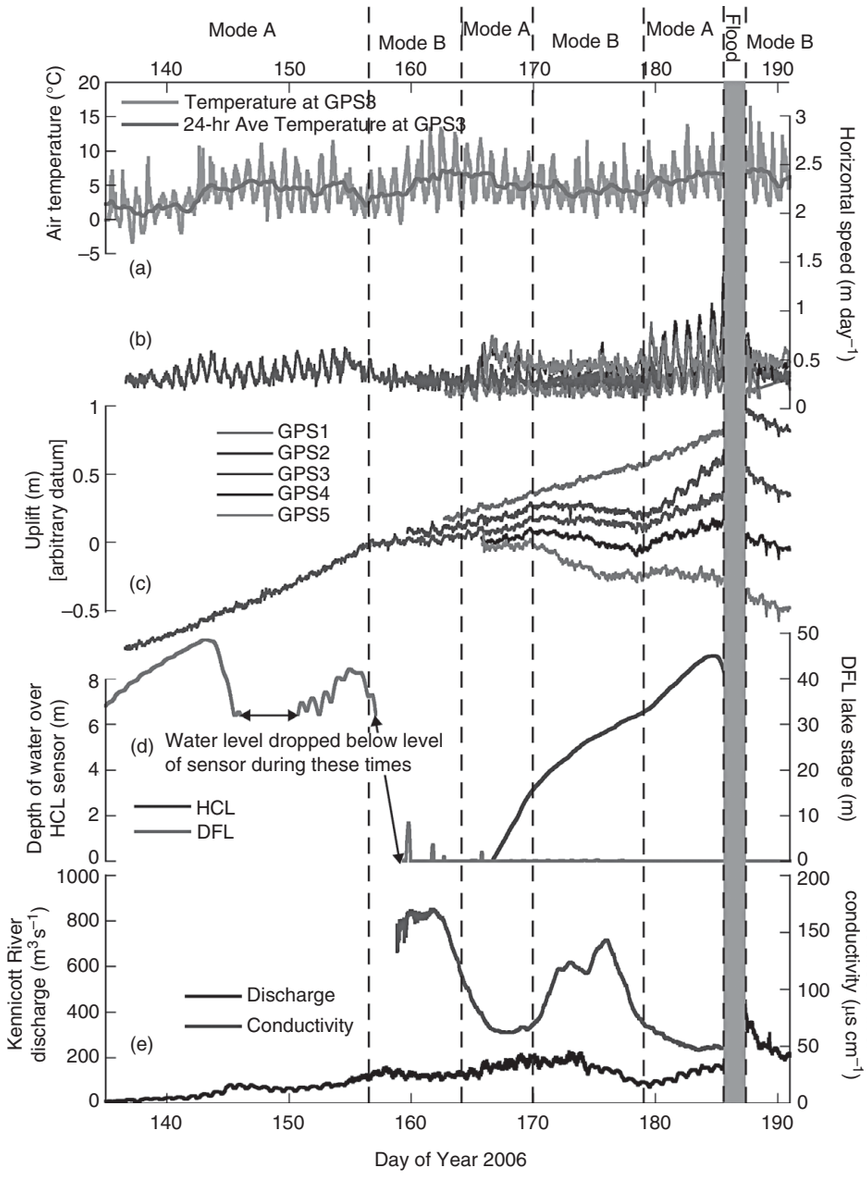


**Figure 8.20** Melt season 2006 record of glacier motion and associated meteorological and hydrological histories. Vertical dashed lines identify two distinct glacier modes, A and B. Period of HCL outburst flood is shaded light blue. (a) Half-hour and 24-hr averaged air temperatures at GPS3. (b) 4-hr averaged horizontal ice speeds at each GPS receiver. (c) Uplift (vertical motion minus the surface-parallel trajectory) at each GPS receiver. (d) Lake level record at Hidden Creek Lake (HCL) and Donoho Falls Lake (DFL). DFL stage is relative to the lake basin floor, while HCL record captures the uppermost 9 m (of ~100 m) of lake filling and draining. (e) Kennicott River discharge and electrical conductivity. (after Bartholomaus *et al.*, 2007, Figure 2, with permission from Nature Publishing Group)

the ice surface from bed-parallel: during rapid sliding the ice appears to rise above this trajectory, while during slow-down of the ice after such events the ice surface appears to subside, eventually returning to bed-parallel motion. This should not be viewed as the insertion of a slab of water at the bed, but instead as sliding of the glacier up stoss sides of bumps in the bed. In the aftermath of the rapid sliding, the drop in water pressure that promoted the slow-down also allows the cavities in the lees of the bumps to collapse, which in turn causes the subsidence of the ice surface. Interestingly, by contrasting Figures 8.18 and 8.20, the collapse appears to be roughly eightfold faster (about 1 day) beneath the thick (400 m) ice of the Kennicott than beneath the thin (180 m) ice of the Bench Glacier (about 1 week). We argue that this difference is what one would expect from the difference in the stresses causing collapse: the nonlinear flow law of ice should

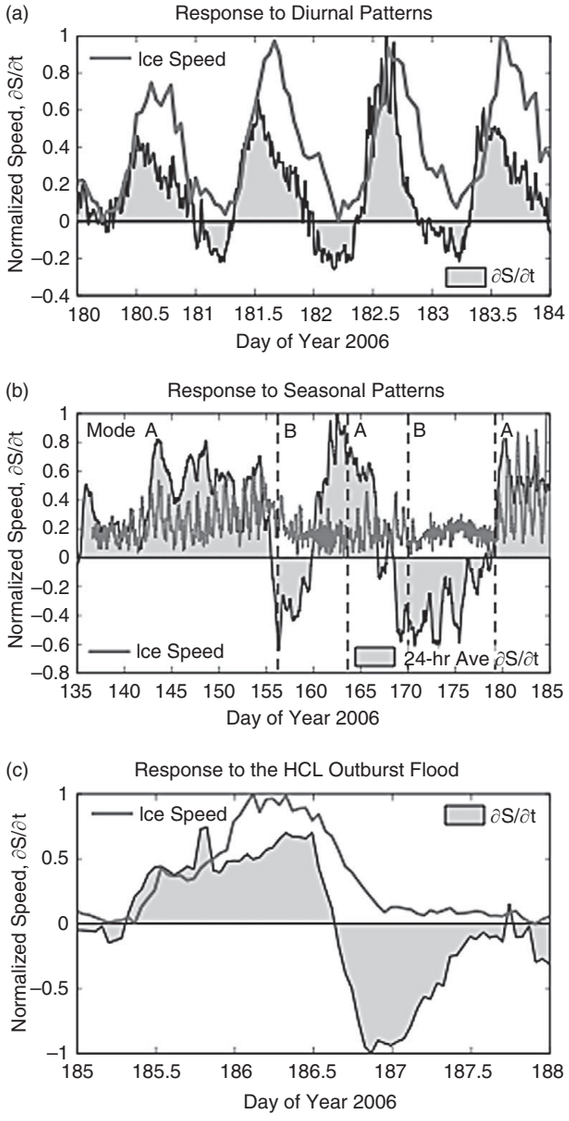


**Figure 8.21** Relations between sliding and water budget of the Kennicott Glacier on three timescales: (a) diurnal, (b) seasonal, (c) the outburst flood from Hidden Creek Lake. In all cases, the motion of the glacier associated with basal motion (normalized by its maximum value in the period depicted) occurs whenever more water is being supplied to the glacier than its plumbing system can accommodate. This occurs when the rate of change of storage within the glacier, d*S*/d*t*, is positive (also depicted as normalized within the specified period). (after Bartholomaus *et al*., 2007, Figure 3, with permission from Nature Publishing Group)

allow collapse of voids to be $2^n$ faster for stresses that are twofold higher. If $n = 3$, as in Glen's flow law, this should result in an eightfold difference in the rate of collapse.

### Basal motion by till deformation

In some and perhaps many glaciers, the glacial ice is separated form the bedrock floor of the valley by a layer of till. In these cases, the basal motion is accomplished not by sliding of the glacier over bedrock bumps, but by deformation of water-saturated till. Till is glacially produced sediment with a wide distribution of grain sizes. The rate of deformation of this granular mixture is dictated by whether the water in the till is frozen or not, and by the pressures of the water if it is liquid. In Black Rapids Glacier in Alaska, which occupies a strike valley localized by the Denali Fault, concurrent observations of ice motion, and of till deformation at the bed using measurements in a borehole, reveal seasonal variations in deformation rate. These too are no doubt associated with the water pressures at the base of the glacier.

Boreholes through the great ice streams that drain the Antarctic Ice Sheet toward the Ross Sea (check this) reveal that they ride on layers of till. These streams has been shown to turn on and off at century timescales in an ice stream cycle. When the ice is thick and slow the thermal structure through the ice is such that the temperatures in the till can reach the freezing temperature, allowing it to deform. Given the high stresses at those times, the till deforms rapidly which in turn drains ice from the path of the stream, thinning it. The thinning brings the very cold surface temperatures closer to the bed, allowing heat to be lost more rapidly, which in turn eventually freezes the water in the till. Once the speed slows, the ice stream re-loads, thickening over the next centuries until the cycle is repeated.

## Applications of glaciology

### Glacier simulations

Simulations of alpine glaciers are now being performed in two plan view dimensions (e.g., Kessler *et al*., 2006, on Kings canyon; Plummer and Phillips, 2003, on Bishop Creek glaciers, California). This allows modeling of glaciers on real-world topographies represented by DEMs, on which one may explore the proper characterization of the climate required to generate glaciers that extend to LGM positions documented by end-moraines, the effects of

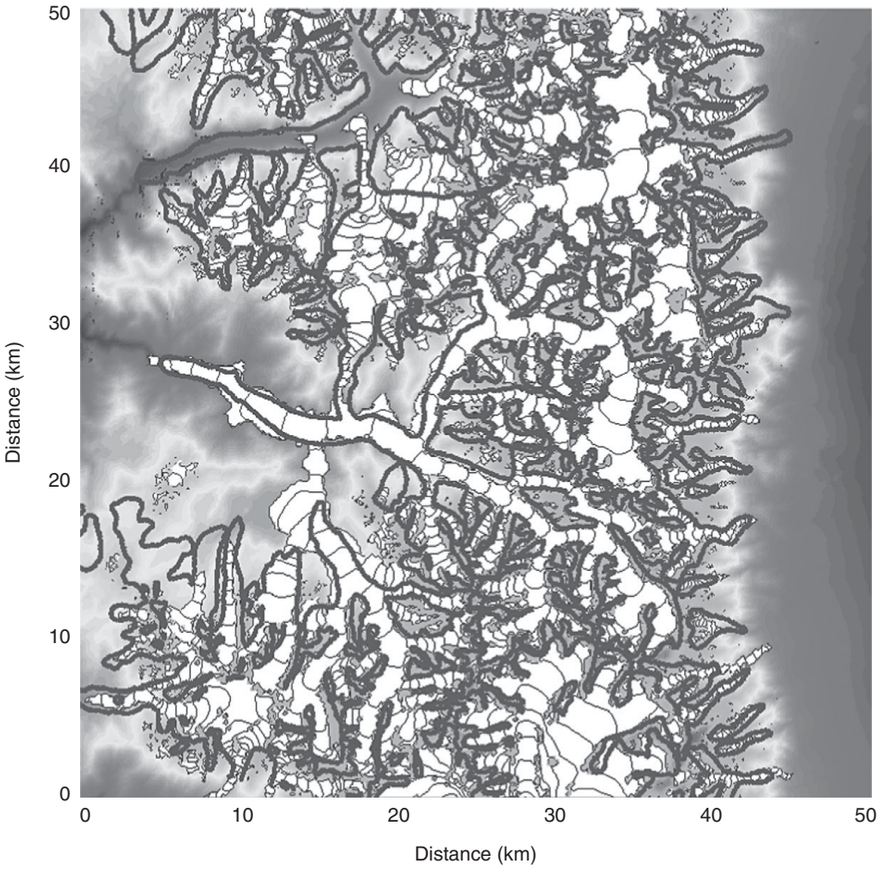


**Figure 8.22** Steady-state glacier extents for experiment 4 from Kessler et al. (2006), in which the mass balance was determined using an orographic model and a positive degree day melt model. Blue line indicates mapped LGM glacial extents extracted from Moore (2000) for this 50 × 50 km area of the southern Sierras centered on Kings Canyon. (after Kessler *et al*., 2006, Figure 13, with permission from the American Geophysical Union)

radiation input to the glacier surface, and so on. One stringent test of such a coupled model of climate and glacier response is in the southern Sierras, where the tilted mountain block results in a strong difference in the precipitation across the range. The mapped moraines reveal a strong asymmetry in glacier length, with much longer glaciers on the western windward side of the range than on the steep, faulted eastern range front. The two-dimensional glacier simulation shown in Figure 8.22 can only reproduce this LGM moraine pattern only if a strong gradient in precipitation is employed. The resulting difference in the estimated ELA, plotted in Figure 8.23, is about 150 m lower on the west (windward) side of the range than on the east.

## Paleo-climate estimates from glacial valleys

Now that we know something about how glaciers work, let us use this knowledge to address questions raised by past glaciers. One of the goals of glacial geology is to estimate the past footprints of glaciers, and from them determine the past climate needed to produce glaciers of that size. It is often assumed that the mean annual 0°C isotherm roughly coincides with the ELA. Above it, temperatures are too cold to melt all the snow that arrives, and vice versa below it. If one assumes that the temperature structure of the atmosphere obeys a lapse rate of say 6.5°C/km or 0.0065°C/m, then the depression of the ELA in meters can be translated into a cooling of the climate in °C. But how do we find the paleo-ELA? We use two methods illustrated in Figure 8.24. First, we note that the up-valley ends of lateral moraines correspond roughly to the ELA. If these can be located in a particular valley, then one can estimate the paleo-ELA from the up-valley elevation of their ends. We will discuss these moraines further at the end of the chapter. The second method utilizes an empirical relationship of the map view of

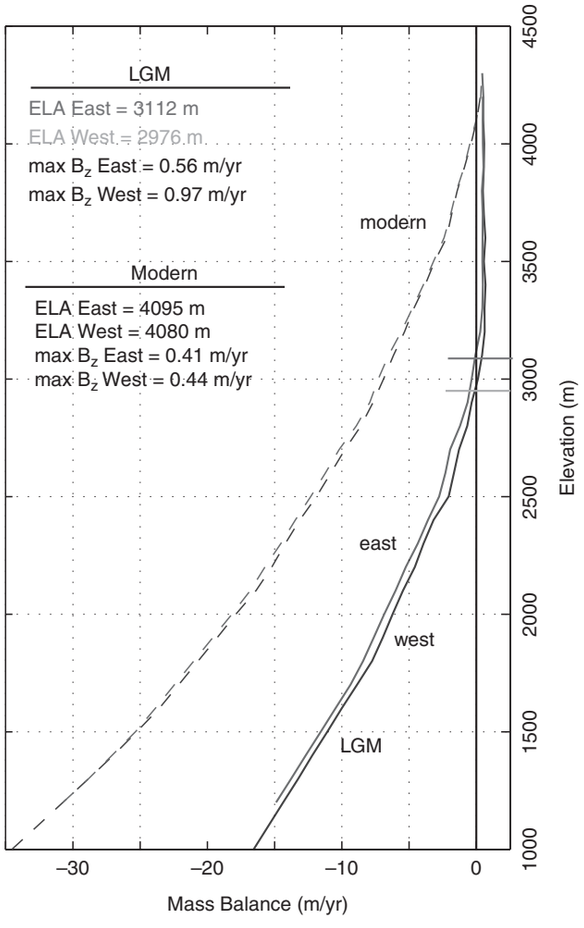


**Figure 8.23** Average net mass balance profiles for modern and LGM (–7°C) climates (dashed and solid lines, respectively). Profiles are derived from an orographic precipitation model and a positive degree day melt model. Red and blue lines indicate mass balance on the eastern and western flanks, respectively. Note 140 m offset of ELAs at LGM time required to match the moraines (after Kessler *et al.*, 2006, Figure 12, with permission from the American Geophysical Union)

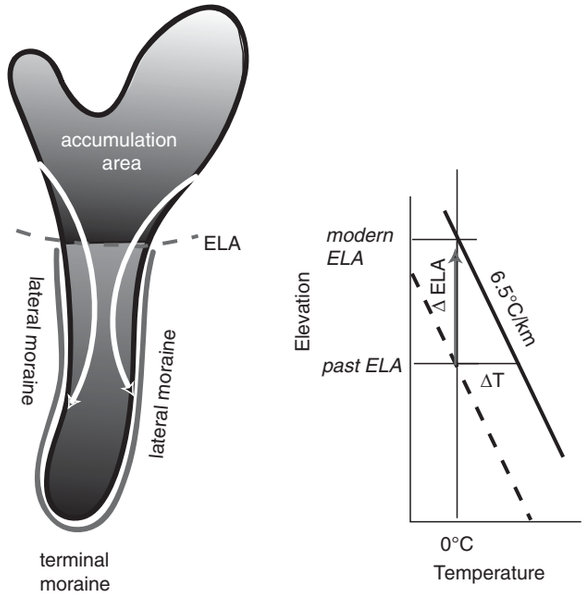


**Figure 8.24** Methods for estimating paleo-ELAs are based upon features of glaciers illustrated. Up-valley ends of lateral moraines coincide with the ELA on a glacier because the trajectories of blocks falling onto the ice are as shown in white arrows: they move toward the glacier center in the accumulation area, and outward to the edge in the ablation zone, responding to the local slopes of the glacier. Typical AARs, ratios of accumulation area to total area of a glacier, are 0.65. If the paleo-area of a past glacier can be measured using terminal moraines, the ELA can be estimated using this AAR. Translation of the change in ELA into an estimate of change in mean annual temperature is based upon application of an assumed lapse rate shown in the figure at the right.

modern glaciers: the accumulation area is roughly 65% of the total area of the glacier. The accumulation area ratio (AAR = accumulation area/total area) is therefore 0.65. If this holds true for glaciers in the past, and one can map the footprint of the past glacier using its terminal moraine, then one can determine at what elevation a contour would enclose an accumulation area of 65% of this. This method is more commonly used than is that based upon lateral moraines because terminal moraines are more likely to remain visible than are the upper ends of lateral moraines. We have already seen in Figure 8.2 how this has been used to estimate ELA lowering during the LGM. In many ranges such estimates suggest a lowering of several hundred meters, from which climatic cooling is estimated to have been 6–10°C. While this is valuable information, we note several weaknesses in the method: AARs vary from 0.6 to 0.8 on modern glaciers, past lapse rates are not necessarily equivalent to those of today, and glacial health is dictated not solely by temperatures, but by rates and patterns of snowfall that can vary with climate as well.

## Ice sheet profiles

Ice sheets are always steepest at their outer margins, and decline in surface slope toward their centers. Why is this? The argument goes as follows. An interesting manifestation of the nonlinearity of ice rheology captured in Glen's flow law is that one may treat ice to

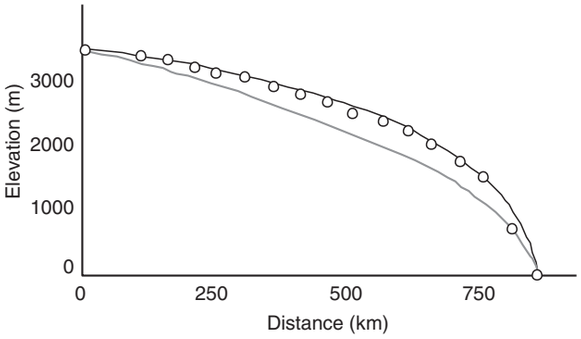


**Figure 8.25** Profile of the Antarctic Ice Sheet from Mirny (circles), along with theoretical profiles: parabola (gray line) and curve that incorporates a uniform accumulation rate (black line). (after Paterson, 1994, Figure 11.4, reproduced with permission from Elsevier)

first order as a plastic substance. A plastic material is one in which there is no deformation up to some "yield" stress, beyond which there is an infinite ability to flow. It has no strength beyond this limit. On a rheological plot, this looks like the broken line in Figure 8.10. As you can see from this plot, a nonlinear substance with a power $\gg 1$ approaches the behavior of the plastic substance. If a glacier were plastic, there must be no place within it that falls above this failure envelope.

Now consider the ice sheet profile sketched in Figure 8.25. At some point on the bed, the shear stress is $\rho g H \sin(\theta)$. If the substance is plastic, and this shear stress is above the yield strength, then infinite strain rates would occur and the ice at the bed would rapidly move, thinning the ice there. This thinning would continue until the shear stress diminished below the yield strength. The argument is therefore that the ice sheet maintains a shape at which the shear stress at the base of the sheet is exactly the yield strength for ice. All we need to know is what this value is, and the handy number to carry in your head is: 1 bar, or, in SI units, $10^5$ Pa. Conceptually, then, given that the shear stress involves the product of surface slope and ice thickness, near the edge of the ice sheet the slope must be high in order to reach the yield stress, and as the ice thickens toward the center the surface slope must decline. We can cast this a little more mathematically. Let's consider an ice sheet on a flat continental surface. All we need is to set shear stressasa constant:

$$\rho_i g H \sin\theta = C \tag{8.25}$$

Given that the surface slope can be expressed as $\mathrm{d}H/\mathrm{d}x$, where $H$ is the thickness of the ice, we can separate the variable $H$, yielding the ordinary differential equation

$$H\mathrm{d}H = \frac{C}{\rho_i g}\mathrm{d}x \tag{8.26}$$

This can be solved by integrating both sides:

$$H^2 = \frac{2C}{\rho_i g}x$$
or
$$H = \sqrt{\frac{2C}{\rho_i g}x} \tag{8.27}$$

The shape of the profile should be a very specific one, obeying a square root dependence on distance from the terminus. There are several things we can do with this relationship. If we have an ice sheet to measure, given that we know the density of ice, the acceleration due to gravity, and can measure both $H$ and $x$, we can deduce the best-fitting value of $C$, the yield strength of ice. We show in Figure 8.25 the shape of the present day ice sheet in Antarctica. The simple model we have just described is shown as one of the lines on the plot. While the fit is not great, only slight modification of the theory is required to accommodate the data very well.

Another use of this simple analysis is reconstruction of past ice sheet thickness profiles. For this reconstruction problem, all we know is the outline of the ice sheet, derived from say the map view pattern of terminal moraines. Using the yield strength derived from present day ice sheets in the above exercise, we can reconstruct how thick the ice must have been as a function of distance from the margin.

Note that we have made many simplifying assumptions in the above analysis, including the characterization of the rheology as a simple plastic. More detailed reconstructions of ice sheets take into account better representations of the nonlinear (Glen's flow law) rheology, and must also handle the thermal problem that dictates where an ice sheet is frozen to its bed (behaving as a Type I polar glacier), and where it is Type II polar or temperate, and therefore can slide.

## Surging glaciers and the stability of ice sheets

We have focused so far on glaciers that will likely look the same next year as they do this year. Exceptions to this rule are surging glaciers, whose surface speeds can increase by orders of magnitude during a surge phase. Surges of valley glaciers may last one or two years, and be separated by decades to centuries. Surging glaciers generate beautifully looped medial moraines, making the glacier tongue look more like a marbled cake than a glacier. A famous example from the Susitna Glacier in Alaska is shown in Figure 8.26. A surge also leaves the glacier with a chaotic pattern of crevasses that should be avoided at all costs as a climbing route. (You would be hard-pressed to climb the glacier photographed in Figure 8.29 in its state at that time.) And on a larger scale, ice streams in Antarctica bear some resemblance to surging glaciers surrounded by non-surging ice. Understanding surge behavior, therefore, has been a major focus within the glacial community.

Our understanding or surges comes largely from the intense and long-lasting study of the 25 km-long Variegated Glacier near Yakutat, in coastal southeast Alaska, mapped in Figure 8.27. This glacier was apparently in surge when photographed in 1905, again in the 1920s, then in the 1940s, and was well documented by a pair of air photos in 1964 and 1965. The apparently approximately 20-year intervals between surges suggested that the next surge might happen in the mid-1980s, and a study was initiated in the late 1970s with the intent of characterizing a glacier as it approached its surge, and then to document well the behavior during the surge. Several teams from at least four institutions poked and prodded and photographed and surveyed the glacier as it approached its surge, which culminated in a two-phase period of rapid motion in 1982 and 1983.

The surge itself can be characterized as a wave of rapid motion that translates through the glacier. In front of the wave, the glacier might be moving at 0.1–0.3 m/day, while in the middle of the high-velocity region it might be moving at 60 m/day, as shown in Figure 8.28. This wave of high velocity translates into yet higher velocities (several times 60 m/day). The crevasse patterns result from the pattern of velocities. At the leading edge of the wave, the ice is in extreme compression, to which it responds by thickening, by thrust faulting, and by folding, in a dramatic analog to the structural geologic evolution one might expect in convergent tectonics. It thickens so much more in the center of the ice than at the edges that it actually fails in tension, generating longitudinal crevasses. On the trailing limb of the high-velocity wave, velocities again drop to lower values, and the ice is put into tension in the longitudinal direction, which in turn generates transverse crevasses. The two sets of crevasses chop up the glacier surface into an amazing chaos of ice pillars that are the signature of the

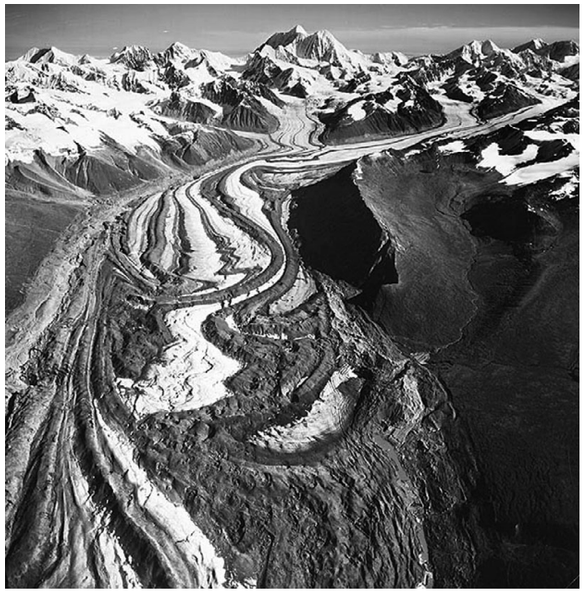

**Figure 8.26** Air photograph by Austin Post of Susitna Glacier, Alaska, taken on September 3, 1970. Medial moraines are highly contorted due to repeated surging of a tributary glacier in the headwaters. (Image susitna1970090301, held at National Snow and Ice Data Center/World Data Center for Glaciology, Boulder)

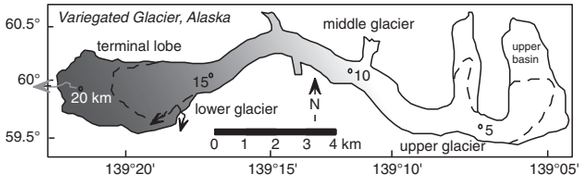


**Figure 8.27** Map of the Variegated Glacier, Alaska, showing the up-glacier and down-glacier limits of the area involved in the 1982–1983 surge (dashed lines), a few of the stake locations spaced at 1 km intervals, and the locations of the major outlet streams near the terminus. (after Kamb *et al*., 1985, with permission from the American Association for the Advancement of Science)

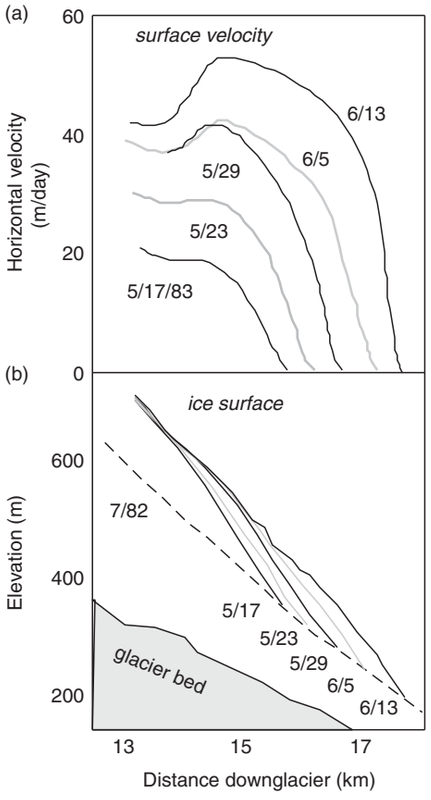


**Figure 8.28** (a) Ice surface velocity profile, $u(x)$, and (b) ice surface topography, $z(x)$, in a 3 km reach of the lower part of the Variegated Glacier, during the 1983 surge. (after Kamb *et al.*, 1985, Figure 4, with permission from the American Association for the Advancement of Science)

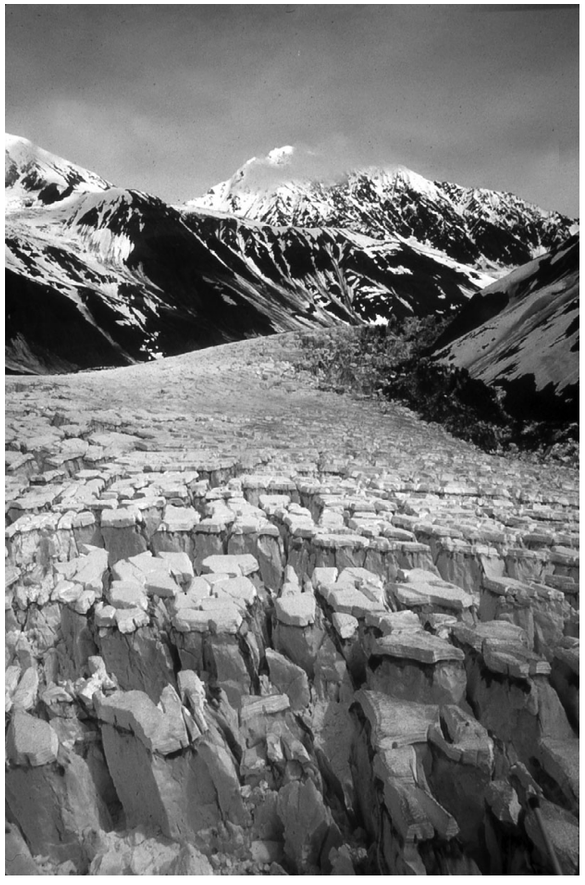

**Figure 8.29** Aerial view looking up-valley of Variegated Glacier near the termination of its 1982–1983 surge. Both longitudinal crevasses, formed early in the surge, and transverse crevasses, formed late, serve to dissect the glacier surface into square pillars of ice, some of them many tens of meters tall. (photograph by R. S. Anderson)

passage of a surge that is obvious in Figure 8.29. Interestingly, the abrupt halt of the surge on July 4, 1983 was coincident with a huge flood of very turbid water reported in Figure 8.30 (see Humphrey *et al.*, 1986).

The data taken together lead to this simplified schematic of a surge. In the aftermath of a surge, the glacier is left with a lower than average surface slope throughout, and has been significantly thinned. It therefore moves slowly, as both slope and thickness dictate lower internal deformation and sliding speeds. The net balance in the following years then rebuilds the glacier accumulation area, and thins the ablation area, as there is smaller than average transfer of ice from accumulation to ablation areas. So the glacier thickens and steepens, as shown in Figure 8.31. Accordingly, you can see in Figure 8.32 that each year its maximum sliding speed rises. Finally, the sliding speed increases sufficiently to disrupt the subglacial fluvial network, and the water that would normally find its way out the glacial conduit system is trapped beneath the glacier. High water pressures result, with attendant positive feedback on the sliding speed. This runaway process is the surge. The surge terminates when, for whatever reason, the water finds a way out, usually resulting in a catastrophic flood.

## Tidewater glaciers

When a glacier extends its terminus down to the ocean, we call it a tidewater glacier. Some of the

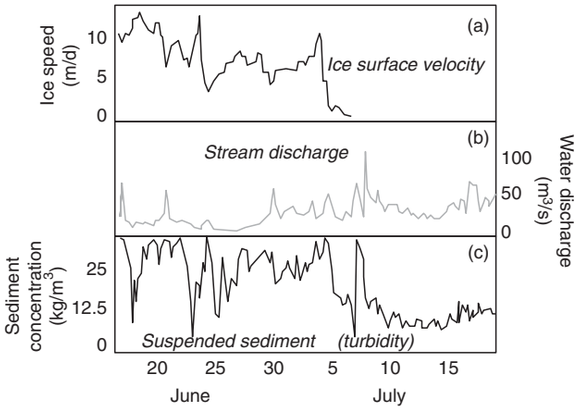


**Figure 8.30** (a) Ice surface velocity at the 9.5 km point on Variegated Glacier, Alaska (see Kamb *et al*., 1985), (b) water discharge, and (c) sediment concentration from turbidity measurements in the weeks surrounding the abrupt termination of the 1983 surge. (after Humphrey and Raymond, 1994, Figure 6, with permission of the authors and the International Glaciological Society)

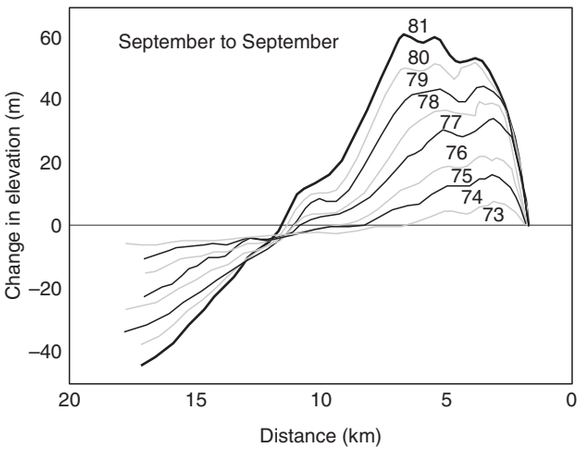


**Figure 8.31** Evolution of the elevation anomaly in the decade leading up to the 1982–1983 surge of Variegated Glacier, Alaska. The glacier thickened more than 60 m in the accumulation area, while thinning by more than 50 m in the ablation area. (after Raymond and Harrison, 1988, Figure 4, with permission of the authors and the International Glaciological Society)

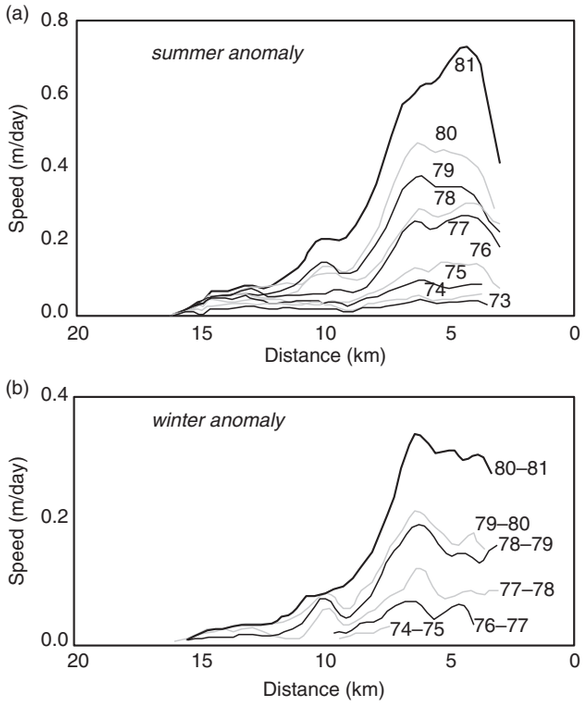


**Figure 8.32** Summer (a) and winter (b) velocity anomalies on Variegated Glacier centerline in the decade preceding the 1982–1983 surge. Note different scale for the summer vs. winter anomalies, attesting to the enhancement of sliding in the summer melt season. The anomaly grows by at least an order of magnitude over the decade. (after Raymond and Harrison, 1988, Figure 5, with permission of the authors and the International Glaciological Society)

largest and fastest glaciers are tidewater glaciers. While the snout of a tidewater glacier may be in the water, the glacier is still grounded, still in contact with a solid substrate. The ice tongue is not floating. In Antarctica now and not long ago in the Arctic, ice shelves also exist, which are indeed floating beyond a point called the grounding line. Tidewater glaciers differ from typical alpine glaciers in several ways, all due to their interaction with the ocean. Most importantly, they can lose mass through a mechanism other than melting – they can lose mass by calving of icebergs, which can be seen cluttering the terminus area in Figure 8.33. This can be very efficient. On Alaska's Pacific coastline the termini of these tidewater glaciers are the targets of tourist ships, as the terminal cliff is the scene of dramatic iceberg calving events. But this is not all. Because the ice extends into a water body, the lowest the water table within the glacier can get is sea level. We have already seen the importance of the state of the hydrologic system within the glacier on its sliding rate. In particular, as we have seen, our simplest working model for sliding speed involves the effective pressure at the base of the glacier in the denominator of the expression (Equation 8.24). As

**Figure 8.33** Aerial photograph of tidewater glaciers calving into a fjord near NyAlesund, Svalbard archipelago. Note prominent plume of sediment-laden water exiting from beneath the uppermost portion of the foreground glacier. The medial moraines separate ice emanating from various tributary valleys in the headwaters. Ice cliff at the sea is roughly 100 m tall. (photograph by Suzanne Anderson)

the flotation condition is approached, or as water pressure increases, sliding speeds ought to increase dramatically. As the glacier extends into deepening water, the effective pressure at the bed must dramatically plummet. If the sliding speeds obey our simple rule, then the sliding speed ought to increase dramatically as well. This pattern of sliding is one of the factors that leads to the extensive fracturing of tidewater glacier snouts. In effect, the glacier ice therefore arrives at the terminus already prepared for calving. It is already riddled with fractures.

## Calving

Given its importance in the operation of these massive glaciers, we know surprisingly little about the mechanics of calving. This is a complicated process involving the propagation of fractures within the ice, either from the bed upward or the surface downward. Interactions with the body of water include melt-notching of the terminal cliff by seawater, buoyancy of the seawater, and tidal swings in sea level. Where calving rates have been measured, they have been shown to be related closely to water depth; the greater the water depth the greater the rate of calving. In Figure 8.34 we show data collected by Brown *et al.* (1982), reveal a nearly linear relationship of calving rate to water depth, $D$:

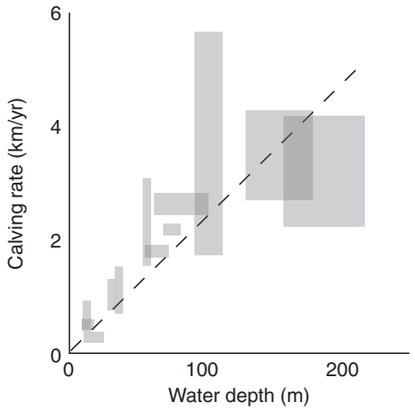


**Figure 8.34** Dependence of calving rate on water depth. (after Brown *et al.*, 1982)

$$U_{\text{calve}} = aD^p \tag{8.28}$$

From the plot one may deduce that $p = 0.92$, which is sufficiently close to 1 to allow simplification to $U_{\text{calve}} = 0.02D$.

## Tidewater glacier cycle

The implications of this dependence of calving on water depth were recognized in the 1960s by Meier

and Post, who proposed what has been called the tidewater glacier cycle. If a tidewater glacier is to extend across deepening water, it must effectively bring along some protection against this calving loss. The proposed mechanism involves a morainal shield. These are big glaciers, and they deliver large amounts of sediment to the sea, presumably both as till at the base of the ice and as sediment delivered to the terminus in the subglacial drainage system. One can see well the muddy plume of water marking the position of one such exit stream in the photo in Figure 8.33. As well, one can imagine sediments at the bed of the fjord being distorted or pushed by the advancing front of ice. All of these sediments get smeared along the glacier terminus by marine processes (Powell and Molnia, 1989). The resulting shoal acts to guard the glacier terminus against the more efficient calving that would otherwise attack the ice front. This allows the glacier tongue to propagate into deeper water by bringing with it the protective shoal. The rate of advance is slow, and is presumably dictated by both the rate of delivery of ice to the front and the rate at which the shoal can be built into deeper water. Notice the vulnerability as the ice extends, however. If for some reason the snout retreats off its shoal, the terminus will experience increased water depth, and the calving rate should increase. Once started, this should result in a retreat that will last until the glacier is once again in shallowing water. Meier and Post suggested that tidewater glaciers undergo periodic cycles of slow advance and drastic retreat in this sort of bathymetric setting. These cycles can have little to do with the mass balance of a glacier. This is an instance in which the retreat of a major tidewater glacier could be completely decoupled from climate. One tidewater glacier may be advancing slowly while another in an adjacent fjord may be in dramatic retreat. The behavior is self-organized.

In coastal Alaska, these tidewater glaciers have retreated up their fjords, exposing brand new landscapes within the last century. When John Muir visited what is now Glacier Bay National Park in the late 1800s, the bay was fully occupied by a large glacier. Now one must paddle a kayak tens of kilometers up the fjord to find the remnants of this glacier, each tributary of which has pulled its toe out of the water.

The most recent example of this retreat is presently occurring on Columbia Glacier, just north of Valdez. The retreat has been dramatic, as captured in repeat photographs summarized in Figure 8.35. This glacier was of special interest due to its proximity to the terminus of the Alaska pipeline. As icebergs calved from the Columbia could potentially enter the shipping lanes traversed by oil tankers, the behavior of the calving front of the Columbia has been closely watched. Indeed, the retreat predicted in the 1980s is now in full swing. Luckily, the terminal moraine serves as a very effective barrier to the transport of icebergs. They must melt, grind, and smash each other into smaller bits before they can escape the moraine sill, and are therefore small enough not to pose a significant risk before they are cast into the open ocean. We expect the retreat to last into next decade, opening a new fjord: Columbia Bay. The story of the retreat, and of the scientists who have studied this glacier for now a century, serves as an introduction to glaciology as a science. It is lovingly told and beautifully illustrated by Tad Pfeffer in his *The Opening of a New Landscape: Columbia Glacier at Mid-Retreat* (2007).

## Contribution to sea level change

Sea level is now rising at a rate of about 3 mm/yr. The rise reflects two phenomena: (1) new water added to the oceans, much of which is coming from glaciers, and (2) warming and expansion of the oceans (see Nerem *et al*. (2006)). The prospect for the coming century is not good, as both of these rates will increase. As is summarized in Figure 8.36, much of the contribution of new water comes from glaciers and ice caps, despite their being dwarfed in total ice volume and area by the big ice sheets of Greenland and Antarctica.

That tidewater glaciers extend to the sea implies that they have large accumulation areas in high elevations, that the accumulation rates are high due to proximity to the storms coming off the ocean, or both. The low elevations of the ablation zones also lead to very high melt rates, rates of many meters per year. In a recent study of glacier change in Alaska (Arendt *et al*., 2002), comparison of the glacier centerline profiles collected using a laser altimeter mounted on a small plane with those derived from 1950s USGS maps showed that the glaciers in Alaska alone could account for roughly half of the sea level rise attributable to glaciers worldwide.

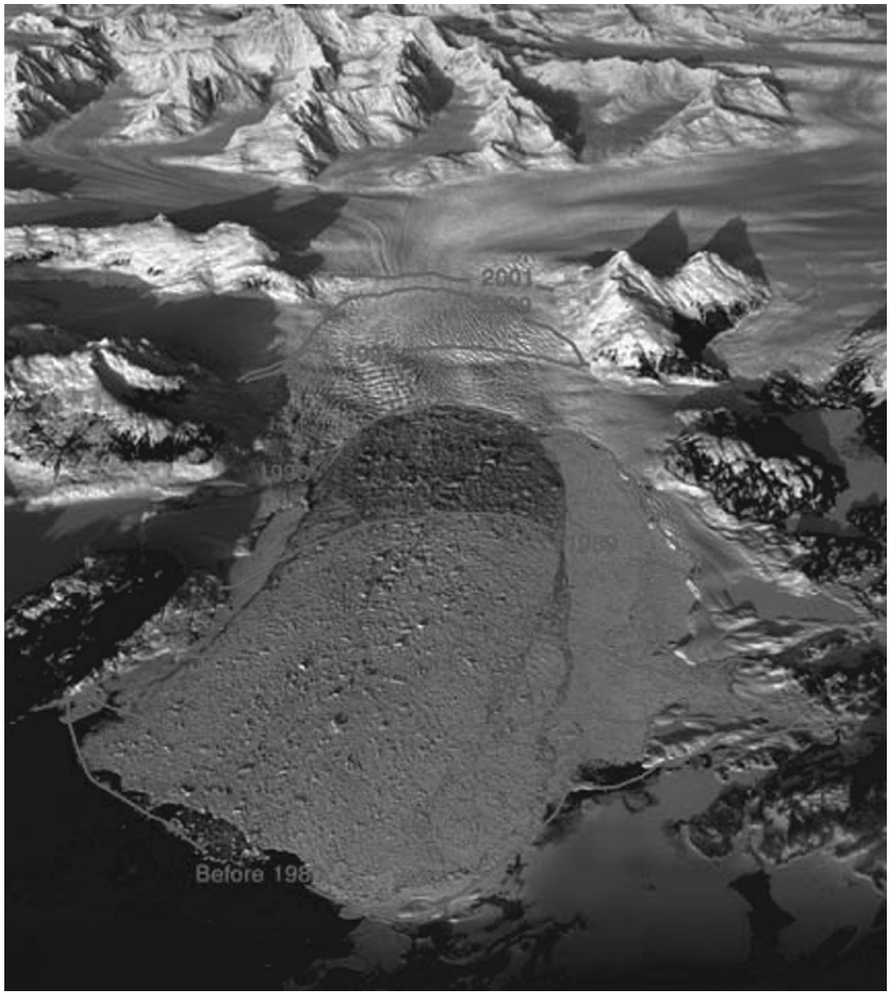


**Figure 8.35** Columbia Glacier in retreat, view looking roughly east toward headwaters in the Chugach Range, Alaska. The retreat between 1988 and 2001 is 13 km, averaging roughly 680 m/yr. (image courtesy of Mark Meier and Tad Pfeffer)

## The great ice sheets: Antarctica and Greenland

Most of the mass of ice in the present cryosphere is contained in the two great ice sheets that cover Greenland and Antarctica. It is from these ice sheets that the longest terrestrial records of climate change have been extracted from ice cores now reaching back almost a million years in Antarctica. Antarctica has had major ice cover since roughly 30 Ma. The Antarctic Ice Sheet presently holds the equivalent of 70 m of sea level, while that in Greenland represents a potential sea level rise of 7 m.

These are cold places, with mean annual surface temperatures that fall as low as −50°C. In Antarctica, there is very little melt of ice on the surface. The ice is polar, meaning that for the majority of the volume of each ice sheet the temperature is well below the freezing point. As we have discussed above, this means that the transport of ice is accomplished solely by internal deformation. Basal sliding is limited to a few special places; it is on these places that we focus because it is here that ice can be pulled rapidly from the continents to contribute to sea level rise in the short term – on human timescales.

As you can see from the image in Figure 8.37, Antarctica is subdivided into two ice masses, the west and east ice sheets. The east is wider, thicker, and contains the majority of the ice. The West Antarctic Ice Sheet (WAIS), however, is the target of

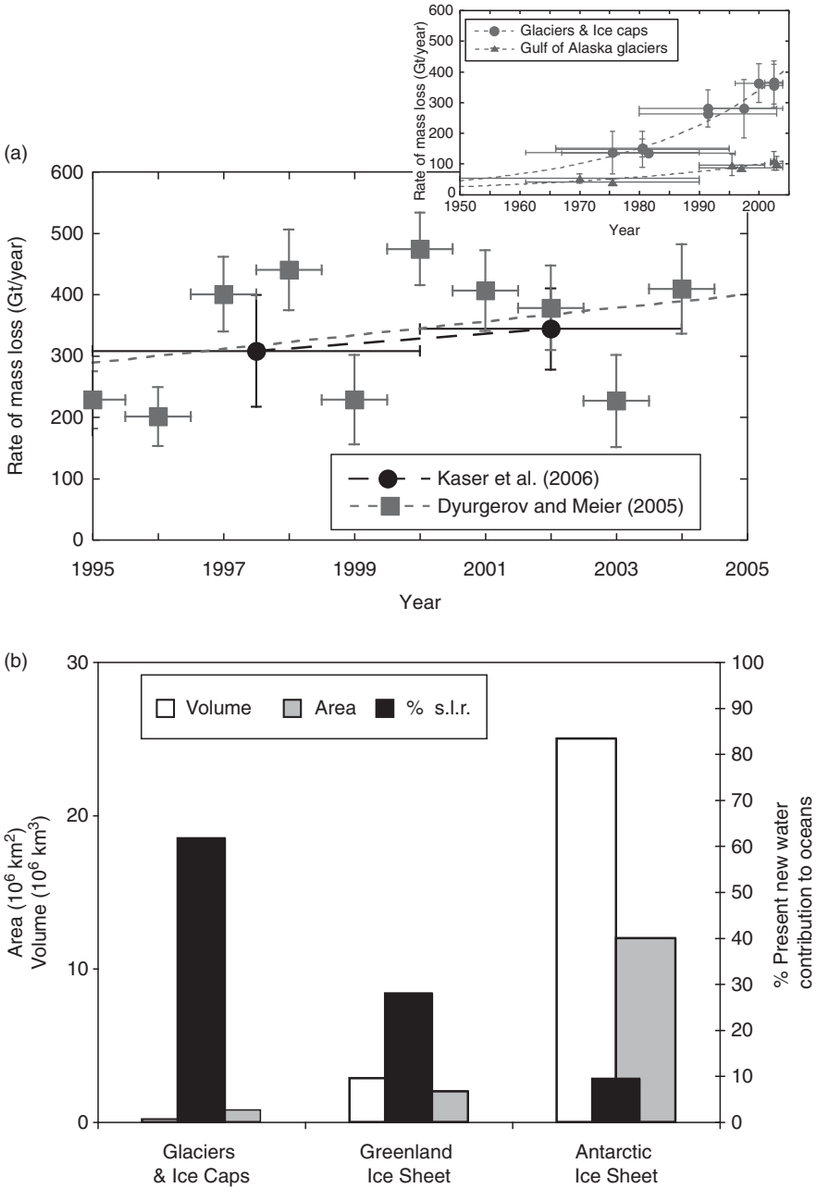


**Figure 8.36** (a) Rate of loss of ice mass from small glaciers worldwide over the last decade (1995–2005), and since 1950 (inset). Also shown in inset is the loss attributable to glaciers draining into the Gulf of Alaska. (b) Comparison of present area (gray) and volume (white) of glaciers and ice sheets. The relative contributions to sea level rise (s.l.r., black) reveal that while area and volume of ice recently stored in glaciers and ice caps is small, they contribute 60% of the new water to the world's oceans. Projections over the next century suggest that this will continue. (after Meier *et al*., 2007, Figures 1 and 2, with permission of the American Association for the Advancement of Science)

considerable research because it is viewed to be more vulnerable to rapid ice loss. This comes from the fact that it is grounded well below sea level, information that we have gleaned by flying airborne radar surveys that can detect both internal layering in the ice and its bed. It is also warmer, with the Antarctic peninsula poking well north. It is from this peninsula that Ernest Shackleton landed his party after abandoning their ship, *Endurance*, and from which he launched his journey across the raging southern ocean, ultimately to find help in South Georgia (read Alfred Lansing's *Endurance*, or Roland Huntsford's *Shackleton*).

Antarctica is bounded by a set of thick ice shelves also shown in Figure 8.37 that serve as intermediaries between the continent and the ocean. The boundary between the ice sheet and an adjacent ice shelf occurs where the ice lifts off the bed to become floating. Subglacially, this is an important interface, as it is

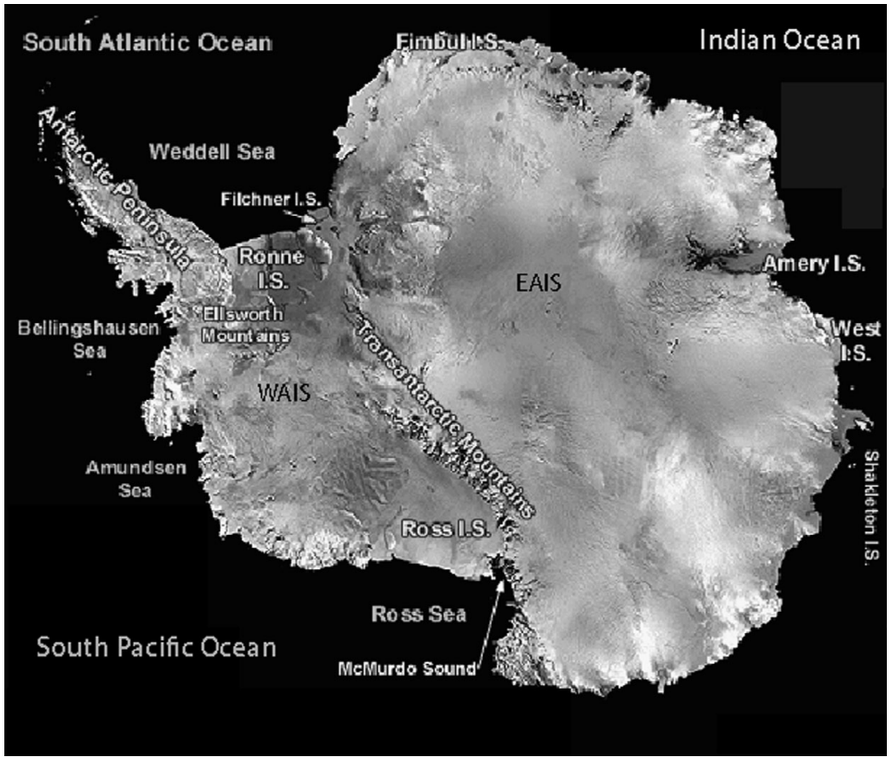


**Figure 8.37** Map of Antarctica showing main topographic features, from AVHRR Mosaic color composite. EAIS and WAIS are the East and West Antarctic Ice Sheets, separated by the Transantarctic Mountains, a rift-flank uplift. I.S. = Ice Shelf. (modified from USGS http://TerraWeb.wr.usgs.gov/TRS/projects/Antarctica/AVHRR.html)

here that sediment delivered from the continent is dumped in the ocean, generating grounding line fans. Subaerially, the location of the grounding line can be sensed using inSAR, as the ice shelf responds to tidal forcing while the grounded ice does not. Interest in these bounding ice shelves has increased recently as more than one of these shelves has experienced disintegration. The demise of a large portion of the Larsen B ice shelf has effectively unpinned the grounded glaciers that feed the ice shelf, leading to their acceleration (Hulbe *et al*., 2008).

With very few exceptions, there is no melting of ice in Antarctica. In such cold places the ice budget must closed by a different mechanism. Ice leaves the continent either by calving of icebergs, or by blowing of snow in the sustained high winds that drain the chilled air from the polar plateau (see discussion of katabatic winds in Chapter 5).

Greenland's ice sheet shown in Figure 8.38 also covers the majority of the landmass, and in its center is more than 2 miles (about 3 km) thick. Its center is also a smooth, windblown plateau. Those small portions of the landmass that are visible reveal highly dissected plateau-like edges, deeply indented by steep-walled fjords. In contrast to Antarctica, the outer edges of the Greenland Ice sheet experience melting. While some of this snow and ice meltwater makes its way to the bed and out of the ice sheet, some refreezes in the subsurface and cannot be counted as part of the negative mass balance.

Most of the ice is lost from these ice sheets through a relatively few rapidly moving "ice streams". These can be tens of kilometers across, and move at rates of a large fraction of kilometers per year. These speeds are best documented from satellite using the same inSAR methods employed to assess tectonic deformation. A recent summary image of ice stream speeds is presented in Figure 8.39. The best known of the ice streams drain toward the Ross Ice shelf from the West Antarctic Ice Sheet. First named A through E, some have now begun to take on the names of researchers who have long studied them. And the ice streams are odd. It has now been shown that they move very rapidly for a while, and then shut down to

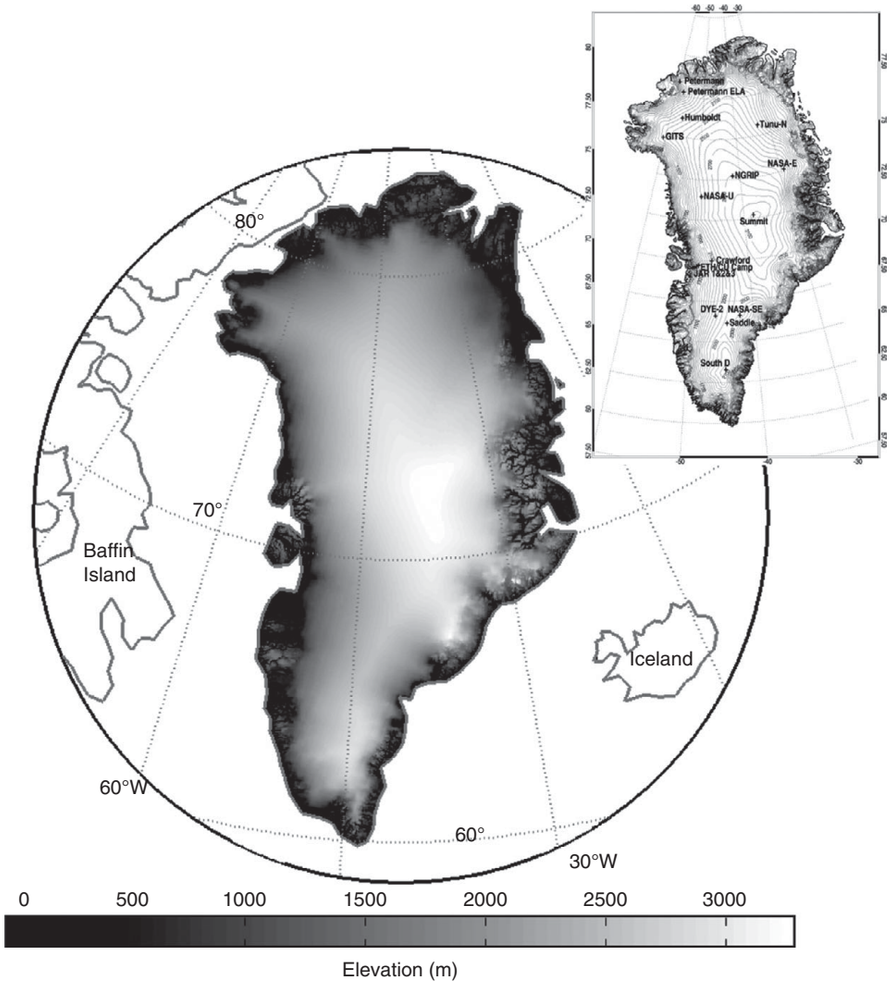


**Figure 8.38** Satellite radar produced map of Greenland. (from A. Bamber, courtesy Liam Colgan, after Fahnestock *et al*., 1997, *Digital SAR Mosaic and Elevation Map of the Greenland Ice Sheet*. Boulder, CO: National Snow and Ice Data Center)

become dormant for decades to centuries before another burst of activity. Drilling to the base of ice stream B has shown that the base of the ice stream rides on a layer of till that is implicated in the rapid motion (e.g., Tulaczyk *et al*., 2000a and 2000b; Bougamont *et al*., 2003). Briefly, we think this works as follows. When the temperature at the base of the ice stream is near the melting point, the water-saturated till shears rapidly and the ice stream above it goes along for the ride. But this slowly drains the ice from upstream and the ice stream thins to the point where the cold surface temperatures can conduct to the base to refreeze the till. Now that the ice spigot has been turned off, ice can build back up the thickness that was lost. This slow thickening in turn decreases the temperature gradient through the ice, reducing the rate at which heat is lost to the atmosphere, and the base begins to warm. The cycle repeats when the temperature rises sufficiently to melt the water in the till. At present ice stream C is turned off, and the huge crevasse field that delineates the boundary of the stream when it is in motion is now buried in tens of meters of new snow.

In Greenland, ice leaves the ice sheet through major fjords that presently compete with Alaska's tidewater Columbia Glacier for the fastest ice on Earth. The recent increases in the speeds of these outlet glaciers, largely documented using inSAR methods and shown in Figure 8.40 (e.g., Rignot and Kanagaratnam, 2006; Howat *et al*., 2008; Nick *et al*., 2009; Joughin *et al*., 2008), have drained a significant volume of ice from the outer fringe of the ice sheet. Just as in tidewater glaciers in Alaska, the acceleration has resulted in a thinning of the ice, which in turn results in further

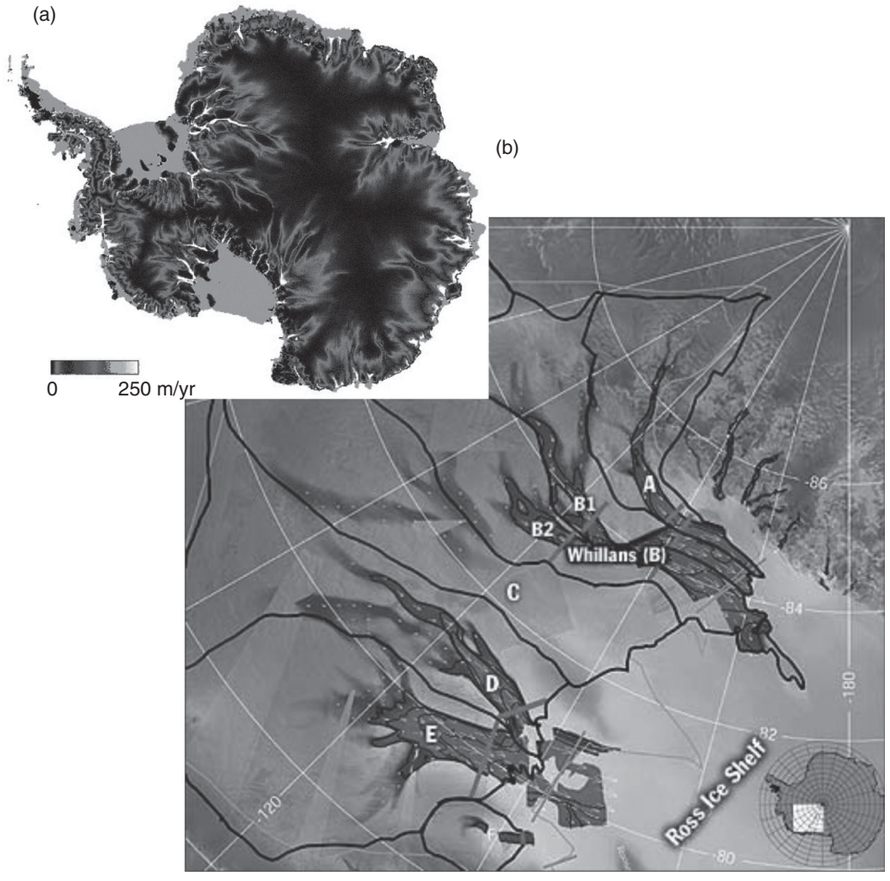


**Figure 8.39** Antarctic ice speeds documented using inSAR methods, (a) covering all of the continent, and (b) focused on the ice streams draining the West Antarctic Ice Sheet toward the Ross Ice Shelf. (after Ian Joughin, image courtesy RADARSAT Antarctic Mapping Project)

acceleration. The termini of several of the largest outlet glaciers have receded many kilometers.

## Glacial geology: erosional forms and processes

Now that we have some understanding of how glaciers work, let us turn our focus to how glaciers modify their physical environment. Glaciers both erode landscapes, generating characteristic glacial signatures (see N. Iverson, 1995, 2002), and they deposit these erosional products in distinctive landforms. We will describe the origins of these features, starting with erosional forms, and starting at the small scale. Again, the goal is not to be encyclopedic, but to address the physics and chemistry of the processes that gave rise to each of the forms.

## Erosional processes

Any visit to a recently deglaciated landscape will reveal clues that it was once beneath a glacier. The bedrock is often smooth, sometimes so smooth that it glints in the sun as if it has been polished. The bedrock is also commonly scratched. The small bumps have been removed, leaving a landscape dominated by larger bumps and knobs that have characteristic asymmetry. And at the large scale we see U-shaped valley cross sections, hanging valleys, fjords, and strings of lakes dotting the landscape. At an even larger scale, fjords bite through the margins of most continents that have been subjected to repeated occupation by ice sheets. Each of these features cries out for an explanation, beyond "this valley was once occupied by a big moving chunk of ice."

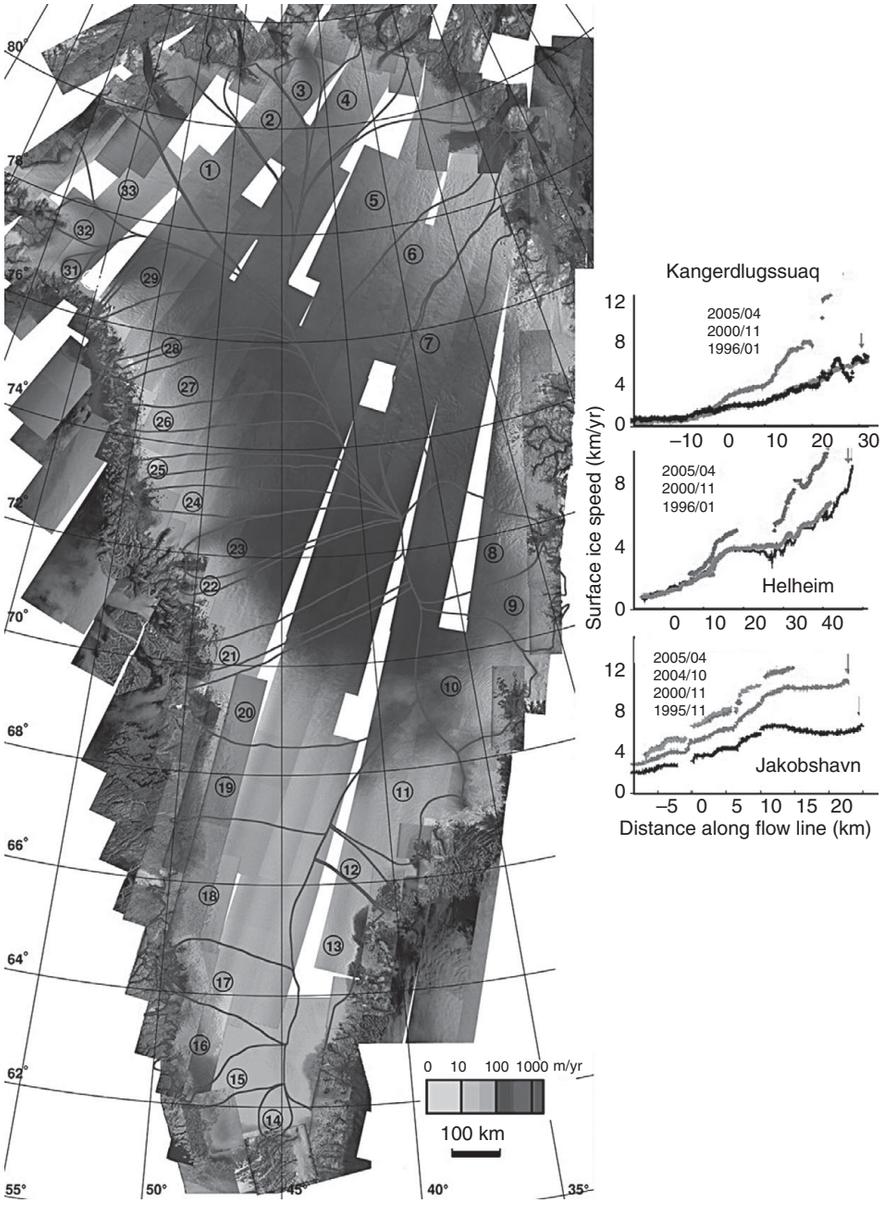


**Figure 8.40** Surface ice speed mosaic of the Greenland Ice Sheet assembled from year 2000 Radarsat-1 radar data, color coded on a logarithmic scale from 1 m/yr (light) to 3 km/yr (dark), overlaid on a map of radar brightness from ERS-1/Radarsat-1/Envisat. Drainage boundaries are shown. Right: Ice speed profiles down flow lines, showing speed-up over the decade 1995–2005. (after Rignot and Kanagaratnam, 2006, Figures 1 and 2, with permission of the American Association for the Advancement of Science)

## Abrasion

The scratches, called striations, are the products of individual rocks that were embedded in the sole of the glacial ice as it slid across the bedrock. The erosion resulting from the sum of all these scratches is the process called subglacial abrasion. It is abrasion that smoothes the bed. It is the short wavelength bumps in the bed that are gone, making it look smoother. This should trigger recollection of the regelation process by which glaciers move past small bumps. Consider again that bump, and think about a rock embedded in the ice approaching the bump. The bottom line is that while the ice can get around the bump with its regelation magic act, the rock cannot. Instead, it is forcefully pushed against the bump, as we illustrated in Figure 8.14, the force being great enough to cause the rock to indent, scratch or striate the stoss side of the bump. As the

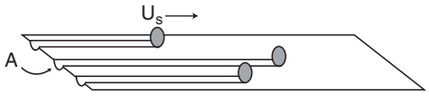


**Figure 8.41** Sketch of glacial erosion by abrasion. Multiple striations of the bedrock by rocks embedded in the sole of the glacier, moving at the sliding speed $U_{slide}$, lead to lowering or erosion of the bed. The rate depends upon the number of striators per unit area of bed, the cross-sectional area of the eroded striation, $A_s$, and the rate of lengthening of the striation, $U_s$. The cross-sectional area of the groove is proportional to the drag force imposed by the ice as it regelates past the rock clast.

rock is still being dragged along by the ice, this indentation stretches out to gouge a micro-channel that is the striation.

The theory of glacial abrasion requires that we handle the effects of each such striator, and that we have some knowledge of the number of them in the basal ice. The theory was worked out by Bernard Hallet (1979), and is summarized in Figure 8.41. The abrasion rate, $e$, goes as the number of indentors per unit area of bed, $C$, the cross-sectional area of the indentation that they induce in the bedrock, $A_s$, and the rate at which the striators are dragged across the rock, $U_c$:

$$e = CA_sU_c \tag{8.29}$$

We must determine what controls the cross-sectional area of the indentation. Experimental work shows that the depth of the indentation increases as the force imparted by the indentor increases. Hallet argued that one should consider the clast doing the work as being embedded in a fluid (ice) that is moving toward the bedrock at a rate comparable to the sliding rate, $U_{slide}$. If ice is disappearing at the stoss side of the bump, and the rock is not, then ice has to move past, around the rock. In this view, the force involved is that associated with the viscous drag of the ice as it moves around the rock to disappear at the stoss side of the bump. From the theory of fluid flow past obstacles, such as that employed in thinking about settling of clasts in a fluid, and recognizing that the flow is likely to be very low Reynolds number (viscous as opposed to turbulent) flow, the drag force can be written

$$F_d = \frac{1}{2}A\rho_f C_d U_{rel}^2 \tag{8.30}$$

where $C_d$ is the drag coefficient, $A$ the cross-sectional area of the clast, and $U_{rel}$ the relative velocity of the fluid and the rock. For low Reynolds numbers, Re [$= UD\rho/\mu$], the drag coefficient is 24/Re, or $24\mu/D\rho U_{rel}$. This leaves the expression for the drag force as

$$F_d = 3\pi D\mu U_{rel} \tag{8.31}$$

But the relative velocity of the ice relative to the clast is some fraction of the sliding speed, $U_{sl}$. Combining these expressions reveals that the abrasion rate should go as the square of the sliding speed:

$$e = \gamma U_{sl}^2 \tag{8.32}$$

We note for completeness the other view of the origin of the drag force. Why is the relevant force not the weight of the overlying column of ice? This overlying column of ice has to be pretty heavy, given that ice is about one-third as dense as rock. The problem with this view is that the ice is not a solid, but must be considered a fluid. The rocks at the base of the glacier are engulfed in the fluid, so they not only do not support the weight of a column of ice overhead, but instead are buoyed up by the surrounding fluid. It is the buoyant weight of the rock that counts. In this view, then, the depth of the scratches that could be imparted to the bed are greater when you drag a rock across the bed *in air* than they would be under ice. Try it. The scratches are very minor compared to the striations that must have occurred subglacially.

We note that recent work (Iverson *et al.*, 2003) has suggested that the rock–rock friction associated with these striators provides a significant brake on the sliding of the glacier. This would serve as a negative feedback in the glacial erosion system, as the more clasts there are the more the glacier will be slowed, and the less rapid the erosion will be.

Given a pre-glacial irregular bed consisting of bumps of all wavelengths, this abrasion process will most effectively remove bumps of small wavelength, leaving the bed smoother at these scales. At some scale, however, larger bumps persist. No glacial valley is perfectly smooth. When we look closely at these larger bumps, they often have an asymmetry, with a smooth up-valley stoss slope that shows signs of abrasion, and an abrupt, steep down-valley or lee side that looks like it has been quarried. These forms are called roche moutonee, apparently named for the similarity of their shapes with that of the rear of a sheep. Their

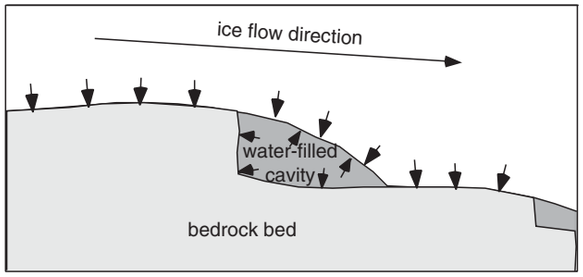


**Figure 8.42** Schematic diagram of a water-filled cavity beneath a temperate glacier. Arrows represent normal stresses.

origin requires introduction of the other major subglacial erosional process: quarrying.

## Quarrying

Larger bumps in the bed can generate the subglacial cavities on their lee sides illustrated in Figure 8.42, as the ice flowing over the top of the bump separates from the bed in the lee. All but those subglacial cavities at the very edges of the glacier will be filled with water. The quarrying process involves the generation of cracks in the bedrock at the edge of the cavity, and results from imbalance of forces on the top and sides of the rock bump. The theory of subglacial quarrying has been recently addressed by Neal Iverson (1991; see also 1995 and 2002) and by Bernard Hallet (1996), quite independently. Cracks grow at a rate dictated by the stresses at their tips. It is therefore the magnitude and the orientation of the stresses within the bedrock bump that are crucial to the problem.

Consider the down-glacier edge of the bump, which is often quite abrupt due to quarrying and can be idealized as a square corner. The ice presses downward against the bedrock that comprises the top of the bump. The water pressure in the cavity, which acts equally in all directions, presses against the lee side of the bump. If there is a large difference between the water pressure and that exerted by the overlying ice overburden, then there will be a large stress difference, and crack growth will be promoted. Iverson generated a model of the magnitude and orientation of the stresses, and hence the expected orientation of cracks under various pressure difference scenarios. Figure 8.43 summarizes the stress fields associated

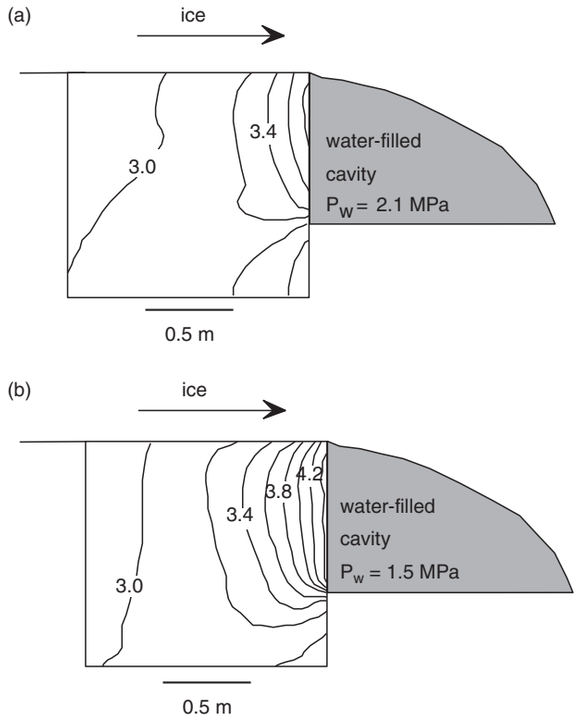


**Figure 8.43** Contours of stresses (in MPa) within bedrock corner at ledge edge. Ice sliding from left to right. No vertical exaggeration. (a) With water pressure steady at 2.1 MPa, and (b) with water pressure reduced to 1.5 MPa. Note strong stress concentrations at ledge face. (after N. Iverson, 1991, Figure 6, with permission of the author and the International Glaciological Society)

with two different water pressures. One can see that the orientation of cracking to be expected is that parallel to the lee face of the cavity. The growth rate would be proportional to the pressure difference. One end-member situation is one in which the water in the cavity is abruptly removed, reducing its pressure to atmospheric. For the period of time required for the cavity to fill with ice as it relaxes into the low-pressure void, the entire weight of the ice overburden would be borne by the top of the bump, very large pressure gradients would exist, and cracks would grow that are nearly vertical. It is therefore the temporal fluctuations in water pressure at the bed that matter: it is transience in water pressure associated with pressure drops that generates the greatest stress gradients in the rock mass.

In a clever physical experiment installed beneath a Norwegian glacier, Cohen and coworkers (2006) have

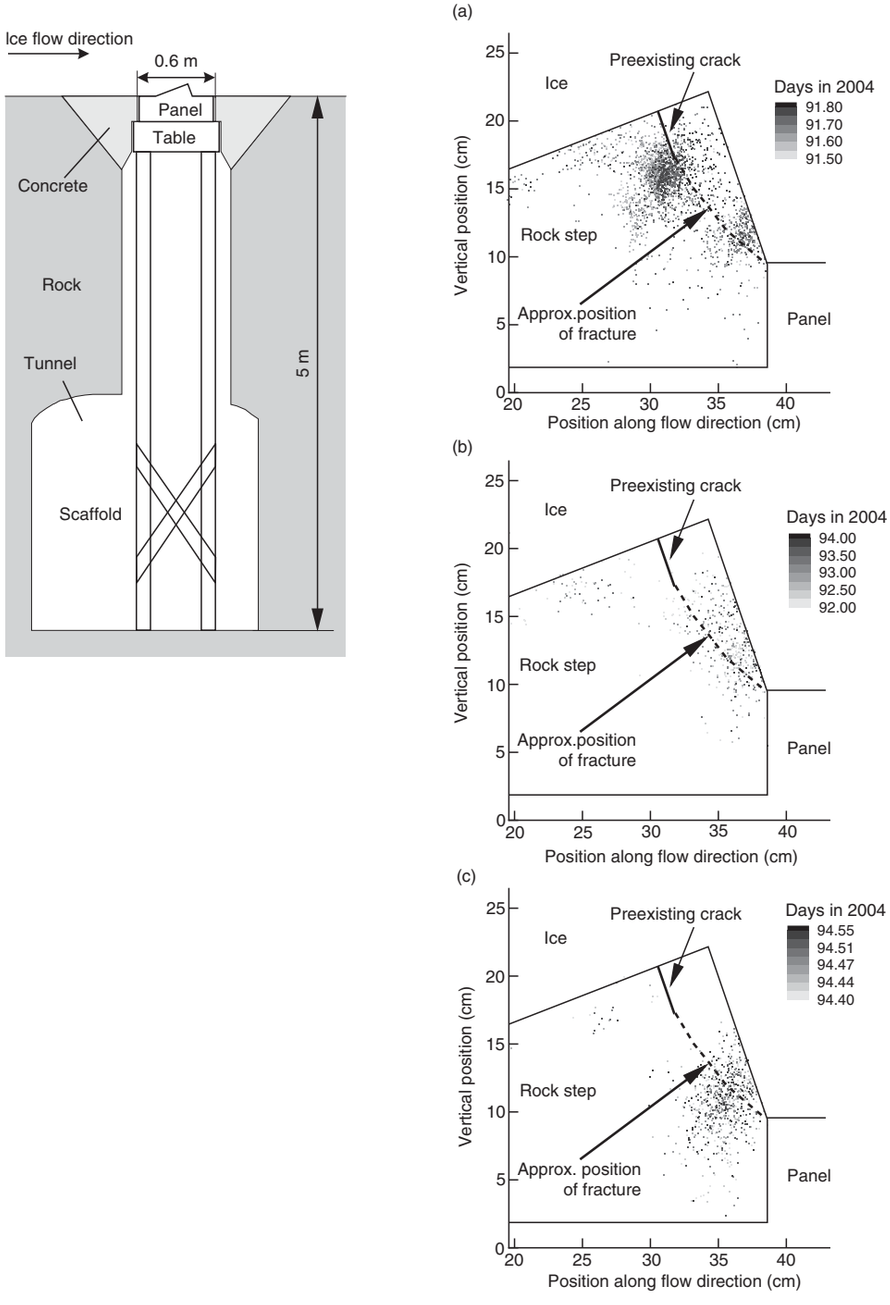


**Figure 8.44** Experiment beneath Engabreen, Norway, designed to explore the dependence of transient water pressures on subglacial quarrying. Left: experimental setup showing how the artificial triangular bump was inserted at the bed of the glacier through a vertical shaft from a tunnel. Right: locations of acoustic emissions (AEs), reflecting crack growth, after three pump tests during the experiment. Early AEs (a) cluster near the tip of a pre-cut initial crack, but progressively migrate downward toward the base of the bump (b and c). The bump ultimately failed along a plane (dashed) roughly following the trend of the AEs. (after Cohen *et al*., 2006, Figures 1 and 8, with permission of the American Geophysical Union)

demonstrated that the basic ideas captured in this quarrying model are appropriate. They took advantage of the fact that in several places in Norway hydropower generation taps subglacial water, which in turn leads to considerable funding for subglacial research. Researchers can access the bed of Engabreen (*breen* is Norwegian for *glacier*), through a tunnel that ends beneath 210 m of ice. They installed an artificial ramp in the bed into which a cut had been made to simulate an existing crack in the stoss side of a bed bump. This is shown in Figure 8.44. Ports in the lee of the ramp allowed them to pump in water to

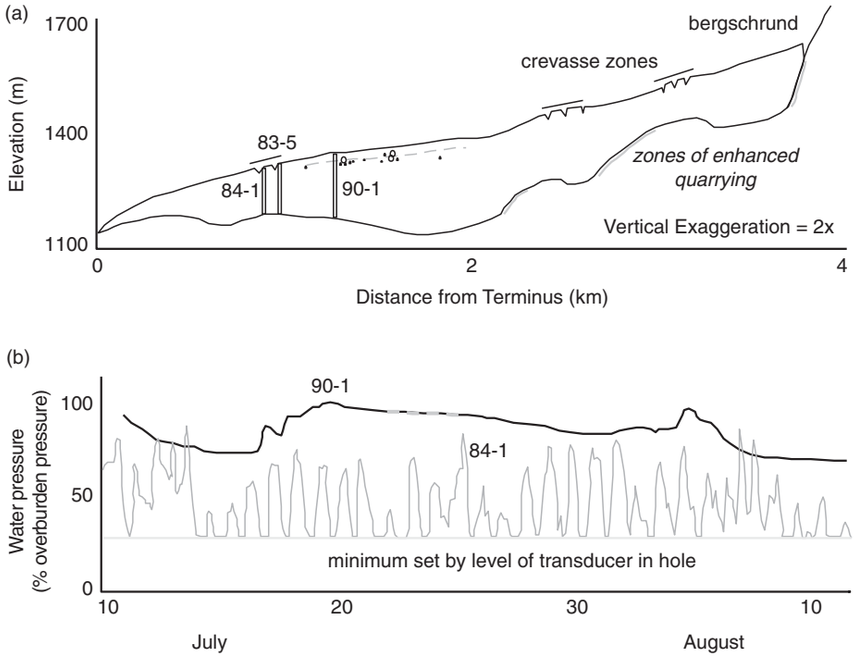


**Figure 8.45** Topographic profiles of ice surface and bed (a), and water pressure records (b) from Storglacieren, Sweden. Profile shows several overdeepenings of the bed and major crevasse zones in regions of extension. Borehole locations in major overdeepening and at crest of bedrock bump are shown, along with spot measurements of the water pressure in the middle of the overdeepening. These measurements are all close to the level expected for flotation of the ice: 90% of the ice thickness, shown in gray line. Pressure records are very different for two sties, that in the middle of the overdeepening showing little variation around 90–100% of flotation, that at the crests of the bump showing major diurnal fluctuations between 70–90% flotation and that pressure associated with the depth of the transducer (gray line). Similar pressure fluctuations are inferred to promote enhanced quarrying of the bed at sites shown in (a). (redrawn from Hooke, 1991, Figures 2 and 3).

melt away a cavity in the lee. When the water pump was turned off, the pressure in the lee of the bump decayed rapidly as cavity collapse could not keep pace with the rate of pressure drop. Iverson's theory would lead us to expect that at these times large gradients in stress should occur that are conducive to the propagation of existing cracks normal to the stoss face of the bump. The experiment allowed them to check this notion: they instrumented the bump with eight acoustic emission (AE) transducers to listen to any cracking that occurred, and to triangulate the location of the cracking within the bump. Remarkably, after several pumping episodes that resulted in growth and decay of the cavity in the lee, and the associated cycling of pressures to which the bump was subjected, they could see the enhancement in the number of acoustic emissions, and the migration of the AEs downward in the bump. Inspection of the bump at the end of the experiment revealed that the edge of the bump had been quarried; the crack had indeed propagated as the AEs had indicated.

This experimental confirmation of the basic quarrying mechanism leads us to ask why pressures in a subglacial cavity system should vary at all? The origin of the water in the cavity system is melt of the glacier surface. At some level, variations in the rate of production of melt, which occur on both daily and seasonal timescales, are the most likely culprits. Boreholes drilled to the base of glaciers have recorded huge swings in the subglacial water pressure on quite short timescales. In the example shown in Figure 8.45, from Storglacieren in Sweden, the water pressure fluctuations are much greater over the crest of a bedrock rise than within a slight overdeepening. This may lead to large spatial variations in the rate of quarrying of the glacier bed.

As discussed in the section on glacial sliding, the detailed records of surface velocity during sliding

events on alpine glaciers all suggest that cavities grow during rapid sliding induced by high water pressures, and that they subsequently collapse as the sliding event wanes. In order for the pressure differences in the edges of subglacial bumps to rise above the threshold for driving cracks, the water pressure in the cavity must drop faster than the ice roof can collapse to maintain contact with the water in the cavity. The intimate connection between water pressure, sliding, and quarrying should be apparent. So too should its complexity.

How do we know these cavities exist at all? There are a couple ways. The most direct evidence is from air-filled cavities (caves) at the edges of some glaciers. Here subglacial spelunking allows us to walk around in the cavity system and to observe first-hand the operation of the plucking mechanism. By their nature, such air-filled cavities are overlain by only minor thicknesses of ice. Nonetheless, direct observation of the edges of the ledges from one year to the next have shown significant modification of the ledge takes place in a single year's sliding (Anderson *et al*., 1982). A time lapse movie taken of the ice roof as it slides by such a ledge edge beneath the Grinnell Glacier, Montana, reveals that numerous small chips and blocks are torn off the ledge over a single winter. They become embedded in the basal ice (the roof of the cavity), and are therefore available to act as abraders when the ice roof reattaches to the bed at the downstream boundary of the cavity.

In limestone bedrock, the nature of the subglacial water system may be carefully mapped out after deglaciation of the valley. Numerous studies, notably Hallet and Anderson (1981), produced maps of these surfaces, making use of the solutional forms of the bedrock when it is in intimate contact with liquid water, and the evidence of clear abrasional erosion elsewhere. These maps commonly show sets of cavities, occupying significant fractions of the bed, linked to one another through relatively narrow passages. As we have seen above, this "linked cavity" system is now a dominant feature of many conceptual models of the subglacial hydrologic network.

## Large-scale erosional forms

This brings us to the large-scale erosional forms imposed by glaciers on the landscape. We all learn in introductory geology classes that one can identify a valley that has been shaped by glaciers when it has a U-shaped cross section, and when it is dotted with alpine lakes. Hanging valleys whose floors are perched well above the floor of a main valley are also attributed to glaciers. But just how do these features become imprinted on the landscape? This is in fact a topic of considerable recent and ongoing research.

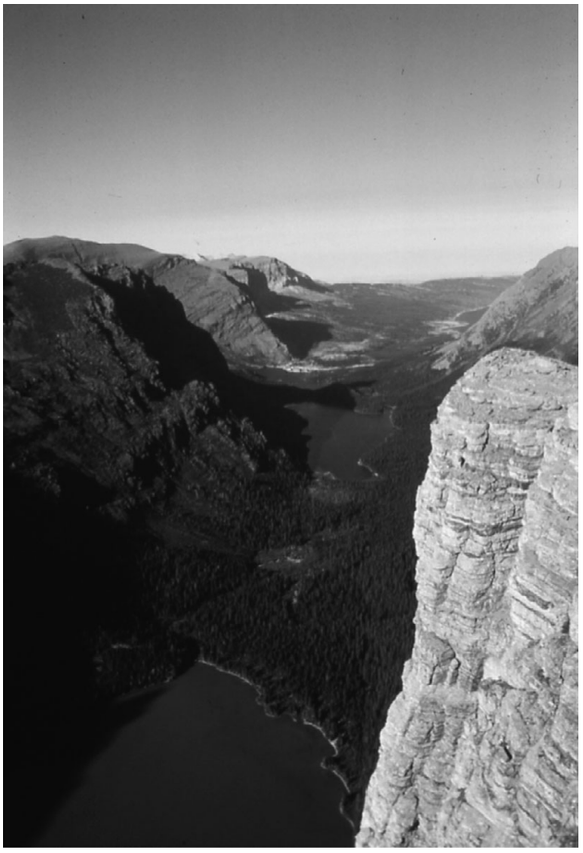

**Figure 8.46** U-shaped valley in Glacier National Park, Montana. View from Angel Wing looking east. Valley long profile is punctuated by numerous water-filled depressions separated by bedrock sills. (photograph by R. S. Anderson)

### The U-shaped valley

First let us deal with the cross section of a valley, an example of which is shown in the photograph in Figure 8.46. How does a classic V-shaped cross section indicative of fluvial occupation of a valley get replaced by a U-shape? And how long does it take?

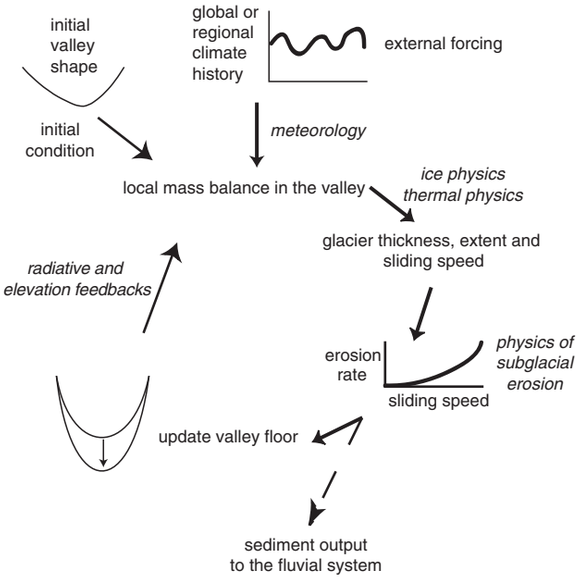


**Figure 8.47** Structure of a glacial landscape evolution model. Relevant processes are in italics. Model is initiated by a specified valley geometry (the initial condition), and is driven by a specific climate history (external forcing, which here serves as a boundary condition on the glacier surface). Local valley geometry modifies the global or regional climate to generate the local mass balance profile on the glacier. Ice physics determines motion of the ice, which is thermally dependent in that both the viscosity of the ice and the ability to slide are dictated by the temperature of the ice. The sliding pattern dictates the pattern of subglacial erosion, which then both modifies the bed and generates sediment that is passed to the river downstream. The modified valley profile can then modify the local mass balance by both radiative feedbacks (hiding in a deeper valley) and elevational feedbacks that dictate both local temperatures and rates of snow accumulation. The red arrows form a loop that is repeated, interacting with the external world through climate forcing and delivery of sediment from the system.

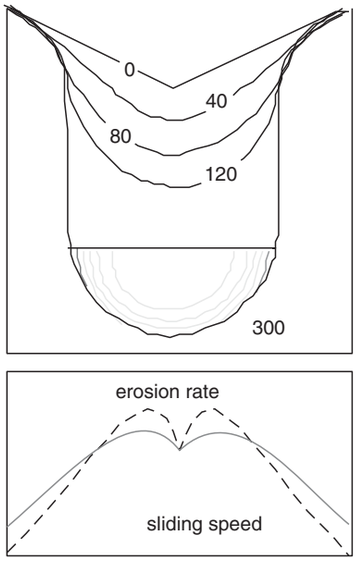


**Figure 8.48** Numerical simulation of cross-valley profile evolution during steady occupation of the valley by a glacier. Initial fluvial V-shaped profile evolves to U-shaped profile characteristic of glacial valleys in roughly 100 ka, given the sliding and erosion rules used. Bottom graph shows initial distribution of sliding speed and corresponding erosion rate. Low erosion rates in valley center allow faster rates along the walls to catch up. Final erosion rate is roughly uniform, causing simple downwearing of the U-shaped form. (redrawn from Harbor, 1992, Figure 5)

Jon Harbor has addressed this problem using a two-dimensional glacier model (Harbor, 1992, 1995). We summarize the model strategy in Figure 8.47. As in most models of landscape evolution, an initial landscape form is assumed (the "initial condition"), the glacier flow through that landscape is assessed, the pattern of erosion is calculated, the landscape shape is updated, and the flow is then recalculated. In the first suite of model runs, the glacier is allowed to achieve a steady discharge through the cross section, after which the ice discharge remains the same. In other words, climate change is ignored. The pattern of sliding, and hence of erosion, in the valley bottom is non-uniform, leading to the evolution of the shape. In particular, the sliding is reduced in the bottom of the triangle, and the sliding rate reaches a maximum in the middle of the valley walls. This results from the dependence of the sliding rate on the water pressure field assumed in the glacier, which Harbor assumed to be steady at 80% of flotation. As seen in Figure 8.48, his leads to widening of the valley walls with time. The form of the valley evolves toward one in which the form no longer changes (a steady form), and that subsequently propagates vertically as a U-shape form. In more elaborate model runs, Harbor explored the role of glacial cycles on the evolution of the valley cross section. He found that sufficient shape change occurred over roughly 100 ka that the imprint of glacial occupation of alpine valleys could be imparted in as little as one major glacial cycle.

## Cirques, steps, and overdeepenings: the long valley profile

The shape of a glacial valley in the other dimension is just as characteristic. In contrast to fluvial bedrock

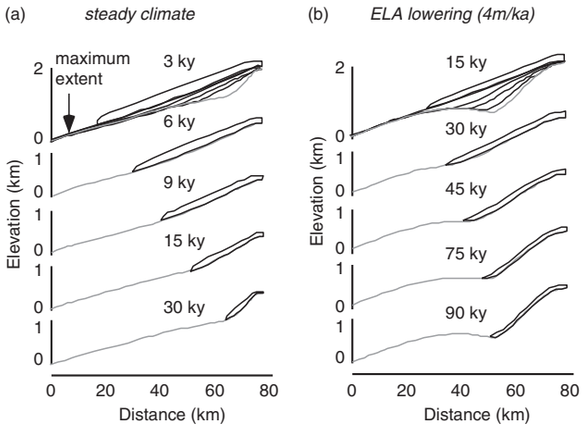


**Figure 8.49** Numerical models of long valley profile evolution of a glaciated valley in the face of (a) steady climate, over 30 ka, and (b) climate in which the ELA lowers at 4 m per thousand years, for 90 ka. Initial profile is a linear (uniform slope) valley. Top diagram shows all time slices in the respective simulation as light lines. (redrawn from Oerlemans, 1984, Figure 4)

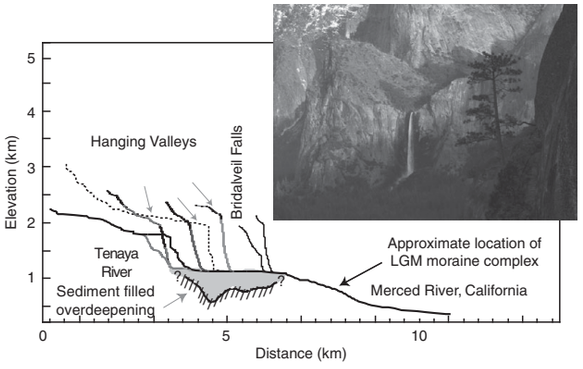


**Figure 8.50** Longitudinal profile of Yosemite Valley the Merced and Tenaya Rivers, and several of their tributaries, showing steps, hanging valleys and overdeepenings (after MacGregor *et al*., 2000, Fig. 1), and photograph of Bridal Veil Falls, which occupies a classic hanging valley tributary to the main valley of the Merced River. (photograph by Greg Stock)

valleys, which display smooth concave up profiles, glacial valley profiles display steps and flats. Many of these steps occur at tributary junctions. In addition, the upper portions of alpine glacial valleys display knobby less well-organized topography rather than the expected smooth U-shape. Finally, many tributary valleys are said to hang above the trunk valleys upon deglaciation. The valley system disobeys what has come to be called "Playfair's law," which states that the trunk and tributary streams join "at grade" (see discussion of this in Chapter 13 on bedrock rivers).

Oerlemans (1984) was the first to attempt to model these features numerically. By embedding an erosional rule in a one-dimensional glacial model, he simulated the evolution of valley long profiles. His chief results in alpine glacial settings are shown in Figure 8.49. The model glaciers were driven by a simple climate in which the ELA was allowed to vary sinusoidally through time, which in turn moved a mass balance profile up and down. Interestingly, the glacial valley deepened so dramatically over several glacial cycles that the glaciers declined in size through time. While Oerlemans countered this by asserting a net cooling of the climate, the effect may be real. Glaciers likely do deepen their valleys through time. In so doing they both hide more effectively from direct insolation, reducing the melt rate, and decline in elevation, which should both reduce accumulation and increase melt rate.

More recently, MacGregor *et al*. (2000) targeted the stepped nature of the long valley profile. The bedrock profile from Yosemite Valley reproduced in Figure 8.50 serves as a target for such models. Again a one-dimensional glacial long valley model was employed in which a net mass balance pattern was imposed. A simple balance profile pivoted about the ELA, and climate change was modeled by an imposed history of ELA scaled to the $\delta^{18}O$ deep sea record. Glacier dynamics included both internal deformation, and a rule for sliding. As in Harbor's models, the algorithm for sliding included an imposed water table, and assessed the sliding rate based upon the effective stress. The rule for the erosion rate was varied between model runs, but in all cases involved the sliding rate. The basic patterns produced were found to be insensitive to the rule chosen. As you can see in Figure 8.51, models of the single trunk glacier valley inevitably resulted in flattening of the valley floor down-valley of the long-term mean ELA and steepening of the valley profile up-valley of this. Only when more complicated valleys were modeled did a discrete step in the valley floor appear. In model runs including a single tributary valley, the erosion of the tributary valley floor was outpaced by that of the adjacent trunk stream, leading to disconnection of the two profiles, and a step appeared in the main valley. This led to the generation of model hanging valleys,

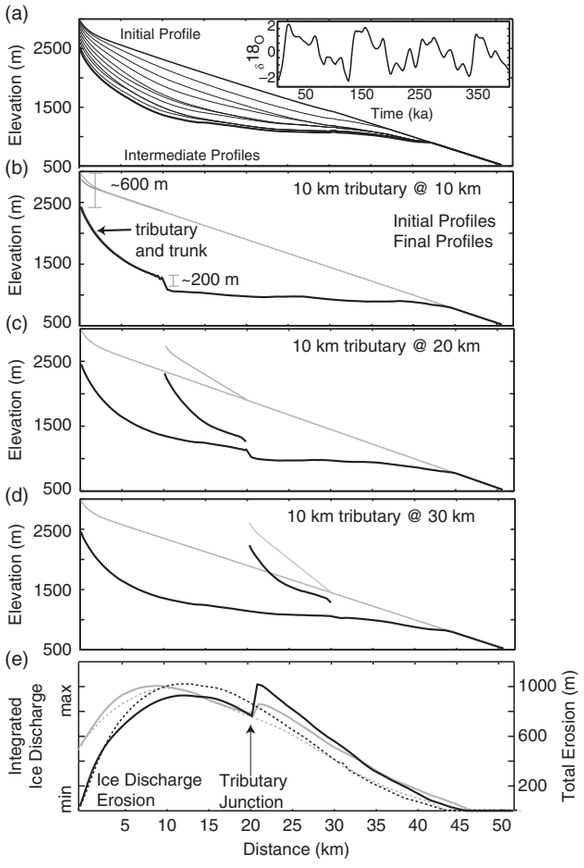


**Figure 8.51** Modeled evolution of the long profile of a valley with one tributary subjected to repeated glaciation. Steps develop in the valley profile, and the tributary valley is hung. The height of the step and the height of the hang depend upon the position of the tributary, and the long-term ice discharge. (after MacGregor *et al*., 2000, Figure 3)

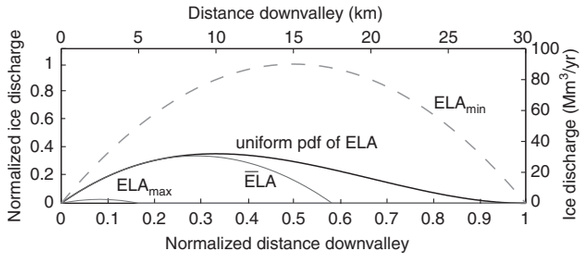


**Figure 8.52** Analytic solution for ice discharge patterns resulting from steady-state glaciers driven by a simple mass balance function, in a linear valley profile, and a uniform distribution of ELAs. Maximum and minimum glaciers corresponding to minimum and maximum ELAs, respectively, are shown along with the glacier discharge expected from the average ELA, and a long-term average resulting from a uniform distribution of ELAs between maximum and minimum. The symmetry is broken when a distribution of ELAs is permitted. Maximum discharge occurs down-valley from that corresponding to the mean climate, at roughly one-third of the glacial limit (the maximum terminus position), and smoothly tapers to zero discharge there. Distance and ice discharge are normalized using glacier length and ice discharge associated with the lowest ELA. (from Anderson *et al*., 2006a, Figure 7, with permission of the American Geophysical Union).

and associated steps in trunk valleys depicted in Figure 8.51. A chief result of the calculations was that the long-term pattern of erosion mimicked the pattern of long-term discharge of ice. Tributary valleys see less ice discharge than trunk streams that drain larger areas. Trunk streams immediately down-valley of a tributary must accommodate the long-term discharge of ice from the tributary, and therefore see more ice.

That the time steps in these complex models had to be very small in order to maintain numerical stability meant that it was difficult to explore a wide range of valley shapes. Anderson *et al*. (2006) build upon the observation that ice discharge was a faithful proxy of erosion rate in MacGregor's models. They employ analytic models of ice discharge patterns based upon the assumption that the glacier is at all times close to steady state. This implies that the discharge must at all times reflect the integral of the mass balance up-valley of a point, as we deduced from Equation 8.3. These simplifying assumptions allow efficient exploration of the roles of climate variability and valley hypsometry (distribution of valley width with elevation). They show in Figure 8.52 that in the simplest case of a linear mass balance profile and a uniform width glacier, a parabolic divot should be taken out of the valley floor, with the maximum of erosion located where the ELA intersects the valley profile. As in MacGregor's models, the valley flattens down-valley of the ELA and steepens up-valley of it. Incorporation of climate variability can be accomplished in a couple ways. One could simply assert a history of the ELA, and numerically chop out parabolas of differing magnitudes and lengths. More efficient still, one can assert a probability distribution function (or probability density function, pdf, see Appendix B) that captures the spread of ELAs. The pdf of the $\delta^{18}O$ curve, reported in Figure 8.53, looks approximately Gaussian over the last 3 Ma since global scale glaciations began in the last glacial cycle.

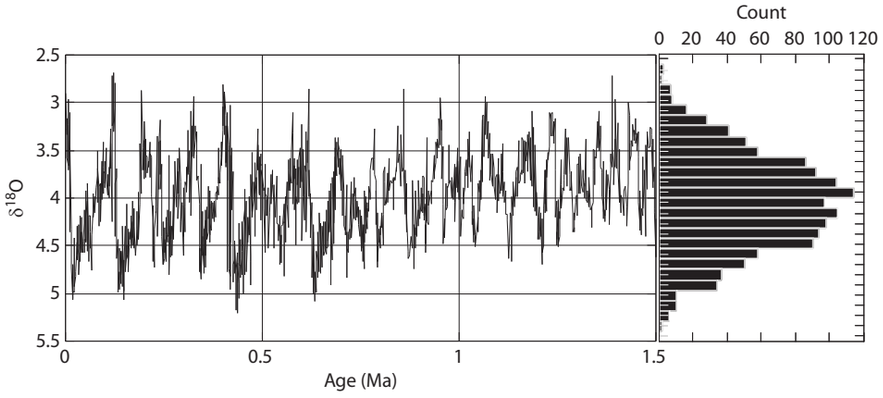


**Figure 8.53** Marine isotopic record for last 1.5 Ma (after Zachos *et al*., 2001), and a histogram of it. The distribution is roughly symmetric, and appears to be normally distributed (after Anderson *et al*., 2006a, Figure 10, with permission of the American Geophysical Union)

Using this pdf, they show that the erosion pattern should feather into the fluvial profile down-valley, and that again the maximum of erosion occurs where the long-term ELA crosses the valley profile. This simple expectation can break down when more realistic plan view shapes of valleys are acknowledged. Most glacial valley systems are much wider in the headwaters than they are in their lower elevations, reflecting the inheritance of the dendritic fluvial network. The ice discharge pattern predicted from Equation 3 must therefore include both the pattern of mass balance and of valley geometry (width). But recall that the principal driver of erosion is the sliding rate. Ice discharge per unit width of the valley should be a better proxy for the sliding rate. This means that where the valley narrows, more ice is being shoved through per unit width than in a wider portion of the valley. When this element of reality is incorporated in the analytic models, the pattern of erosion begins to include a bench in the upper valley, below which the erosion rate increases dramatically. This reflects funneling of the ice into a narrower throat as the tributary valleys coalesce in the headwaters.

**Figure 8.54** Kilometer-tall walls of Precambrian granite tower above Sam Ford Fjord, eastern coast of Baffin Island. Sea ice covers an 800 m-deep fjord, which reaches its greatest depth where it crosses the island-bounding mountain range. (photograph by R. S. Anderson)

## Fjords

The ornamentation of coastlines and shelves by fjords is a characteristic of continents that have harbored large ice sheets in the past. An example from eastern Baffin Island is shown in the photograph of Figure 8.54. The coastlines of Greenland, Fennoscandia, New Zealand, Patagonia, and Antarctica are decorated with deep fjords that indent the coastline by many tens of kilometers. Fjords reach depths of more than 1 km below present sea level. For example, Sognefjord in Sweden is more than 1.2 km deep. This greatly

exceeds the lowstands of sea level during glacials (order 100–150 m), and therefore requires submarine erosion of rock. Rivers cannot accomplish such erosion, as their power dissipates upon entering the ocean, which in turn generates the sedimentary deltas that characterize their entrance. Fjords are instead gouged into the continental margins by glaciers. They bite deeply into the landscape, reaching more than 100 km inland from the coast, in places punching through coastal mountain ranges (for example, in Baffin (Kessler *et al*., 2008), in the Transantarctic Mountains (Stern *et al*., 2005), and in British Columbia. The first two cases correspond to the mountain ranges that correspond to the uplifted flanks of rift margins. Here recall the isostatic rebound calculation of rebound associated with these fjords, reproduced in Figure 4.35. In such situations, the greatest depths of the fjords occur as they pass through the crest of the range. You can see this by inspecting the profiles in Figure 8.55. At their upstream heads, fjords gradually lose definition and feather into the landscape in "onset zones." At their downstream edges, fjords extend onto the continental shelf as fjord troughs and often terminate in a bedrock sill. The deep water in the base of a fjord is therefore somewhat isolated form the ocean, and houses a distinct ecology. In detailed mapping and cosmogenic radionuclide analysis of fjorded landscapes on Baffin Island, Briner *et al*. (2006) have shown that significant erosion in the last glacial occupation of the landscape was limited to the fjords themselves. They interpret the lack of erosion in inter-fjord regions to the polar thermal condition of the bed there. Ice was presumably thin, cold, and slow on the inter-fjord flats, while it was thick, temperate, and fast in the fjords.

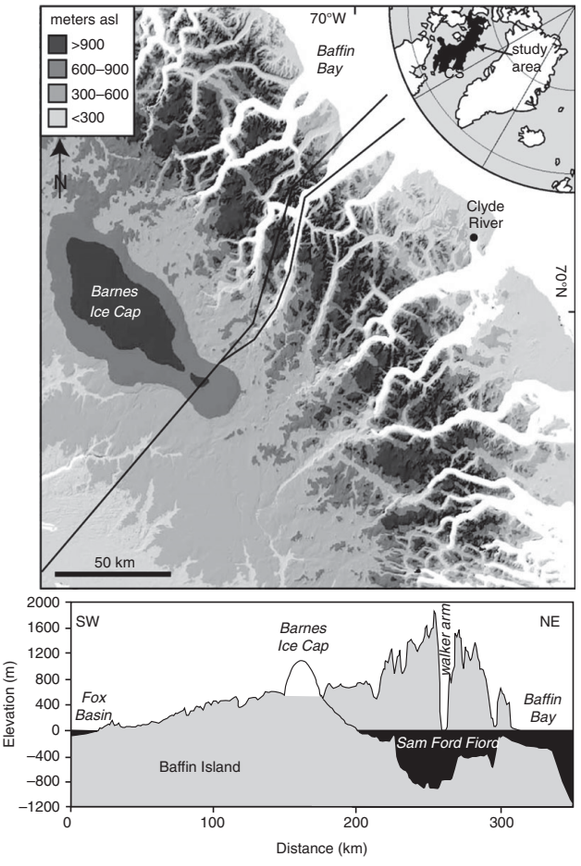


**Figure 8.55** Baffin Island fjorded topography. Top: the fjorded continental edge of northeastern Baffin Island showing the inland plateau, on which the Barnes Ice Cap sits, and the fringing mountain range. Inset: location of Baffin Island in the western Arctic. Bottom: topographic cross section of Baffin Island, along Sam Ford Fjord and neighboring topography, following transect lines shown in map. (after Kessler *et al*., 2008, Figure 1, with permission from Nature Publishing Group)

Fjords serve as the major conduits through which ice from present-day ice sheets enters the ocean. In Greenland, for example, 40% of the ice leaving the continent leaves through the three main fjord-occupying outlet glaciers of Jacobshaven, Kangerdlugssuag and Helheim (Bell, 2008). Combining this observation with the fact that fjords owe their origin to erosion by glacial ice leads us to ask (1) how the early icehseets of the last glacial cycle, say 2–3 Ma, operated in the absence of such efficient conduits for ice from the interior, and (2) how rapidly the present fjords were eroded into the continental edges?

While the latter question awaits analysis through thermochronology, the former can be addressed through modeling. Employing a two-dimensional glacier model, Kessler *et al*. (2008) have simulated how fjords might have evolved through time in a simplified landscape that includes a circular continent with a bounding mountain range meant to mimic a rift flank range. The model setup is shown in Figure 8.56. They demonstrate that once the ice sheet is thick enough to overtop the mountain range, ice from the interior is steered through any mountain pass. As erosion rate is tightly correlated with ice discharge, this leads to preferential erosion of the passes relative to the surrounding range. This dimples the contours of the ice sheet well upstream from the mountain pass, which steers yet more ice toward

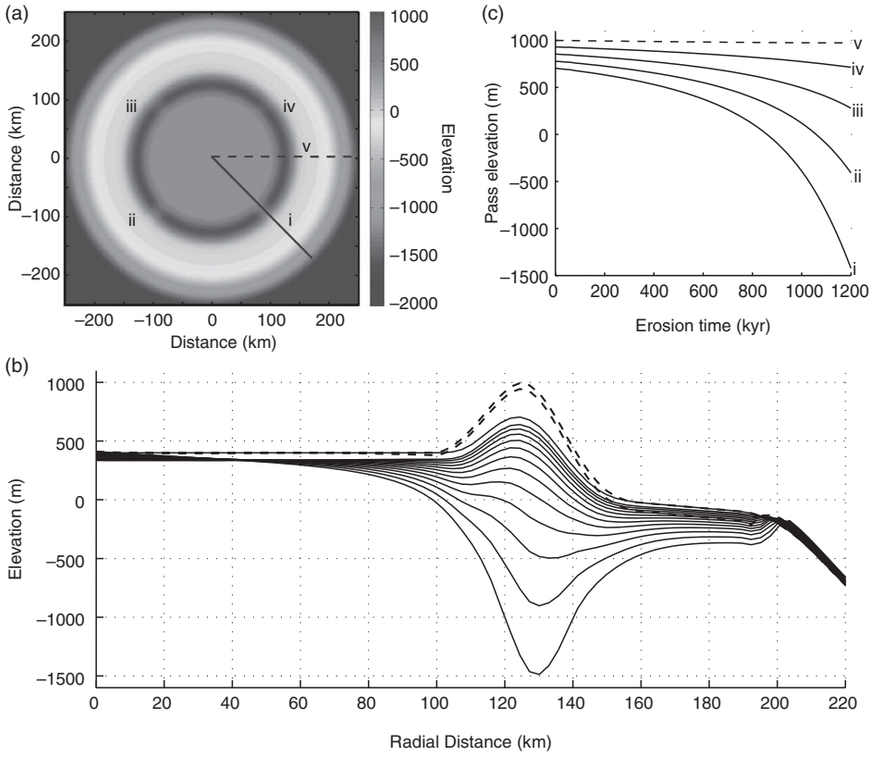


**Figure 8.56** Evolution of model topography. (a) Initial synthetic bed topography. Fringing mountain range is dissected by four valleys with varying depths. (b) Evolution of a fjord; thin solid lines indicate bed profiles at 100 ka time steps for the deepest valley at transect "i" in (a); dashed bold lines indicate the initial and final topographic profile at the range crest at transect "v" in A. (c) Elevation through time at the radial position of the initial crest for each of the four passes (i, ii, iii, iv) and the crest (v). (after Kessler *et al*., 2008, Figure 2, with permission from Nature Publishing Group)

the pass. The deeper mountain passes out-compete their neighbors, leading to a few dominant fjords that efficiently tap ice from the interior. Just as those in Baffin Island, the simulated fjords are deepest as they cross the range crest. This reflects the fact that ice discharge per unit width is greatest there: as seen in Figure 8.57, upstream, the ice is converging; downstream, the ice diverges. Because the two-dimensional model employed in these simulations did not have a thermal component, meaning that it could not simulate the variation in thermal conditions at the bed, the authors argued that the ice steering–erosion feedback was sufficient to allow deep fjords to form. The thermal feedbacks should serve to magnify this pattern.

The exploration of the effect of presence or absence of fjords and associated outlet glaciers on the behavior of ice sheets has only begun. In preliminary experiments, Kessler *et al*. (2008) have shown that the presence of fjords indeed influences the behavior of the ice sheet, for example by altering its response time to variations in climate. This could potentially influence the degree to which ice sheets are controlled by the various periods of orbitally controlled insolation.

## Depositional forms

Glacial deposits come in many shapes and forms, including isolated glacial erratics (an example of which is shown in Figure 8.58), and are the subject of numerous books. The reader is pointed to Menzies (1996), to Bennett and Glasser (1996), and to Benn and Evans (1998) for more comprehensive summaries of this portion of the glacial system. We treat here only the basics. Many glacial deposits consist of poorly sorted sediments that run the gamut in terms of grain size; they were once called boulder clays and are now called simply tills. The first-order classification comes from distinguishing those materials that have seen the bed of the glacier, from those that have not.

### Moraines

Many moraines, be they lateral (on the edges), terminal (at the terminus), or medial (down the middle), are derived from supra-glacial debris, debris that has never seen the bed of the glacier. While this might be

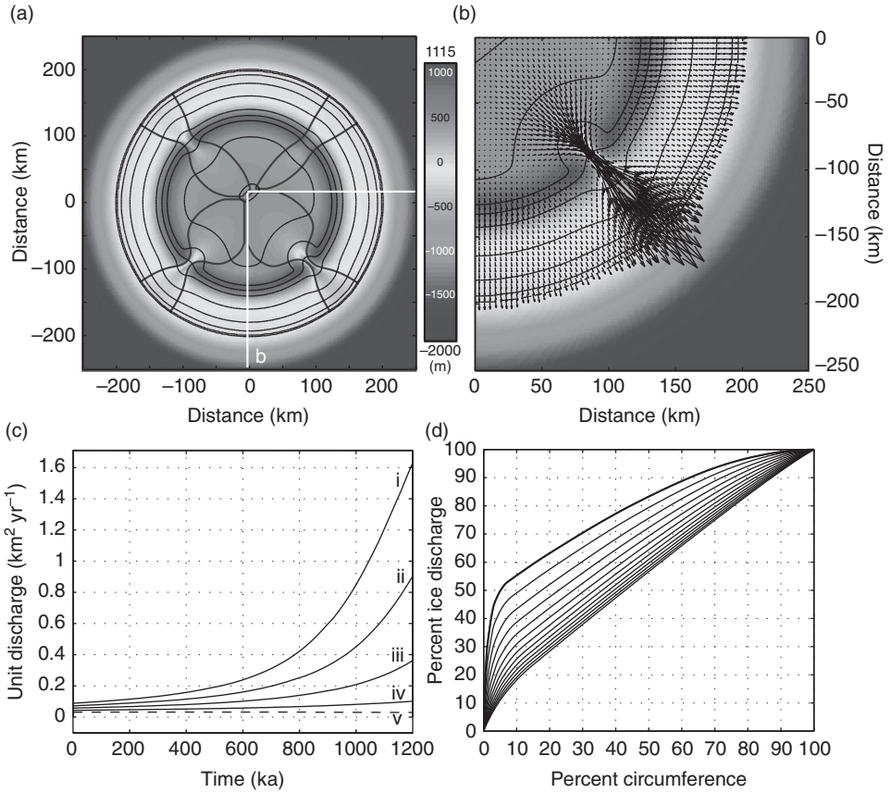


**Figure 8.57** Modeled ice surface, bed elevation, and ice velocity pattern after 1.2 Ma. (a) Bed elevation in false color. Thin black lines denote ice surface contours. Bold lines demark interior regions that drain through each of the four valleys. (b) Ice velocity vectors in the quadrant of the deepest valley (outlined in (a)). (c) Maximum specific ice discharge versus time along the five transects in Figure 8.56(a). (d) Percentage ice discharge along the crest (125 km from center) versus percent crest length through which that discharge passes; curves show time intervals of 100 ka. The discharge of ice from the landmass becomes increasingly dominated by that exiting the fjords. (after Kessler *et al*., 2008, Figure 3, with permission from Nature Publishing Group)

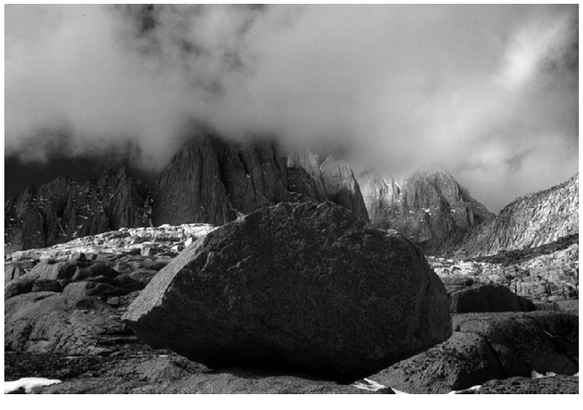

**Figure 8.58** Glacial erratic in glacial valley floor east of Mt Whitney in the Sierras. Isolated block of granite lies on granitic bedrock, but was transported into place in the last glacial maximum glacier. (photograph by R. S. Anderson)

obvious in the case of the lateral moraines, which are accumulations of debris found along the margins of a glacier, and are often delivered to those sites by hillslope processes, it is less clear for the other two classes of moraines. Lateral moraines consist largely of angular blocks riven from the valley walls by periglacial processes, and delivered by individual rockfall events, landslides, or avalanches that incorporate rocky debris as they slide against the wall. Rarely are there blocks that show striated facets indicating time spent at the glacier bed. A point of caution: it is worth noting that some lateral moraines near present day margins of glaciers are ice-cored. These are not the simple triangular piles of rock that they look to be, but are instead a rather thin carapace of angular rock covering glacial ice.

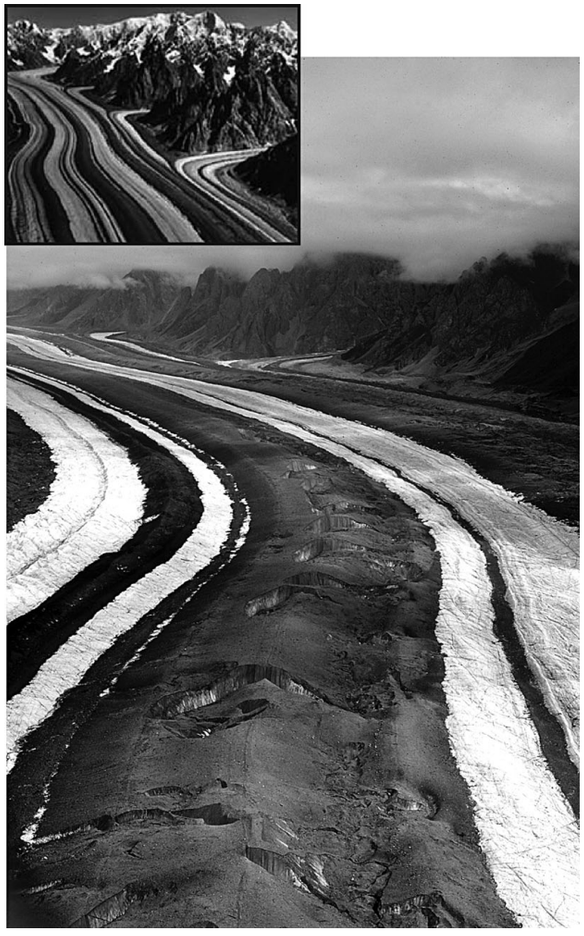

**Figure 8.59** Barnard Glacier, in Alaska's Wrangell–St. Elias National Park. This glacier's many tributaries make it famous for its medial moraines. Inset: Austin Post air photograph held at World Climate Data Center. Main image: lower flight allows view of the main medial moraine in the glacier centerline, showing how thin the debris cover is – one clast thick in most places. It also reveals how each moraine is a ridge with debris-rich ice emerging at its center. (photograph by R. S. Anderson)

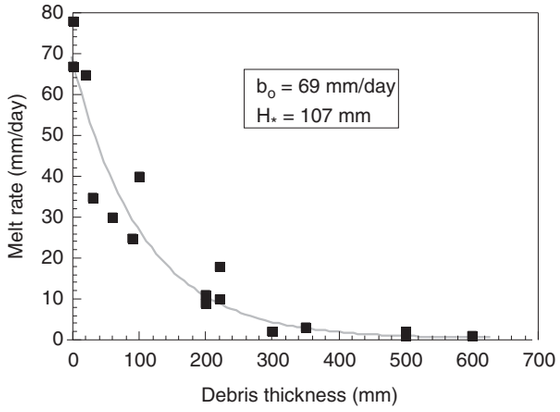


**Figure 8.60** Dependence of ice ablation rate on debris thickness. Note scale length for exponential decay of ablation rate is roughly 11 cm. (after Anderson, 2000, Figure 5, with permission from International Glaciological Society; data from S. Lundstrom, 1992).

Terminal moraines are accumulations of debris at the snout or terminus of a glacier. The larger terminal moraines are generated when a glacier remains in the same position for some time, continuing to deliver debris to the margin on an annual basis. Upon retreat, this pile of debris is left behind. Smaller piles may be generated each year (annual moraines) as a signature of the retreat history.

Medial moraines are the dark stripes we see gracing the interiors of many longer glaciers. Some of the more famous are in Alaska. There is no less striking evidence that the flow of ice is laminar, and that most glaciers are very steady in their motion, than that these debris stripes are so parallel to the margins of the glacier. In fact, it is the rare exceptions to the straightness of these medial moraines that indicates that something has "gone wrong" up one or another tributary; the looped moraine signature of a surging glacier is telltale, as seen in Figure 8.26. While there are exceptions, by far the majority of the medial moraines result from the welding together of lateral moraines at interior tributary junctions such as those on Barnard Glacier in the photos of Figure 8.59. The debris is swept into the seam between the two ice streams. It is angular debris, and has never seen the bed. The ice on either side of the seam has very little debris content, while that in the seam has at least some. In the ablation zone, below the ELA, this debris emerges at the surface as the ice melts. Because the ice can melt (and therefore vanish), while the debris cannot, the debris accumulates on the surface of the glacier. At this point another element comes into play, however. The presence of any significant debris on the surface of the ice leads to reduction of the melt rate of the ice. As shown in Figure 8.60, only 10 cm of debris reduces the melt rate by a factor of $e$ (2.72). So the adjacent debris-free glacier surface melts faster, leaving the debris covered ice higher. This produces a slope away from the debris cover, which in turn promotes the downslope motion of

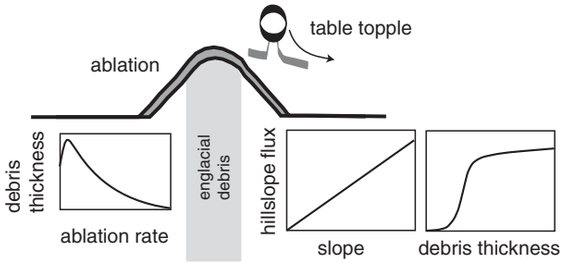


**Figure 8.61** Schematic of medial moraine problem. Debris from a debris-rich septum of ice (gray) emerges at the surface at a rate dictated by the ablation rate. Debris ravels down the slope by the "table topple" mechanism at a rate that depends upon slope. The total debris discharge depends on both local slope and debris concentration. The moraine widens beyond the margins of the debris-rich septum through time. The moraine crest is convex, while the side slopes beyond the debris-rich ice septum are straight.

the debris sketched in Figure 8.61. The result is a stripe of debris that widens downglacier as more debris emerges on the surface, and is continually being spread laterally. Walking on practically any portion of a medial moraine will reveal that the hillslope processes are indeed very efficient. The debris is everywhere very thin, usually only one clast thick (see this in crevasses that cut the medial moraines in the low-level air photo of Figure 8.59). Medial moraines typically display a rounded crest and relatively straight limbs. Indeed, this problem has been treated as a hillslope evolution problem (Anderson, 2000), resulting in parabolic profiles. We will see in Chapter 10 that this is the expected steady-state profile of a hilltop. Finally, we note that while these debris stripes add to the visual drama of a glacier, the debris is so thin that medial moraines are rarely preserved in the geomorphic record after deglaciation.

An interesting feedback occurs in complicated glacier networks. As each tributary junction spawns a new medial moraine, and as every moraine widens down-glacier, it is common for these medial moraines to merge, eventually covering the entire glacial cross section with debris. This will inevitably lead to the reduction in the mean ablation rate, and will promote the longer extent of a glacier. This appears to be the case, for example, in the Karakoram Range, where highly debris covered snouts of glaciers extend well down the valleys. Similarly, in the easily eroded volcanic rocks of the Wrangell Range in Alaska, debris-covered glacial snouts abound, as seen in Figure 8.62, as do rock glaciers.

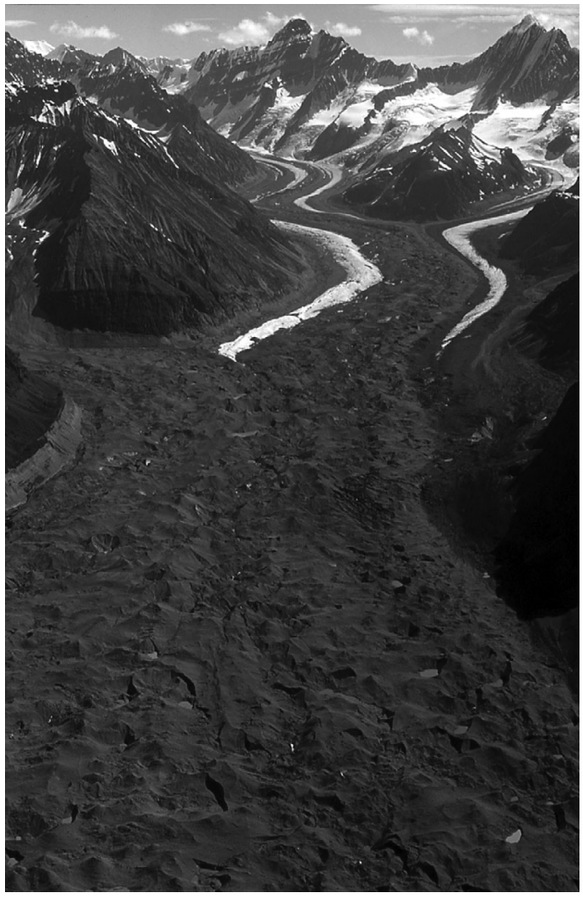

**Figure 8.62** Debris-covered snout of a glacier draining the high Wrangell Mountains of Alaska. The easily eroded volcanics that dominate the geology of this range generate debris in sufficient quantity to create wide medial moraines that merge in the terminal reaches of the glacier. This in turn prevents ablation, and promotes longer glaciers than the climate would otherwise suggest. These debris-mantled terminal reaches are very difficult to travel across. They are dotted by numerous small lakes, the steep walls of which are often the only bare ice in the area.

## Eskers

There is one distinctive depositional feature attributable to the subglacial fluvial system: eskers. These are sinuous ridges with triangular cross sections that consist largely of gravels. They can be up to several tens of meters in relief. An esker represents the operation of a subglacial tunnel through which significant volumes of surface meltwater passed, entraining and transporting the gravel as it did so. As such, their present shape and location in the landscape provides

evidence of the hydrologic and glaciological conditions during which they formed. The most extensive systems of eskers were formed beneath the continental scale ice sheets.

One of the most striking features of eskers is that they do not obey the contours of the landscape on which they currently rest. This could be explained in two ways. The first is that these conduits in which the gravels were initially deposited were englacial rather than subglacial conduits, and were simply laid down over the landscape as the glacier retreated. The second is that they are indeed subglacial, and that something inherent in the subglacial hydrologic system allows water to flow uphill. Sounds outrageous, but this is the most likely. Arguments against the englacial explanation include the fact that the gravel deposits have intact stratigraphy that is not deformed by such a superposition on uneven ground. Most importantly, however, the apparent uphill flow of subglacial water, the details of where this uphill flow occurs, and the style of deposition in the various divides, can all be explained. We are very used to thinking about water responding only to topographic gradients, as it does when running in open channel flow on the surface of the Earth. But eskers represent flow in closed conduits – pipes – beneath the glacier. Just as water in a hose can be made to flow upward by water pressure gradients, so too is the flow in the conduits dictated by horizontal gradients in pressure, running down-gradient. The pressure field is governed not only by the bed topography, but also by the ice thickness profile, which involves both the ice surface and the bed profiles. The tilted nature of the equipotentials is plotted in the schematic cross section of a glacier in Figure 8.63. The equation dictating the potential field is that for the total head, which is the sum of the elevation head, and the pressure:

$$\phi = \rho_w g z + \rho_i g (H - (z - z_b)) \tag{8.33}$$

where $z$ is the elevation, $z_b$ the elevation of the bed, and $H$ the thickness of the ice. Water within a glacier or an ice sheet flows perpendicular to lines of equipotential within the glacier. These lines, or planes of equipotential, can be calculated by setting the gradient, $d\phi/dx$ to zero:

$$\frac{d\phi}{dx} = \rho_w g \frac{dz}{dx} + \rho_i g \frac{d(H - (z - z_b))}{dx} = 0 \tag{8.34}$$

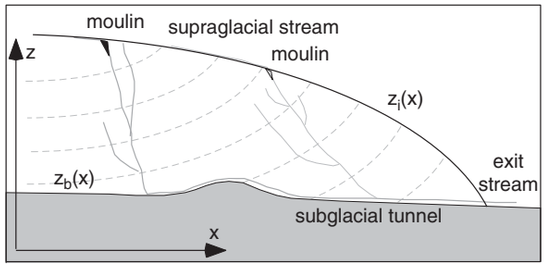


**Figure 8.63** Schematic of the water flow paths within a glacier profile. Melt water enters the glacier through moulins and crevasses. Englacial water flows normal to equipotential lines (dashed) until it encounters the bed. Flow at the bed occurs in tunnels in the ice and/or the bed; flow speed is dictated by pressure gradients. These are more strongly determined by the ice surface gradient than by the bed gradient. (after Shreve, 1985b, Figure 4)

Solving this for the dip of the equipotential lines, $dz/dx$, we find that

$$\frac{dz}{dx} = \frac{\rho_i}{\rho_w - \rho_i} \frac{d(z_b + H)}{dx} = \frac{\rho_i}{\rho_w - \rho_i} \frac{dz_s}{dx} \tag{8.35}$$

As we can see from Equation 8.35, and from Figure 8.63, the lines of equipotential essentially mirror the topographic contours of the ice surface, but dip $11 \times (917/(1000 - 917)$ times more steeply than does the surface. The flow field of water within the glacier is therefore canted at a high angle to the surface, pointing down-glacier. When the englacial channels intersect the bed, of course, the flow is trapped at the ice-rock interface. It must still obey the potential gradient. The equation for the head gradient (the derivative of Equation 8.33) has two terms, one related to the ice surface slope, the other to the bed slope. We now seek the expression for the potential gradient along the ice-rock interface, i.e., when $z = z_b$:

$$\frac{d\phi}{dx}|_{bed} = (\rho_w - \rho_i) g \frac{dz_b}{dx} + \rho_i g \frac{dz_s}{dx} \tag{8.36}$$

The term associated with the bed slope, $dz_b/dx$, is one-eleventh as important as that associated with the slope of the surface of the ice, $dz_s/dx$. The flow will go in the down-glacier direction, i.e., in a positive $x$-direction, as long as this gradient is negative (flow is driven down potential gradients). This requires that

$$\frac{dz_b}{dx} < -11 \frac{dz_s}{dx} \tag{8.37}$$

For example, if the surface of the ice slopes at −0.01, or 10 m/km downglacier, then water will continue to flow downglacier as long as the bed slope is less than 0.1. This is a steep *upward* slope. When the ice sheet is removed to reveal the esker deposit, it looks as if the water in the subglacial tunnel had flowed uphill, while in fact it had flowed down the potential gradient. The bottom line is that the surface topography of the glacier is 11-fold more important in dictating the direction of flow than is the topography of the landscape over which it flowed.

One of the classic examples of esker systems is the Katahdin esker system, in Maine. This system extends 150 km from central Maine to the calving margin at roughly the present coast. In a pair of papers, Shreve (1985a,b) uses the physics of water flow in a subglacial conduit to explain a wide variety of the features of these eskers. As one follows any particular esker down-ice, the esker disobeys present day contours in a particular way, and it changes shape in a characteristic pattern. Shreve first explained these patterns, and then made use of them to reconstruct the shape of the ice sheet covering this portion of Maine around 14–16 ka. As shown schematically in Figure 8.64, the shape change is such that on the flat the esker tends to be sharp-crested, and triangular in cross section. As it climbs toward a divide, it first becomes multiple-crested, and then broad-crested, losing its triangular cross section altogether. Over the top of the divide, there may be a gap in the esker before it resumes its course, again sharp-crested. Shreve focused on what is happening to the water in the ice-walled tunnel. Heat is generated as the water flows, due to frictional interaction with the walls. This energy can be used either to warm up the water or to melt the walls or both. Note also that as the water flows into regions of thinner ice, it is moving into warmer ice (recalling the thermal profile within a Type II polar glacier). The faster the ice is thinning, the more of this energy being released must be consumed in warming the water to keep pace with the warming of the walls. If this pace of warming is not sufficient, the water will be below the pressure melting point of ice, and will freeze onto the wall. Shreve deduced that the condition for freezing is when the bed gradient is positive, and is more than 1.7 times the magnitude of the ice surface gradient. It is at this point that the ice is thinning too rapidly for the water to warm up fast enough. Rapidly melting walls allow ice with all its basal debris to move toward the ice conduit; in addition, the shape of the conduit is tall, the melting rates being highest where the water is deepest. Freezing walls pose the opposite case. With no new ice moving toward the conduit, the roof is low-slung, the freezing rates being highest there. New sediments are not supplied, and sediment already in the pipe is simply reworked, generating better sorted deposits.

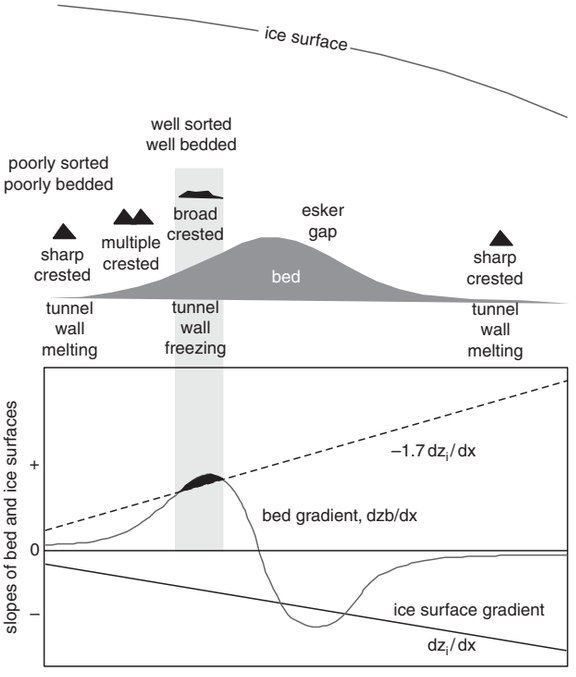


**Figure 8.64** Esker styles. Types of eskers and their locations in the topography beneath an ice sheet. Eskers evolve from sharp-crested on flat topography to multi-crested and broad-crested as the water in the subglacial tunnel is forced over a pass in the basal topography. (after Shreve, 1985b, Figure 6, with permission from Elsevier)

Shreve also reconstructed the ice surface morphology. Wherever he found well-defined transitions from sharp-to-broad crested, he could pin down the ice surface slope. In addition, he made use of the divergence between modern topographic gradient and the path of the esker over it to deduce the ice surface slope. As reproduced in Figure 8.65, at seven places along the 140 km Katahdin esker system, surface gradients constrained the shape of

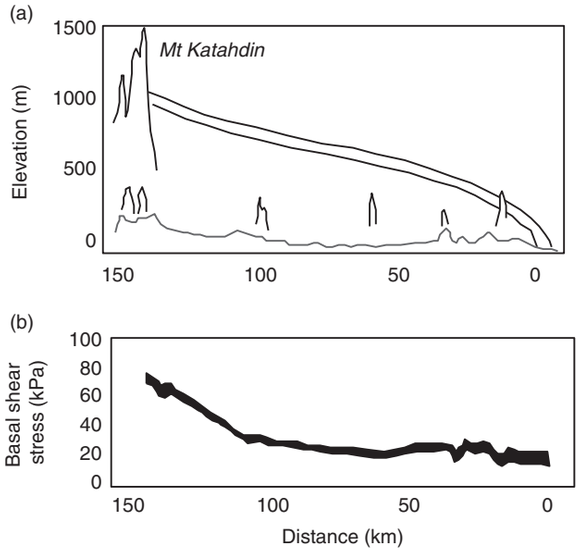


**Figure 8.65** (a) Profile of the ice sheet along flow line over Maine, through Mt. Katahdin, at roughly 11 ka, as deduced from esker topography (bottom continuous line) as it crosses various passes (isolated bumps). Two profiles shown bracket maximum and minimum estimates. (b) Basal shear stress profile for same section of the ice sheet. Stress is everywhere below 1 bar (100 ka) and over much of the profile is only 20–30 kPa. (after Shreve, 1985b, Figure 3, with permission from Elsevier)

the ice sheet, allowing recreation of the ice sheet profile at the time of operation of the esker system. The thickness profile was then integrated, constrained to have the proper surface gradient at each location. In other words, knowing $dz_i/dx$ at several locations, $z(x)$ was obtained by integration. Note that no assumptions were made about the rheology of the ice, its thermal profile, whether or not it was sliding, or the nature of the underlying material. This independently documented ice sheet profile could then be used to assess the pattern of the basal shear stress of the ice sheet. Recall that we used the assumption that the basal shear stress was uniform, and of the order of 1 bar ($10^5$ Pa), in our simple reconstructions earlier. Shreve found that the shear stress varied from $0.2–0.3 \times 10^5$ Pa (relatively low compared to estimates from modern ice sheets of about $1 \times 10^5$ Pa), and viewed this as supporting the claims of others that the history of the demise of the local portion of the Laurentide ice sheet from its last glacial maximum had been first to deflate (lower in slope), and then to retreat from its margins. This implies that the eskers were formed when the ice sheet was in its deflated state.

## Erosion rates

Just how efficient are glaciers at eroding the landscape? What means do we have of constraining erosion rates beneath hundreds of meters of ice? Our principal probe is the sediment output from glacial streams. By its nature, this yields only a spatially (and perhaps temporally) averaged measurement of the erosion rate. It is impossible to tell unambiguously where the sediment has come from beneath the glacier. Even so, this number is useful in that it allows comparison with fluvially dominated systems, and it allows comparison amongst glacial systems from which one might ferret out what variables are the dominant ones. If we can measure well the sediment discharge, $Q_{\text{sed}}$, then the spatially averaged rate of erosion of the glacier whose basal area is $A_{\text{glacier}}$ is

$$\bar{e} = \frac{Q_{\text{sed}}}{A_{\text{glacier}}} \tag{8.38}$$

It is not at all trivial to measure sediment load in a river, however. As discussed in the fluvial chapter (Chapter 12), one must measure both suspended sediment and bedload transport rates. Using this method, one can obtain a near real-time record of the sediment output from the glacier. There is no doubt that this records the sediment output from the glacier. We are not assured, however, that this is equivalent to the rate at which sediment is being produced by erosion at the glacier bed. The problem is that sediment can be stored temporarily at the glacier bed, to be exported from the subglacial system later.

An intermediate timescale (one to several years) estimate of erosion rates can be obtained in special circumstances. In Norway, some of the hydropower used in the nation derives from water tapped subglacially. Sediment loads in the subglacial water, which could damage the turbine blades, is diverted into reservoirs to trap the sediment. The traps are emptied periodically, and the number of truck loads can be tallied to estimate the volume of sediment involved since the last cleaning.

Another technique yields yet longer-term rates of glacial erosion. This relies upon the volume of sediment in a depositional basin that was transported to the site from a glacial basin over a given period of time. For example, the basin may be a lake (e.g., Loso *et al*., 2004), the interior of a fjord (e.g., Powell and Molnia, 1989), or the continental shelf of Alaska. Drilling the deposit, or seismically imaging it, can constrain the geometry and hence the volume of the deposit. And time lines can be drawn within it by obtaining an age from one or another marker horizon within the deposit.

The results of many studies utilizing these methods have been summarized by Hallet *et al*.. Their summary plot is reproduced in Figure 8.66. The rates vary greatly, but can range up to several milimeters a year. They also vary in a systematic way geographically. The glacial basins in Alaska are very productive of sediment, while those in Norway are one to two orders of magnitude less so. This presumably reflects both the erodibility of the substrate and the delivery of snow to the region. The Alaskan coast is dominated by young rocks of an accretionary prism, while the Norwegian coast is a Precambrian shield. And the Alaskan bight enjoys huge snowfalls relative to Norway. A steady-state Alaskan glacier must therefore transport much more ice down-valley than its Norwegian counterpart. To the degree to which this is accomplished by enhanced sliding, the erosion rate ought to be enhanced.

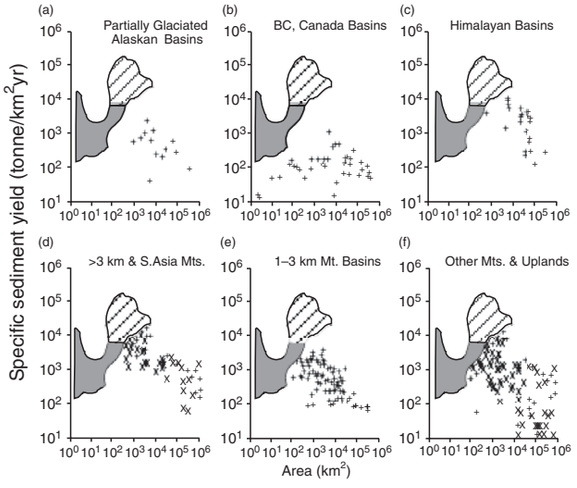


**Figure 8.66** Sediment yield from glacial basins around the world (shaded pattern), and comparison with fluvially dominated basins of specified size or location (marked with X's). (after Hallet *et al*., 1996, Figure 3, with permission form Elsevier)

### Box 8.1 Yosemite Valley

We are now in a position to ponder the origin and evolution of the classic glacial landscape of Yosemite Valley and, more broadly, Yosemite National Park. This granitic landscape is dominated by smooth rock walls with large patches of glacial polish that makes the white granitic surfaces yet brighter. These surfaces reflect the light that dazzled John Muir, and that so attracted photographers Ansel Adams and later Galen Rowell. The deep glacial valleys are interrupted here and there by smooth almost hemispherical domes looking like state capitols that peel away in huge graceful onion-like sheets. Several of these, including the graceful Half Dome, are shown in Figure 8.67. The rock of the Park is all granite. It formed 180–80 million years ago from intrusions in a collisional arc setting. These plutons are the roots of the arc volcanoes that once capped the range. The rock has come to the surface simply through erosion and is now well above sea level due to isostatic adjustment to this erosion. The volcanic rocks once on the surface have been eroded from the surface and deposited to the west in what was the forearc, and is now the Great Valley. No tectonic forces pushed the rock up against gravity, cracking it as it was moved along curved faults, as has happened for example in the Laramide ranges of the American West. The rock moved toward the surface gently, and this gentle unroofing leads to the intact, massive character of the rock. This character in turn translates into all of the major features that together are the signature of Yosemite. The lack of cracks means the walls are strong and can maintain near verticality for hundreds of meters. Hence El Capitan. The precious few cracks challenge climbers on far-flung routes up the vertical walls. That the rock is so intact also promotes the formation of the domes. As discussed in Chapter 10, sheet jointing requires massive rock so that compressional stresses do not simply move myriad chunks of rock on pre-existing cracks, but instead generate surface-normal stresses on curved surfaces. But our interest here is in the glacial features. The smooth, glinting polished landscape, dotted with scattered glacial erratics as exemplified by the scene in Figure 8.68, is yet

another corollary to the massive rock quality. The lack of cracks robs the glaciers that repeatedly slid across this landscape of the most efficient of the erosional mechanisms: quarrying was limited, meaning that abrasion was the only method remaining for the glaciers to employ. Hence the polish. The few erratics scattered about on these surfaces speak to the low debris concentration in the ice, also a manifestation of the difficulty of plucking blocks from the bed. These effects are pronounced in the Cathedral Peak Pluton, which is the most massive, least fractured of the plutons in the Park. The limited erosion of the portion of the Yosemite landscape underlain by the Cathedral Peak pluton is now documented by $^{10}$Be concentrations that are far too high to record the time of deglaciation (see Guido *et al*., 2007; Duhnforth *et al*., 2008; Ward *et al*., 2009). Where the spacing between fractures is small, quarrying dominates, sufficient erosion occurs to reset the $^{10}$Be clock, and the measured $^{10}$Be concentration is that one would expect from the time of deglaciation (i.e., $C = P_o T$, see Chapter 6). Where the spacing between fractures is large, insufficient erosion occurs during the last glacial cycle, and the measured $^{10}$Be reflects both the accumulation since deglaciation and some remainder of the inventory from the last interglacial exposure (called inheritance). Perhaps the low erodibility of the Cathedral Pluton is why Tuolumne meadows sits so high, with the deep glacial troughs of the Tuolumne and Merced Valleys plunging off it to the northwest and to the southwest, respectively.

**Figure 8.67** Upper Yosemite Valley seen from Glacier Point looking east. Half Dome graces the right skyline. All rock in view is granitic. The Ahwiyah Point rock fall below Half Dome is visible as a light streak. It occurred on the morning of March 28, 2009 and is estimated to have involved about 40 000 cubic meters of rock, making it the largest in Yosemite in 22 years (pers. comm., Greg Stock, NPS). (photograph by R. S. Anderson)

## Summary

Glaciers modify alpine landscapes significantly, leaving their marks on the landscape in the form of U-shaped valleys, cirques, hanging valleys, stepped longitudinal profiles, and fjords in the erosional portion of the landscape, and characteristic deposits in moraines and eskers. We have reviewed the physics of how these features originate. Sedimentary records from glacial terrain imply that glaciers are efficient at eroding the headwaters. Their actions therefore impact the fluvial landscape downstream by strongly modulating the sediment supply to the river system, charging it with slugs of sediment when glaciers are large, and starving it when they are small. We will see in Chapter 12 that this generates stacks of fluvial terraces.

**Figure 8.68** The essence of the upper Yosemite landscape includes broad bare bedrock surfaces sporting glacial polish and scattered erratics. Note the massive (fracture-free) nature of the bedrock in Tuolumne Meadows. (photograph by Miriam Duhnforth)

In order to understand the erosion by glaciers, we had to understand how glaciers work. Glaciers are charged with the task to transporting snow (metamorphosed into denser pure ice) from the accumulation zone above the ELA into the ablation zone below it, where it is lost to melt or to calving. At steady state, the pattern of ice discharge required to accomplish this task increases to a maximum at the ELA, and declines to zero at the terminus. Glaciers transport ice by two mechanisms: internal deformation of ice, and basal motion that we loosely call sliding. Internal deformation is governed by the nonlinearity of the rheology if ice. This makes the ice discharge very sensitive to ice thickness, meaning that only small changes in ice thickness are required for a glacier to accommodate climate change. Sliding remains a major focus of modern glaciological research both because it governs the erosion by glaciers and because it controls the rate of delivery of ice to the margins of ice sheets. We do know that sliding is strongly governed by the state of the glacial hydrologic system. It appears that whenever the inputs of water to the complex hydrologic system of tunnels and cavities beneath a glacier exceed its ability to pass that water onward to the terminus, sliding is promoted. In addition, basal motion can be accomplished by shearing of underlying till. The rapid motion of the ice streams of Antarctica appear to be governed by the thermal state of this till.

Sliding of the glacier against its bed is the only means by which a glacier can damage the underlying rock. Both abrasion and quarrying rates increase with sliding speed. Quarrying focuses on the down-valley edges of bumps and ledges in the bed. Abrasion smoothes the stoss or upstream sides of these bumps, and serves to remove small-scale bumps, leading to smooth surfaces.

Larger scale forms such as glacial cirques, U-shaped valleys, hanging valleys and fjords must be understood in the light of repeated occupation of the landscape by glaciers that have come and gone through the last several million years. Spatial variation in the long-term ice discharge, some fraction of it accomplished by sliding, is responsible for at least some portion of this pattern of erosion. That alpine valley profiles evolve to flat-floored valleys with steepened headwalls is an inevitable consequence of the pattern of ice discharge, which to some degree mimics the pattern of erosion. Hanging valleys result from the large discrepancy of long-term ice discharge through the tributary vs. the trunk valley. So also is the punctuation of continental edges by glacial fjords. Topographic steering of the ice through any preexisting drainage allows fjords to bite deeply into the landscape. The details of the erosion pattern, however, will also be governed by spatial variations in the susceptibility of rock to erosion. The pattern of glacial erosion in the last glacial cycle in the Yosemite landscape, for example, suggests that fracture spacing strongly controls the erodibility of rock.

## Problems

**1.** The data in the table below shows mass balance data collected in 2006–2007 at Hardangerjøkulen, the sixth largest glacier in Norway. Hardangerjøkulen is a small ice cap that drains in several directions through outlet glaciers. The data we have is for the outlet called Rembesdalsskåka.

Your primary task is to determine whether this was a positive or negative mass balance year for this glacier (the outlet Rembesdalsskåka, for which we have data).

Steps:

- **(i)** Compute the specific net balance for each altitude band.
- **(ii)** Plot the specific winter, summer and net balances as a function of altitude.
- **(iii)** Compute the volume for winter, summer and net balance in each elevation band.
- **(vi)** Plot the volume balances (winter, summer, net) as a function of altitude.
- **(v)** Compute the total net balance for the glacier both as a specific balance (units of depth of water equivalent) and as a volume balance (volume of water equivalent).

In addition to a table showing the results of these calculations, and the plots requested, answer the following questions:

- **(a)** What is the equilibrium line altitude for this glacier in 2006–2007?
- **(b)** Was this a positive or negative mass balance year for this glacier?

Mass balance Hardangerjøkulen 2006–2007

| Altitude (masl) | Area ($km^2$) | Specific winter balance (m w.e.) | Specific summer balance (m w.e.) |
|---|---|---|---|
| 1850–1865 | 0.09 | 2.70 | –1.45 |
| 1800–1850 | 3.93 | 3.45 | –1.50 |
| 1750–1800 | 4.03 | 3.60 | –1.60 |
| 1700–1750 | 3.46 | 3.50 | –1.75 |
| 1650–1700 | 1.94 | 3.20 | –1.90 |
| 1600–1650 | 0.75 | 2.70 | –2.10 |
| 1550–1600 | 0.59 | 2.35 | –2.30 |
| 1500–1550 | 0.57 | 1.95 | –2.50 |
| 1450–1500 | 0.29 | 1.73 | –2.70 |
| 1400–1450 | 0.19 | 1.56 | –2.95 |
| 1350–1400 | 0.10 | 1.39 | –3.20 |
| 1300–1350 | 0.10 | 1.22 | –3.45 |
| 1250–1300 | 0.27 | 1.05 | –3.70 |
| 1200–1250 | 0.36 | 0.80 | –3.95 |
| 1150–1200 | 0.28 | 0.55 | –4.25 |
| 1100–1150 | 0.11 | 0.30 | –4.55 |
| 1020–1100 | 0.05 | –0.05 | –4.90 |

**2.** *Glacial water balance*. We are interested in knowing when water is accumulating within a glacier, when it is steady, and when it is losing water. Kennicott Glacier is 40 km long and 4 km wide. The average (water-equivalent) melt rate at the glacier surface over the melt season is 5 cm/day, as measured using ablation stakes. Water discharge is also measured at the terminus of the glacier.

Estimate what the discharge of water should be, in $m^3/s$, when the water outputs from the glacier equal the water inputs.

**3.** *Glacier thickness*. We wish to estimate the local thickness of a glacier given only a topographic map of the glacier. Assume that the basal shear stress $\tau_b = 0.8$ bars $= 8 \times 10^4$ Pa, and that the walls are far enough away (the glacier is wide enough) that they play no role in supporting the ice. The contours on the map show that the ice slope is 10 m/km or 0.01 at this location. Given the density of ice $\rho = 917$ kg/$m^3$ and $g = 9.8$ m/$s^2$, estimate the ice thickness $H$ at this location.

**4.** *Glacial terminus position*. Given a simple glacial valley with a slope of 0.01, such that the elevation of the bed $z = 3500 - 0.01x$, a uniform valley width, and a mass balance profile $b(z) = 0.01*(z–\text{ELA})$, where the equilibrium line elevation ELA = 3000 m, calculate the expected terminus position for a

steady glacier. The maximum elevation of the valley, at $x = 0$, is 3500 m. Calculate and plot the down-valley pattern of ice discharge.

**5.** *Sea level rise*. Given a recent estimate of the rate of loss of glacial ice to the ocean of 400 Gtonne/year, what rate of sea level rise would this produce?

**6.** Calculate the expected thickness of ice that can be melted from the base of a glacier due to geothermal heat flux. Assume that the glacier is temperate to its base (why is this important?), and that the geothermal heat flux is 60 mW/m$^2$.

**7.** From the plot of GPS-derived horizontal speeds on the Bench Glacier in Figure 8.18(a), estimate (a) the background speed of the glacier that is presumably attributable to internal deformation of the ice, and (b) scale the maximum sliding speeds during the two speed-up events at the GPS 3 site.

**8.** Estimate the flow-law parameter $A$ from the ice speed profile of the Worthington Glacier in Figure 8.12(b). Assume the local slope of the glacier at the borehole location to be 60 m/km, and that the ice obey's Glen's flow law ($n = 3$).

**9.** How thick would ice to be to remain grounded in the middle of Sam Ford Fjord on the eastern edge of Baffin Island, where present water depths are 800 m. How thick would it have to be if sea level were 120 m lower (i.e., during a glacial lowstand)? List what assumptions you are making in such a calculation. Note that it is required that the ice be grounded for some fraction of the time in order to erode the bedrock floor of the fjord.

**10.** *Thought question*. Given the climate oscillations that have characterized the Quaternary, as summarized in the marine isotope record in Figure 8.53, discuss how the alpine landscape ought to respond. The answer should include addressing how glaciers might respond, and how sediment released from the glaciers might drive landscape change in the river system downstream.

**11.** *Thought question*. Ponder the design of a means of measuring the flow speed within a subglacial conduit through which water enters from the glacier surface through a moulin and exits the glacier in an exit stream. For safety reasons, you are not allowed to enter the conduit yourself, meaning you will need to find some remote means of measuring it.

**12.** *Thought question*. Design a field experiment to measure the sliding history of a glacier over the course of a full annual cycle. Talk about the instrumentation that will be required, and where and how you will deploy it. In other words, produce a field plan.

## Further reading

Benn, D. I. and D. J. A. Evans, 1998, *Glaciers and Glaciation*, London: Arnold, 734 pp.
*This broad compilation of the literature provides the student with a snapshot of our knowledge of the field as of the late 1990s.*

Hooke, R., Le, B., 2005, *Principles of Glacier Mechanics*, 2nd edition, Cambridge: Cambridge University Press.
*This book provides an alternative entrance point for the student of glaciology wishing to learn about the mechanics of glaciers. It is both rigorous and accessible, leaning heavily upon the author's broad experience in the field.*

Menzies, J. (ed.), 1996, *Modern Glacial Environments: Processes, Dynamics and Sediments, Vol. 1:*

*Glacial Environments*, Oxford: GBR, Butterworth-Heinemann Ltd.
*An edited volume with chapters by leaders in the field, this book crosses the discipline from glaciers to their influence on the landscape.*

Paterson, W. S. B., 1994, *The Physics of Glaciers*, 3rd edition. Pergamon, Elsevier Science, 480 pp.
*Long the bible of glaciology, and now in its third, edition this textbook provides the basic reference in the field.*

Pfeffer, W. T., 2007, *The Opening of a New Landscape: Columbia Glacier at Mid-Retreat*, AGU Special Publications Series, **59**, 116 pp.
*This slim book provides, quite literally, a snapshot of the landscape emerging from beneath this fast-retreating tidewater glacier in Alaska. Because so many early glaciologists contributed to its study, and the issues involved in such glaciers touch upon many aspects of glaciers, the text also provides something of a history of glaciology. The photography is stunning.*

Sharp, R. P. 1991: *Living Ice: Understanding Glaciers and Glaciation*. Cambridge: Cambridge University Press, **xii**+228 pp.
*As with most things Bob Sharp touched, this little book is charmed. It provides an avenue for the general reader to access how glaciers work, and how the landscape has evolved as they have come and gone in alpine landscapes.*